Mohammad Abdin

Development of Transcritical CO₂ Heat Pump Chillers

Trondheim, 06 2023

Master Thesis

NTNU
Norwegian University of
Science and Technology
Faculty of Engineering
Department of Energy and Process Engineering

NTNU

Kunnskap for en bedre verden
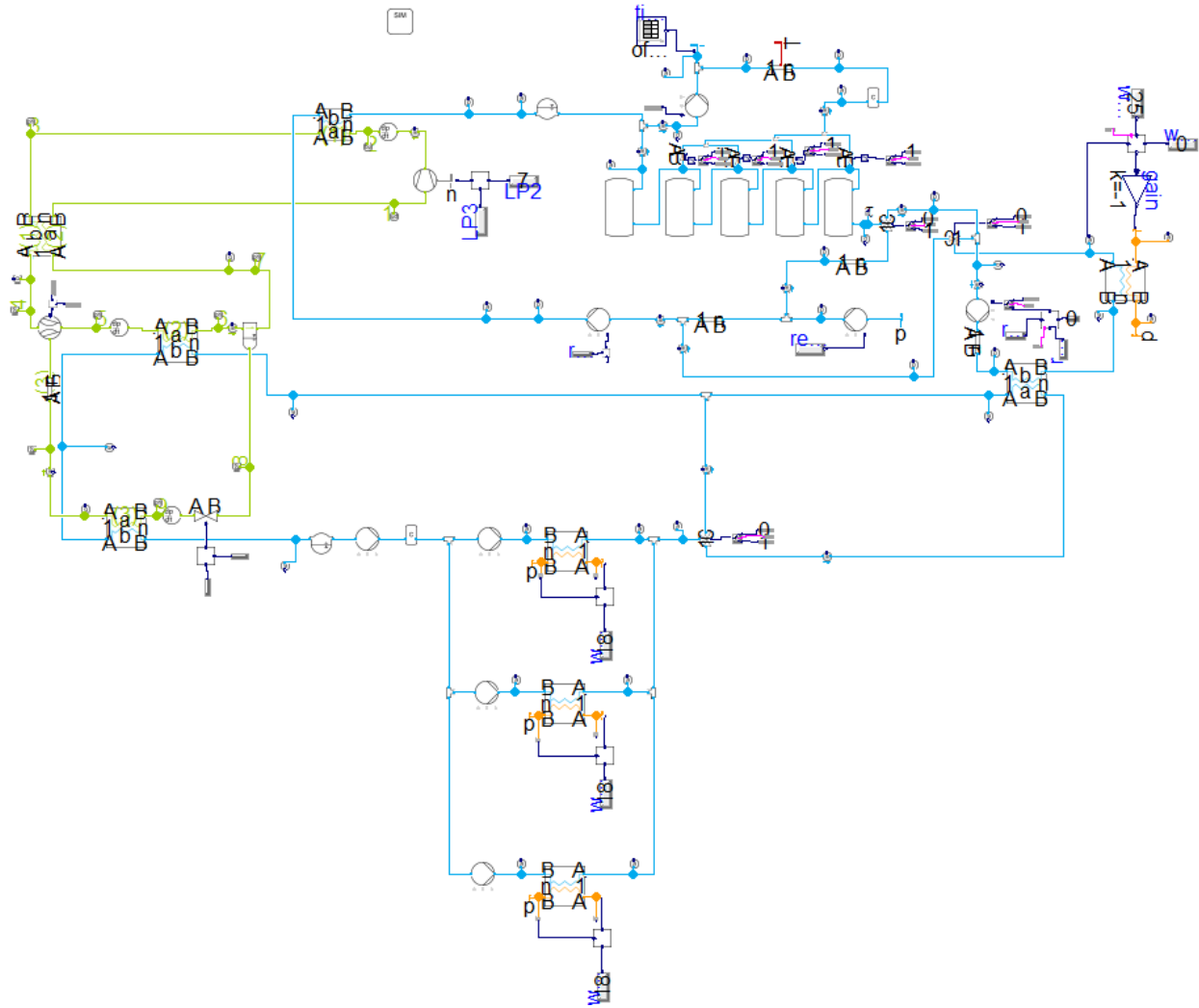
Faculty of Engineering

Department of Energy and Process Engineering

TEP4521 - Specialization Project
of
Sustainable Energy (M.Sc.)
Heat Pumping Processes and Systems

Development of Transcritical CO$_2$ Heat Pump Chillers

Author:
Mohammad Abdin

Supervisor:
Armin Hafner

June 2023

Abstract

Carbon dioxide was first used as a refrigerant in the 1850s, primarily due to its natural abundance, cost efficient and non toxicity. It then started to phase out for the use of hydrochloroflourocarbons (HFC) due to the high operating pressure and low critical temperature of CO_2. With new legislations (The Montreal Protocol, and EU-F gas policies by the European commission) in place that call for a reduction in the use of certain refrigerants for their high GWP factors. After discovering their harmful effect on the ozone and environmental health, with the food storage industry being the most responsible. Hence, the emphasis shifted to the use of natural gases and CO_2 as a working refrigerant was rediscovered for its great physical properties, negligible effect on the environment and and its wide abundance.

CO_2 heat pump and refrigeration systems were initially developed in the 2000s to accommodate the North European weather. Where CO_2 proved to be a very efficient option due to the low ambient northern temperatures that rarely ever exceed 25^OC, where the system easily operated in subcritical mode year round. With the low ambient temperatures the system configurations were simple and proved to be more efficient and very effective when compared to its counterpart the HFC systems. This is another story, for warmer climate conditions were CO_2 will operated in transcritical cycle for long portions of the year, which means the systems had much lower efficiencies than when compared to those in Northern Climate even lower than the efficiency of HFC systems. Moreover, systems working in transcritical mode results in, high discharge temperature and pressures creating reliability issues at that time. As a result, the term CO_2 equator started to be used to refer to the latitude below which CO_2 systems were inefficient and inconvenient.

This thesis, intends to implement a comprehensive review of the evolution of CO_2 refrigeration and heat pump systems covering the most important aspects of the state of the art commercial transcritical CO_2 systems which have emerged to overtake its worst counterpart the HFC technologies, and put an end to the use of high GWP refrigerants. It was concluded that, despite the scepticism around the adoption of CO_2 systems in warm countries, R744 as an only working refrigerant in transcritical operation with the integration of the newest technologies proves wrong. This thesis, develops an R744 heat pump system for a hotel in India, and shows that R744 systems are efficient in warm countries with potential for more upgrades. By the end of the thesis, a transcritical heat pump system capable of achieving great results in all possible conditions was engineered.

Preface

The paper I have written for master thesis covers the evolution of CO_2 systems as well as developing and simulating a transcritical and novel CO_2 heat pump system myself. This thesis, has been submitted to fulfill the some of the requirements to achieve a master's degree in sustainable energy, specialized in heat pumping processes and systems at the Norwegian University of Science and Technology (NTNU). The study submitted, started as project development work from August 2022 till December 2022 and the master thesis final work carried out from January 2023 till June 2023. The supervisor of my work is Professor Armin Hafner. The project belongs under the umbrella group project INDEE+. Which are projects dedicated to support the Indian refrigeration and air conditioning sector, for a transition into a greener environment.

I apologize in advance for some pages having blank spaces, there is not alot of edits and control over the page structure in Latex overleaf.

Acknowledgments

I would like to give my gratitude to where gratitude is owed. First and foremost, I want to thank my supervisor Professor Armin Hafner, for all his support and guidance throughout my period of studies. With him pouring high quality knowledge during all our meetings and emails, as without him I would have not gained the experience and knowledge needed to produce this report. I will forever be thankful for this opportunity. I would also like to give my dearest gratitude to my fellow classmates and colleagues, for all the help they gave me in times of need, pushing me through to the finish line, and inspiring me to work harder and be a better person.

I would also like to thank my family for all their support and advice all my life and I will forever be grateful for.

Table of Contents

List of Figures

List of Tables

Nomenclature

0.0.1 Greek and Latin Letters

Symbol	Explanation
Q or $\dot{Q}$	Capacity [kW]
U	Overall Heat Transfer Coefficient [Wm^{-2}K^{-1}]
A	Area [m^2]
V	Volume [m^3]
T	Temperature [K or ^{O}C]
P	Pressure [Pa or bar]
h	enthalpy [kJkg−1]
s	entropy [kJkg^{-1}K^{-1}]
H	Static height difference [m]
h	Static height difference [m]
ρ	density of fluid [kg/m^3]
L	Length [m]
d	diameter [m]
g	Gravity constant [9.81ms^{-1}]
Δ	Difference between two points
$\sum$	Sum
logP	Logarithmic Pressure [bar]
ω	Entrainment Ratio
π	ejector suction pressure ratio
η	efficiency
m	mass [kg]
cp	Specific Heat Capacity [kJkg^{-1}K^{-1}]
ε	internal heat exchanger effectiveness
C	ratio between the heat capacities of the fluid
Δ t$_a$	Approach temperature [K]
$\dot{m}$	mass flow rate [kgs^{-1}]
u	Velocity [ms^{-1}]
υ	specific volume [m^{3}kg^{-1}]
x	vapor fraction

0.0.2 Abbreviations and Subscripts

HFC	Hydrofluorocarbon
HCFC	Hydrochlorofluorocarbon
CFC	Chlorofluorocarbons
CO_2	Carbon Dioxide
GWP	Global Warming Potential
TES	Thermal Energy Storage
HWS	Hot Water Storage
CWS	Chilled Water Storage
HWP	Hot Water Production
HWD	Hot Water Demand
AC	Air Conditioning
R717	Ammonia
R744	Carbon Dioxide
R290	Propane
R404A	HFC refrigerant
R134a	HFC refrigerant
R448a	HFC refrigerant
COP	Coefficient of Performance
IHX	Internal Heat Exchanger
LT	Low Temperature
MT	Medium Temperature
BPV	By pass valve
Comp.	Compressor
GC	Gas Cooler
HR	Heat Recovery
HX	Heat Exchanger
riser	riser port in gravity fed operation
Exp	Expansion
Evap	Evaporator
Sp or sep	Liquid Separator
HP	Heat Pump
app	Approach
amb	Ambient
PHE	Plate Heat Exchanger
AHU	Air Handling Units
Ph	Pressure Enthalpy
Th	Temperature Enthalpy
mf sen	mass flow rate sensor
Temp.	Temperature
DCV	Directional Control Valve
LP	Low Pressure
l or Liq	Liquid
i	Inlet
o	Gaseous
s	Sensible
i	Initial
f	Final
act	Actual
min	Minimum
max	Maximum
ref	Refrigerant
kg	subscript when the unit is in kg
m^3	subscript when the unit is in m^3
L	length

1 Introduction

Heating, cooling, freezing and chilling has been necessities for humans since the beginning of time, whether it is for storing foods for longer life, protecting themselves from the cold winter, or cooling themselves from the hot summer. These processes have been developed and came a long way. In this day and age they are called refrigeration systems, AC units, space and water heaters.

With the increase in population, comes an increase in the number of buildings, supermarkets, hotels, etc... all these structures require some type of heat pump or refrigeration systems. Unfortunately, these systems requires a lot of energy especially supermarket refrigeration systems, where they roughly account for 50% of the total consumed energy in a supermarket or 300 to 600kWhm^{-2}, with the comparison to office buildings that have specific energy demand of 150 to 200kWhm^{-2} as presented by Armin Hafner, Poppi et al. 2012.

With such high energy demands HFC systems impose a great damage to the environment for the high indirect green house emissions for generating the electricity to keep them running. As well as, they share the responsibility of the largest emitters of high GWP refrigerants, which occurs through leakages during normal operation, extensive pipework, or poor maintenance. Refrigerant leakage is always opted to occur at one point as there is not one system that is 100% leakage free where the estimated average annual leakage is about 15 to 20% of the total charge in the system Armin Hafner, Poppi et al. 2012.

Hence, a solution must be developed to cancel out the high global warming potential (GWP) refrigerants with refrigerants with low GWP, and more efficient systems. In other words, a solution to decrease both the direct and indirect emissions. In spite of the numerous efforts to phase out high GWP refrigerant R404A which has a GWP factor of 3943 $\text{kg}_{CO_{2eq}}\text{kg}^{-1}_{refrigerant}$ is still widely used in the food sector around the world especially in warmer countries.

1.1 CO$_2$

Fortunately, the pressure against using high GWP refrigerants is increasing day by day, with the adoption of the EU F-Gas 517 regulation by the European commission which only allows the use of refrigerants with a GWP of 150 or lower, as well as the Montreal Protocol which also phase out the use of high GWP refrigerants. With these regulation the use of natural refrigerants is increasing such as the use of Ammonia R717, Propane R290, and CO$_2$ R744. With the spotlight shining on the use of R744 as a refrigerant, thanks to its amazing properties and negligible GWP of 1 and Ozone depletion potential factor of 0. R744 is not toxic nor flammable hence no harsh safety factors to take into account, in addition it has high density and volumetric cooling capacity meaning it will have minimal sensitivity to pressure losses, it also have great thermal conductivity, specific and latent heat capacities. If that is not enough, CO$_2$ is also cost effective, since it is cheap to produce and is widely available. One can say its only drawback is its low critical temperature of about 31°C meaning in warmer climate the system will work in transcritical operation which means more system optimizations to keep the system efficient, nonetheless this also makes CO$_2$ to have a long temperature glide which can be very easily utilised to space and water heating via heat recovery. The adoption of CO$_2$ only systems was mainly observed in countries with cold climates, and took a good deal of time for it to start spreading to warmer countries. Even with the great potential in CO$_2$ as a refrigerant the first deployed units were met with scepticism by the scientific community, however, the systems proved to be very efficient and the use of CO$_2$ for heat pumping units and refrigeration systems just increased ever since.

It is worth to note that there is still a risk in investing in upcoming low GWP HFC refrigerants such as the R448A as future regulations could place further limitations on their use just like what happened with CFCs, HCFCs and what is happening now to HFCs. It is also important to note that even though Ammonia and Propane are natural refrigerants with GWPs of 0 and 3 respectively, they have limited use due to their restrictions when it comes to safety as they are toxic or flammable. This what makes R744 stands out from the rest as it does not share the risk of being phased out in the future.

1.2   Project Objectives

The type of refrigerant and system configuration is the main factor that affects the direct and indirect emissions, hence it is of utmost importance to have a detailed understanding of systems for the preservation of the environment, decrease energy consumption and increase the efficiency of installed systems in commercial refrigeration and heating sector. This project will cover these factors and the developments that come alongside it, to develop the knowledge and skills required to build such systems with high quality. The main objectives of the project are:

- Understanding the newest technologies used for R744 systems, and how far such systems have come from the first generation system, and analyze their environmental, economical and energy evaluations with comparison to conventional HFC systems.

- Design a heat pump system with cold and hot water loops for a hotel in high ambient temperature city Goa, India.

- Develop a control strategy for optimum working operation for the system.

- Build and develop a working simulation of the designed system.

- Develop a future plan on ways to develop the analyzed system for future work.

1.3   Report Structure

The focus of this thesis, is to move the CO_2 equator south and allow for the use of R744 to be a great viable option for warm countries. The technological advancements allows for higher potentials of energy efficiency than the currently used HFCs. As well as, bring into attention the viability of modelling and simulating heat pump or refrigeration systems using softwares to analyze their performance before installation. This allows for money, time savings and potential better configurations before installations. Making it the new way of developing and researching systems. In section 2.1, the newest technologies and systems configurations that have been on the rise from other authors have been discussed and most important parts that would be later utilised in this investigation were brought to attention. In section 4, the methodology behind building one CO_2 heat pump unit for water heating and chilling was developed, as well as the steps that were taken to achieve the results which are seen in section 5 and validate them with the installed. In sections 6, 7 and 8 the heat pump system investigated and its results were discussed with future work and developments on enhancing the system further were expressed, which is believed to make the system a much better operating system with higher efficiencies, compared to the investigated model. It must be noted that the simulation results were not validated with the real system due to the big delay in system installation.

2   Literature Review

2.1   Transcritical R744 Refrigeration System Investigation

The increasing popularity of R744 refrigeration systems, is a result of all the investigations that took place in the past and the ones taking place now to develop and improve existing refrigeration systems. In 2007 Cecchinato et al. 2007, investigated both subcritical and transcritical running modes of a R744 system. He was able to develop a control strategy that will allow refrigeration systems to switch from subcritical mode to transcritical mode smoothly and vise versa. The running mode of the refrigeration system is directly related to the outdoor ambient temperatures within the system's operating range. Cecchinato defined the operating range with upper and lower limits based on the operating high pressure as well as the outlet temperature of a gas cooler.

To add to his research, Luca Cecchinato et al. 2009 over-viewed the benefits of adding an inter-stage heat exchanger such as a de-superheater compared to the staged throttling. With his research it was found that such additions to a CO_2 only system will increase its COP by about 29% and 28% when evaporating at -10°C and -30°C respectively.

Similar to Cecchinato, Torrella et al. 2011, experimentally compared two exact CO_2 only systems with the only difference being an internal heat exchanger at three evaporating temperatures (-5,-10,-15 ^{o}C) at high pressures ranging from 74 to 106 bar. It was found that the COP and cooling capacity had an increase of 12% with a negligible increase of power input. Torrela, discovered that the efficiency of the internal heat exchanger (IHX) is dependent on the evaporating temperature and high side pressure.

Daniel Sánchez, Patiño, Sanz-Kock et al. 2014 experimented with a simple one stage CO_2 system to show at which heat rejection temperatures a system is more efficient in subcritical and transcritical mode. It was found that at heat rejection temperature of 15°C the system performs better in subcritical mode, and at temperatures of 20 to 25°C subcritical mode is no longer beneficial and transcritical mode is the way to go. Sanchez, suggested that the founded results were due to the poor effectiveness of the condenser and by installing an inverter compressor increased the COP and cooling capacity significantly at low running compressor speeds in both transcritical and subcritical modes.

Continuing on his work Daniel Sánchez, Patiño, Llopis et al. 2014, experimented with placing an IHX at different positions within the cycle. The results showed that having an IHX after the gas cooler is beneficial under any running conditional mode increasing the COP of the system by 10.6% when compared to the basic system. It also allows the system to run at a lower optimal high side pressure when compared to a system without an IHX, at heat rejection temperatures reaching 20°C. The second position investigated was at the liquid receiver exit, which deemed to not always be advantageous.

Llopis et al. 2015, investigated systems for low temperature use. It was found that using cascade systems with environmental friendly refrigerants are much more successful than the use of high GWP refrigerants as well as they are as applicable as CO_2 only systems.

R744 refrigeration systems were not favorable in the early days, especially in Southern Europe. Sergio Girotto et al. 2004, R744 system layout proved to consume 10% more energy when compared to a R404a system installed in Northern Italy. Hence, improvements had to be researched and it started with Girotto suggesting a flash gas by pass valve to the MT compressor, as well as decreasing the temperature difference between the CO_2 refrigerant and the cooling media in the gas cooler. On the other hand, in Northern Europe it was a different story due to the low ambient temperatures. For example, Sawalha 2008 proposed system was found to consume 4% less energy

when compared to a R404a system in Sweden. In addition Sawalha mentioned that such system will not be able to compete with a R404a system in high ambient temperature conditions.

All CO_2 cascade systems were also investigated, in order to phase out HFC cascade systems. This was very popular for systems in subcritical mode. However, it was found that with every 1K increase in temperature in the gas cooler the system lost 3% in COP which made only CO_2 cascade systems not very popular in warmer areas.

Hence, booster CO_2 only systems took the spotlight for systems with large cooling capacities. This was mainly due to the fact that booster configurations would decrease the components needed in the LT circuit by 75% when compared to the cascade systems as investigated by Sienel and Finckh 2010. Which made booster systems more cost efficient. KM Tsamos et al. 2017 took this investigation one step forward, by investigating the energy savings of the two systems in warm climates. It was found that CO_2 only booster systems saved 2% more energy when compared to CO_2 only cascade systems.

2.2   Basic Booster System 1st Generation

The first ever CO_2 booster system was developed in Denmark under the project name "Life" by the Danish Technological institute Gullo, Armin Hafner and Krzysztof Banasiak 2018 and was installed in March 2007 in a small Danish supermarket. This system offered 4% energy saving and 52% less carbon footprint when compared with previous installed R404a system. The system was comprised of a MT and LT compressor (double stage compression) hence the name booster, combined with a gas cooler, an IHX after the gas cooler with suction line of MT compressor, a liquid receiver, two evaporating temperatures MT and LT. Later on the 1st generation booster system included a flash gas by pass from the liquid receiver to MT compressor due to the immense energy benefits that came with it.

The schematic diagram in figure 1 shows the first generation booster system. Which was then installed in 200 stores in Northern Europe short time after the first installation in Denmark Matthiesen et al. 2010.

Later on Sharma et al. 2015 tested the booster system in a lab to find the COP of the system in ambient temperatures ranging from 10 to 35°C. The COP of the system was found to range from 3.3 to 1.4. On the other hand, Fricke et al. 2016 lab tested an equivalent R404a sized system to the one Sharma tested. The founded results showed that the transcritical booster system had 15% larger COP when compared to the R404a system at temperatures ranging from 15 to 31°C. In addition, Sawalha et al. 2017 collected field measurements of 3 CO_2 booster systems in three different Swedish stores during a time period of 7 to 9 months, where the outdoor temperatures were below 24°C. It was found that the CO_2 booster system had higher overall COP when compared to HFC system with the same size as well as the booster system was able to achieve 20% more energy savings than the HFC system.
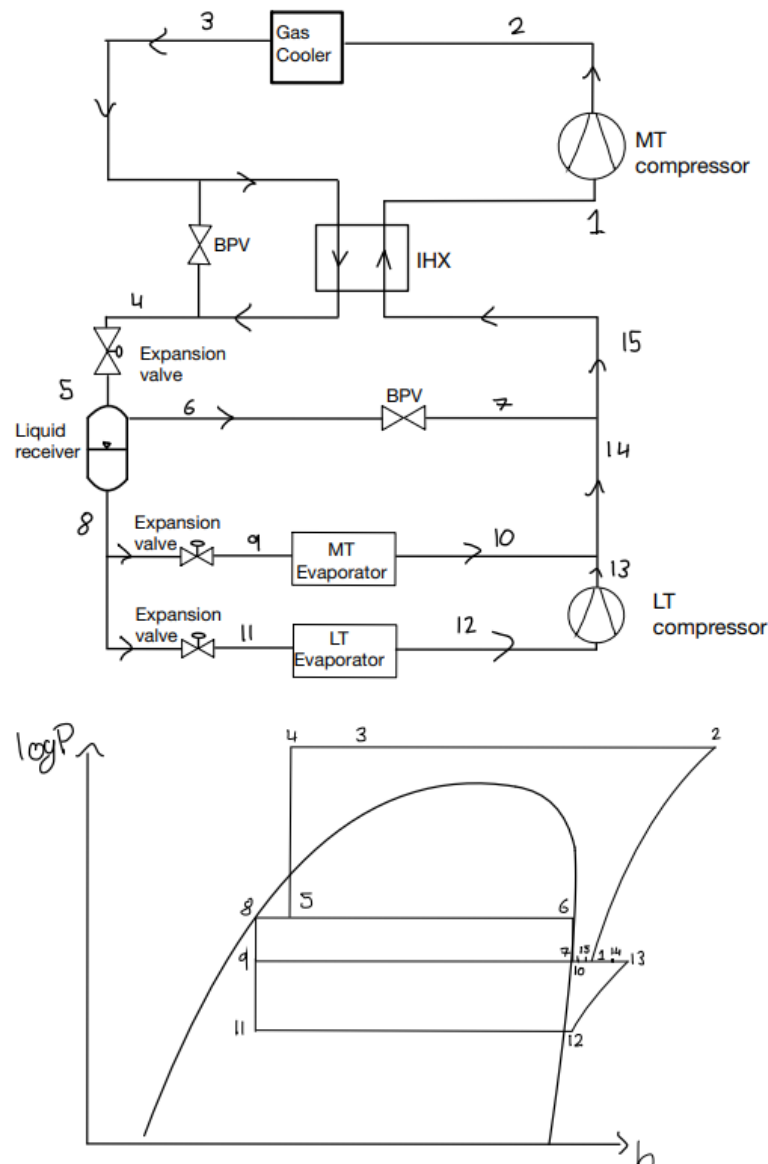
Figure 1: 1st Generation Booster System and its Cycle in PH diagram

With the 1st generation booster system being very popular in cold climate regions and not favorable in the warmer climates, due to the significant differences between the heat rejection and heat absorption pressure in transcritical operation, which leads to huge exergy depletion rates that is directly affected by the expansion valve. This causes the performance of the system to deteriorate with the rise of the cooling media's temperature. This created a so called CO_2 equator line dividing the northern cool areas to the southern warmer areas. Ever since this division researchers worked to push the CO_2 equator line even further down south to enable CO_2 systems to flourish in warm climates and become more popular to allow phasing out the HFC systems easier. To see that come to reality, all the research was being developed to enhance the energy efficiency and cost effectiveness of the 1st generation booster systems to a more promising system configurations that will solve the issue of the so called CO_2 equator.

5

2.3   State of the Art Transcritical Systems 2nd and 3rd Generations

2.3.1   Parallel Compression

The first addition to push the CO_2 equator south was the addition of a parallel compressor, seen in figure 2, which is mainly connected to the flash gas by pass from the intermediate pressure receiver seen in the 1st generation systems. This is due to the fact that, as the outdoor temperature increase the amount of flash gas in the liquid receiver increases significantly up to 45% of the total mass flow rate in the system. Hence the MT compressor will be under high stress and this means less efficiency and poor performance in high temperatures Gullo and Cortella 2016b.

Hence, the addition of a parallel compressor to compress part of or the total amount of flash gas from the intermediate pressure to the high pressure will allow a significant increase in COP of the system. In fact, the addition of a parallel compressor makes the system more efficient than an R404a system for temperatures up to 27^oC when previously the first generation system was limited to outdoor temperatures of 14^oC Gullo and Cortella 2016a. In addition, the use of a parallel compressor will allow to control the pressure of the intermediate pressure receiver allowing a regular pressure at the sale side in a supermarket, as well as, a stable feed to the expansion valves Minetto, Girotto, Rossetti et al. 2015. Hence, it regulates the cooling capacity and power input into the parallel compressor maintaining a system efficiency higher than a system with no control over the intermediate pressure. As the intermediate pressure decrease, the compression power required increases simultaneously the cooling capacity increases as proven by Bell 2004.

Another possibility is to connect the MT compressor suction line with the parallel compressor suction line through the use of a three way valve, this will allow the use of the parallel compressor only when needed as the operating conditions worsen, by doing so the system will save energy and allows the opportunity of running the systems on different modes depending on the outdoor season Javerschek et al. 2016.
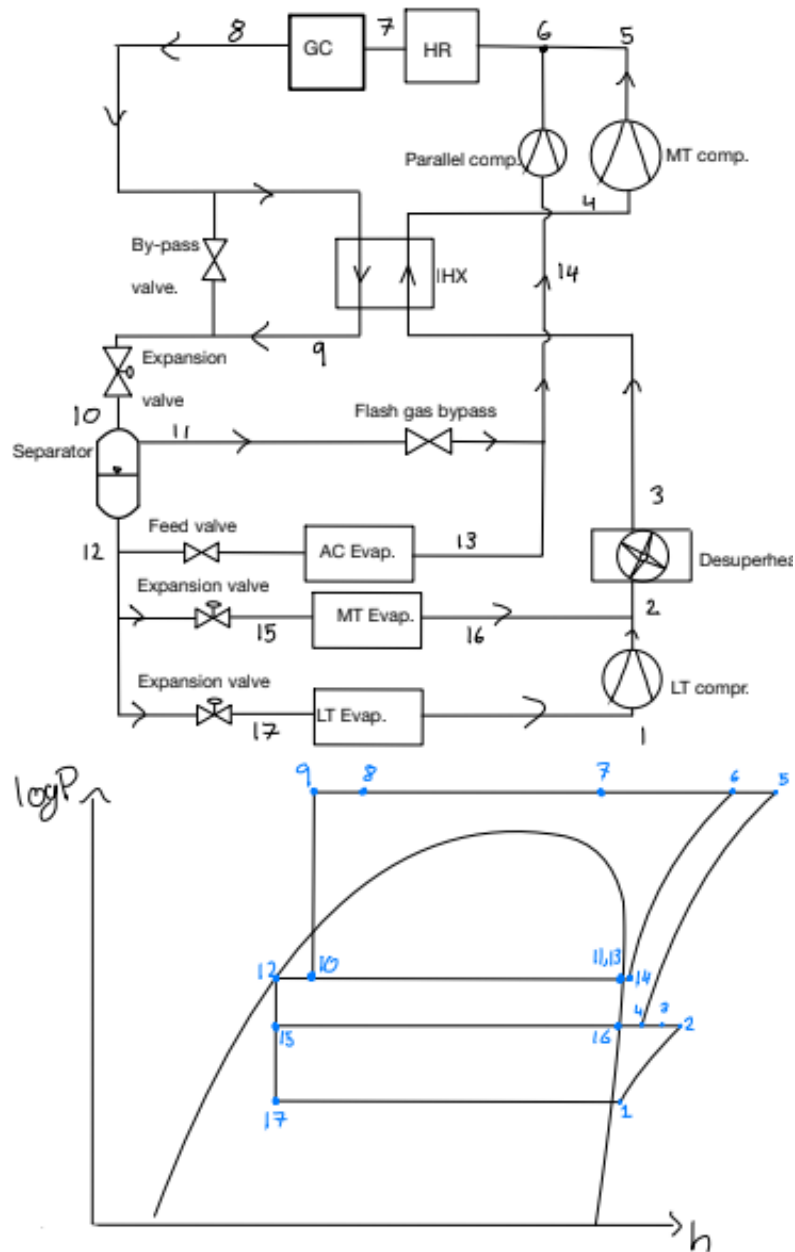
Figure 2: 2nd Generation Booster system with Parallel Compression

Chesi et al. 2014, has evaluated the effect of different operating conditions on the effectiveness of the 2nd generation booster system. Where it was found that, the performance of parallel compression technology is mostly affected by the liquid separator efficiency. Figure 3 shows the effect of liquid separator efficiency on the system's COP at 3 different gas cooler temperature at constant discharge and evaporating pressures. It was also found that the use of parallel compression increased the system's COP by 30% when compared to its predecessor 1st generation system.
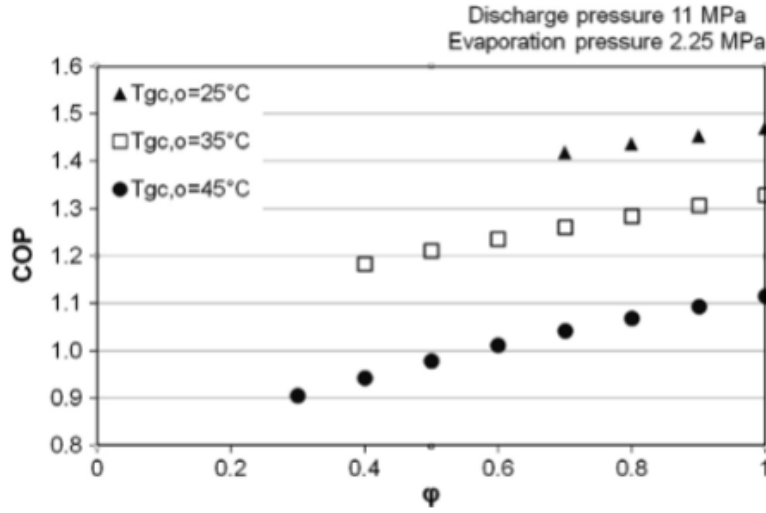
Figure 3: Influence of the Seperator Efficiency on COP by Chesi et al. 2014

2.3.2   Overfed Evaporators

It is no surprise that liquid fluids have a higher thermal conductivity when compared to its gaseous state which is true in the case of CO_2. Hence one way to increase the cooling capacity of an evaporator $Q = UA\Delta T$, where U is the overall heat transfer coefficient and is directly proportional to the thermal conductivity of the working fluid, and efficiency of an evaporator is to over feed it. This means that at the outlet of the evaporator the CO_2 leaves with a vapor fraction less than 1 which ensures that throughout the entirety of the evaporator the working fluid is never fully in its gaseous state. Improving the heat transfer will allow to increase the evaporation temperature, and as reported by Finckh et al. 2011 with each increase on 1K in evaporating temperature an annual energy saving of 3% can be achieved, which leads to a higher overall COP of the system, since less work is required by the compressor as the compression ratio decreases as seen in figure 4 from data researched by Girotto 2017. Moreover, increasing the evaporation temperature will also lead to a reduction in from formation, hence less defrosting cycles.
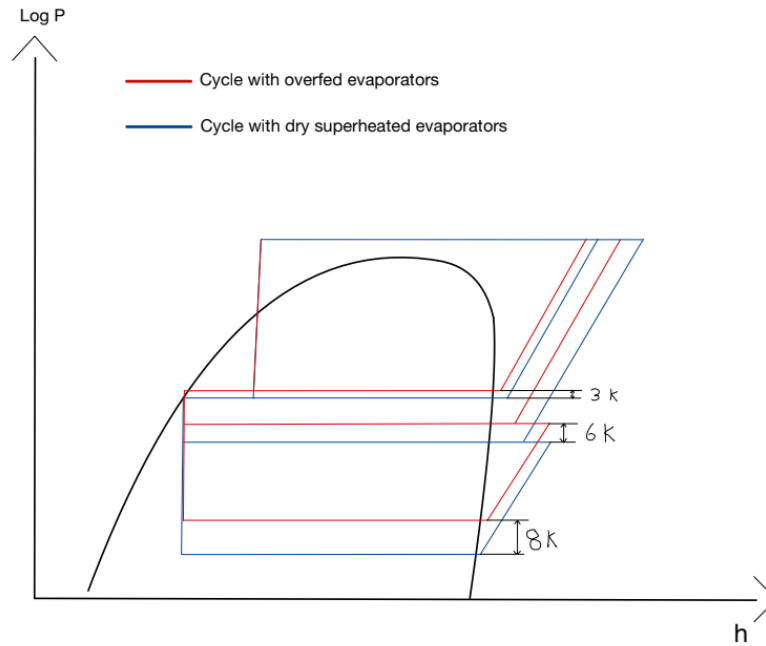
Figure 4: Cycle with overfed vs dry evaporators

This was proved true by Cheng et al. 2008, in this research the effect of vapor fraction on the overall heat transfer coefficient was investigated and the results where as seen in figure 5. Hence, it would be smartest to bound the CO_2 to leave the evaporator at a fraction of approximately 0.75. However, this will require the use of mutli-ejector or liquid ejector which will be described in section 2.3.3, or in the case of not having an ejector, but direct connection to compressor then the use of HX to heat the remaining liquid CO_2 to ensure no liquid return to the compressor as it is detrimental to its life.
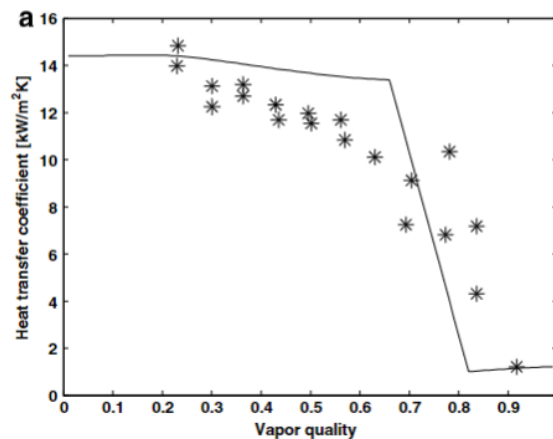
Figure 5: Influence of the vapor fraction on the overall heat transfer coefficient by Cheng et al. 2008

Gullo, Cortella et al. 2016 theoretically investigated the effect of overfeeding the evaporator in an all CO_2 booster system in two different locations Seville, Spain and Rome, Italy to show annual energy savings of 8.2% and 12.3% respectively when compared to a traditional direct expansion R404A system also in Southern Europe. Moreover, Gullo also did a comparison of the possible annual energy savings in a warm country (Athens) and a cold one (Norway) where it was discovered that overfeeding the evaporator will result in energy savings of 12.4% and 22.7% respectively when compared to a R404A unit Gullo, Konstantinos Tsamos et al. 2017.

9

Furthermore, in 2018 Karampour and Sawalha investigated a CO_2 only system with overfed evaporators and parallel compression, and did an energetical and economical evaluation which showed very promising results for warm climates, enough to overtake the now present HFC solutions Karampour and Sawalha 2018.

Gravity Fed Evaporators

A gravity fed evaporator is an evaporator and separator setup that utilizes flooded evaporation seen in figure 6. Where the low or medium pressure separator (based on how it is utilized in the system) is used to supply the evaporator with saturated liquid CO_2 via the downcomer. Hence, the refrigerant at the inlet of the evaporator has a vapor fraction of 0 (allowing a better distribution of liquid refrigerant in the evaporator), with an exit vapor fraction of 0.8 for optimum operation as stated by Hazarika et al. 2022 for highest heat transfer coefficient as seen in figure 7 . The exit of the evaporator is connected to the separator via a riser. The working concept is based on the density differences of the refrigerant at exit and inlet of the evaporator, which in return creates buoyant forces due to the different states of the refrigerant (liquid at inlet, vapor at outlet) which circulates the refrigerant, which is known as a thermo-syphon effect. Moreover, such setup removes the need of an a thermostatic expansion valve as well as the operation is maintained independently of the high side pressure Hazarika et al. 2022.
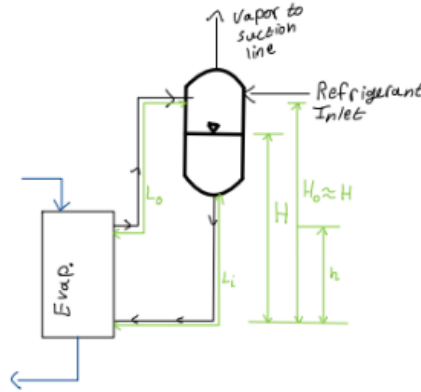
Figure 6: Gravity fed evaporator setup based on Hazarika et al. 2022 model
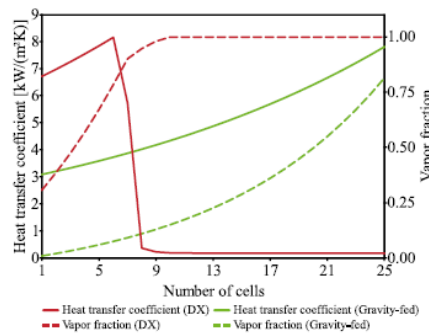
Figure 7: Gravity fed vs DX heat transfer coefficient in evaporator

In order for the setup to run and the refrigerant to flow the total pressure losses (from heat exchanger, pipe bends and frictional losses) (right hand side of equation 1) must be less than the pressure difference between the separator and evaporator due to the height difference depicted as H in figure 6(left hand side of equation 1). Where ρ_l is the density of refrigerant in line L_i, ρ_{evap}

is the average density of the refrigerant in the evaporator(inlet and exit) and ρ_o is the refrigerant density in line L_o. As seen from the equation, the height H is of utmost importance when it comes to running the setup fluently, and in Hazarika et al. 2022 investigation the static height was an independent variable that was used to measure its effect on the cooling capacity of the system. Hazarika et al. 2022 also investigated the effect of changing the riser diameter (Line L_o) on the system's cooling capacity. These can be seen in figure 8. The increase of the static height will increase the cooling capacity until an optimum point around H=0.5m which is then followed by a slight decrease of the cooling capacity as the height was increased further seen in figure 8a.

On the other hand, as seen in figure 8b as the riser diameter is varied from 14 to 28 mm the increase of d_{riser} increased the cooling capacity until d_{riser}=0.028m. However, the increase of the diameter further will not have significant effect on the cooling capacity. Moreover, the increase in diameter the pressure drop in the riser decreased which enhances the self-circulation flow rate. As can be depicted by 9b the flow rate increases significantly at first then it reaches a plateau at diameter of 28mm. Hence it will not be effective to increase the riser diameter further. With the increase of flow rate due to the larger riser diameter, this gives the opportunity to decrease the static height. Hence, it is beneficial to have a riser diameter that is double the diameter of the downcomer.

$$H\rho_i g - h\rho_{evap}g - (H - h)\rho_o g = \sum \Delta p_{losses} \tag{1}$$
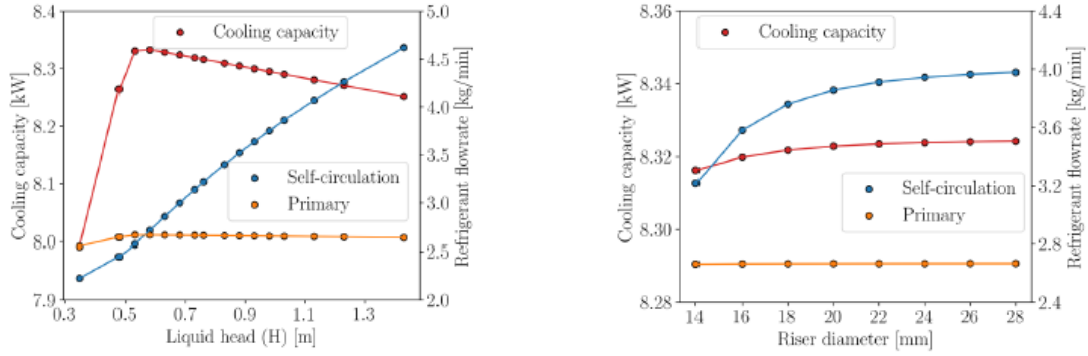
(a) Effect of the static height H on the cooling capacity, self circulation flow rate and primary flow rate of Hazarika et al. 2022 system

(b) Effect of the riser diameter d_{riser} on the cooling capacity, self circulation flow rate and primary flow rate of Hazarika et al. 2022 system

Figure 8: Effect of static height H and the riser diameter d_{riser} on the cooling capacity, self circulation flow rate and primary flow rate of Hazarika et al. 2022 system
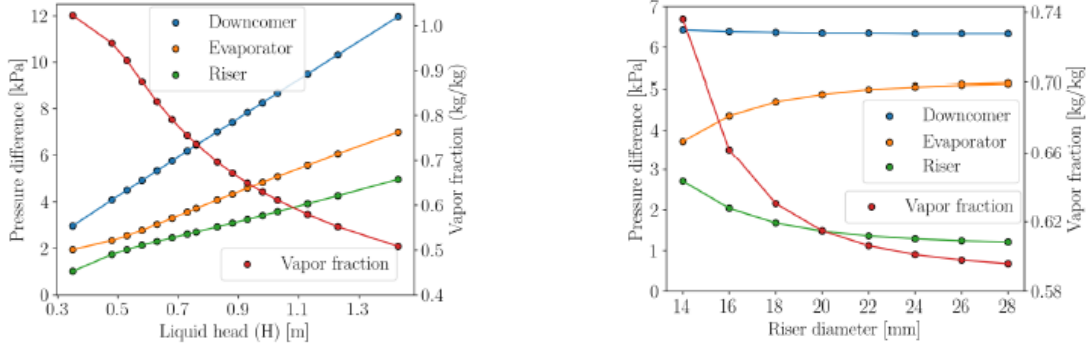
(a) Effect of the static height H on the pressure difference in downcomer, evaporator and riser Hazarika et al. 2022

(b) Effect of the riser diamater d_{riser} on the pressure difference in downcomer, evaporator and riser Hazarika et al. 2022

Figure 9: Effect of static height H and the riser diameter d_{riser} on the pressure difference in downcomer, riser and evaporator Hazarika et al. 2022

2.3.3 Ejectors and Multi-ejector Concept 3rd Generation

One way to be able to achieve higher performances in an all CO_2 system is the utilization of ejectors in the place of the conventional high pressure expansion valve. Ejectors will overcome the drawback of CO_2 system sensitiveness to the increase in cooling media temperature due to its low critical temperature.

With the use of ejectors work can be recovered by compressing a part of the refrigerant from the MT pressure level to the medium pressure liquid separator, hence decreasing the suction compression of the MT compressors, reducing their required work and improving the efficiency of both the system and compressor hence increasing the COP.

The ejector's available compression work is dependent on both the pressure and velocities of the refrigerant. The high pressure refrigerant enters the motive nozzle (point 4 on 10) which is small in diameter; causing the velocity of the refrigerant to increase, with this high velocity the pressure around the nozzle will drop creating a low pressure level(slightly lower than that of the evaporator pressure) in the suction chamber (point 5 on 10). This will allow the refrigerant coming from the evaporator at low pressure to be drawn into the ejector. Then both the high and low pressure refrigerants are mixed in the mixing chamber (point 6 on 10), this will create a common velocity for the mixture which is then sent into the diffuser chamber (point 7 on 10). Here the pressure of the mixture will increase and further slow down due to the steady increase in diameter.

Two-phase ejectors are much more popular than expanders these days, since they are much cheaper, simpler to manufacture and easier to operate and control. Moreover, ejectors are not as sensitive as expanders to liquid refrigerant and will not be damaged that easy. With the research taken place on ejectors they also deemed to be the technology to move the so called CO_2 equator further south as they make the system much more efficient in warm countries as proved by Hafner 2017. Their two main advantages are; the decrease of required compressor power input since the CO_2 is pre-compressed, secondly rise in the refrigeration capacity since the R744 will enter the evaporator at near saturated conditions.
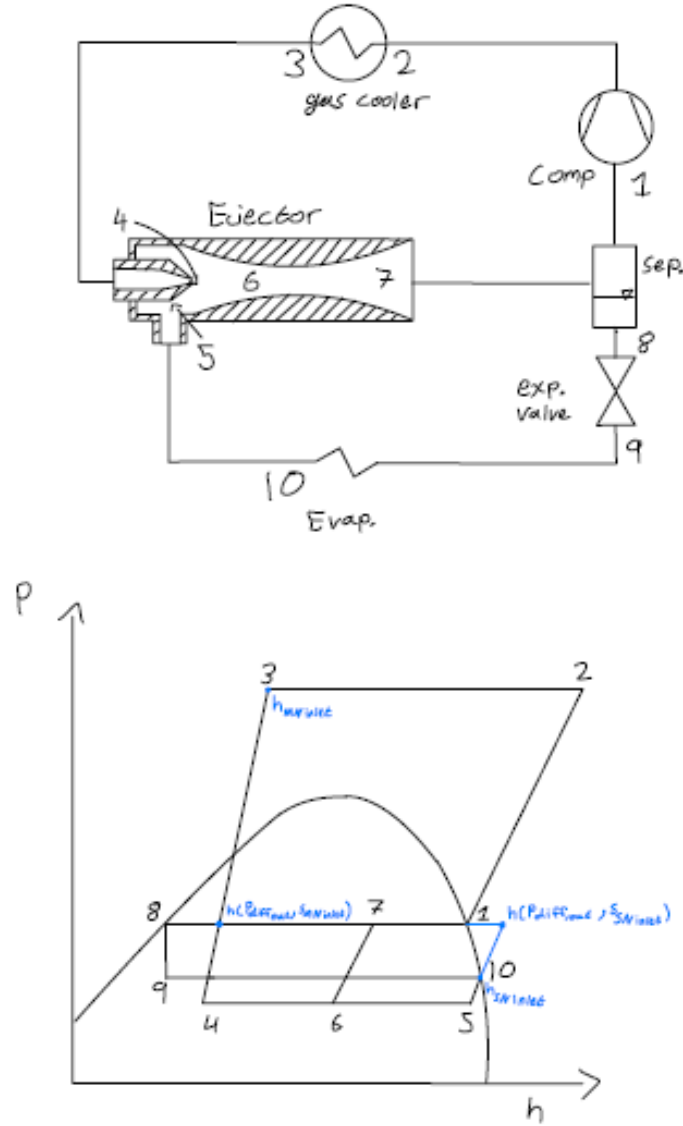
Figure 10: Simple Ejector CO_2 system

To describe the ejector performance and its ability for expansion work recovery, these 4 metrics were developed, the entrainment ratio (ω), suction pressure ratio (π), pressure lift (P_{lift}) and ejector efficiency ($\eta_{ejector}$) as mentioned by Gullo, Armin Hafner, Krzysztof Banasiak et al. 2019. Where the entrainment ratio (Eq.2) is the ratio between the mass flow rate of the refrigerant through the suction nozzle to the mass flow of the refrigerant through the motive nozzle. This will gauge the ability of the ejector to pump the refrigerant.

$$\omega = \frac{\dot{m}_{suction\ nozzle}}{\dot{m}_{motive\ nozzle}} \tag{2}$$

Whereas, the pressure ratio (Eq.3) and pressure lift (Eq.4) are used to quantify possible pressure lift of the refrigerant that the ejector can provide.

$$\Pi = \frac{P_{diffuser\ outlet}}{P_{suction\ nozzle\ inlet}} \tag{3}$$

$$P_{lift} = P_{diffuser\ outlet} - P_{suction\ nozzle\ inlet} \tag{4}$$

13

Finally, the ejector efficiency (Eq.5), which was defined by Elbel and Hrnjak 2008, represents the actual amount of work recovered by the ejector. It is defined as the required power for compressing the suction stream isentropically from the suction pressure to the diffuser pressure divided by the total possible theoretical amount that could be recovered through isentropic expansion from the motive nozzle inlet to the diffuser outlet pressure Gullo, Armin Hafner, Krzysztof Banasiak et al. 2019. These points are seen in figure 10 represented in the blue dots.

$$\eta_{ejector} = \omega \cdot \frac{h(P_{diffuser\ outler}, s_{suction\ nozzle\ inlet}) - h_{suction\ nozzle\ inlet}}{h_{motive\ nozzle\ inlet} - h(P_{diffuser\ outler}, s_{motive\ nozzle\ inlet})} \tag{5}$$

Elbel and Lawrence 2016 compared R744 to R410A and R134a ejector technology, it was concluded that R744 ejectors have an efficiency ranging between 0.2 and 0.3 whereas R410A and R134a has an average efficiency of below 0.2.

With further research and experimental reviews, an individual constant geometry ejector was found to not be able to accurately control the high side pressure and simultaneously do expansion work recovery efficiently as stated by Krzysztof Banasiak et al. 2015. To overcome this drawback, Armin Hafner, Försterling et al. 2014 developed a multi-ejector block concept seen in figure 11. The multi-ejector integrates the use of multiple fixed geometry ejectors of different sizes placed in parallel, this will allow the mass flow rate needed to cover the cooling load to be available in any operating modes. Hence, allow the ejector to cope with variable cooling demand under changing ambient conditions, which is usually the case in commercial refrigeration. The block consists from 4-6 vapor ejectors and usually up to two liquid ejectors.

The running operation of these ejectors are as follow; there is at least one vapor ejectors is in operation, while the other ejectors are operated when a necessary capacity needs to be fulfilled. To fulfill the capacity the ejectors available are always changing their combination based on their sizes, this will guarantee the optimal high side pressure in any conditions. Utilizing liquid ejectors will also allow overfeeding the evaporators for additional energy conservation. As described earlier in section 2.3.2 the importance of overfeeding the evaporators and its effect on increasing the working evaporation temperature. Girotto 2017 remarked that with a liquid ejector with an efficiency of 8% will improve the overall yearly performance of the system by 15% when compared to a vapor ejector with an efficiency of 30% which will improve the annual performance by only 5% of course depending on the ambient temperature log.
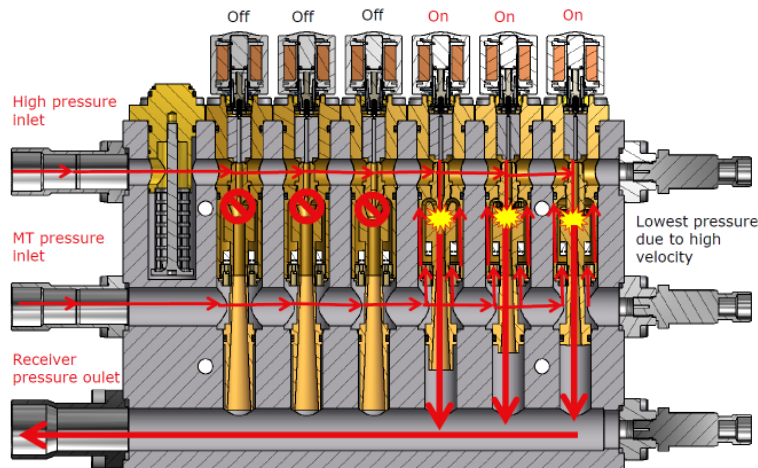
Figure 11: Multi-Ejector block Gullo, Armin Hafner, Krzysztof Banasiak et al. 2019

Figure 12 represents the first R744 system to be proposed with multi-ejectors, use of parallel compressors and overfeeding MT evaporators. The system was installed in a large Swiss supermarket with a medium and low temperature capacities of 120 and 55 kW respectively. To improve on this system Minetto, Girotto, Rossetti et al. 2015 applied extra internal heat exchangers to overfeed the

LT evaporators. This also requires a low pressure accumulator tank to trap the liquid that cannot be evaporated in the internal heat exchanger (IHX D) seen in figure 13, whereas IHX C is used to heat up the refrigerant before entry to the LT compressors at all operating conditions. These improvements proved extremely beneficial, as the system is more energetically efficient making it the preferred solution for end users.

A fully integrated system also known as an all in one system, is a system customized to provide refrigeration at both MT and LT levels, air conditioning and heat recovery including water and space heating as well as ice melting if necessary. Such system was installed in Northern Italy seen in figure 14. Such system are to be expected to replace the HFC solutions and become the standard for commercial refrigeration systems. With more research and improvements to come, these systems are expected to decrease the capital, maintenance and operational costs, other than its extremely beneficial energy savings and higher COPs when compared to the conventional HFC solutions as mentioned by Hafner 2015; Hafner, Banasiak et al. 2016.
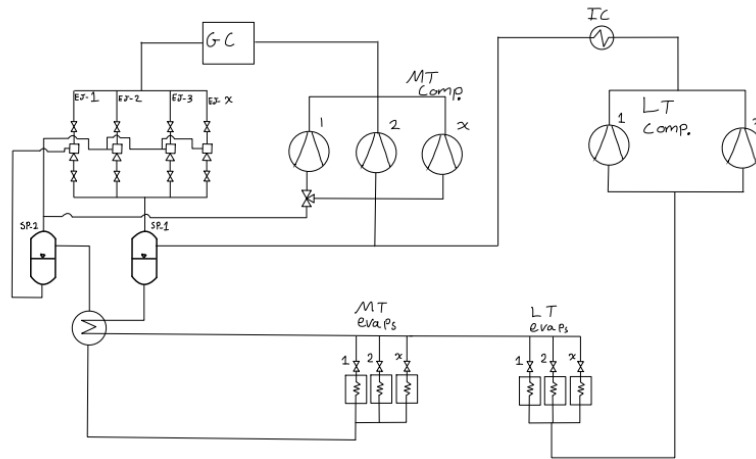
Figure 12: First proposed R744 multi-ejector system with parallel compression
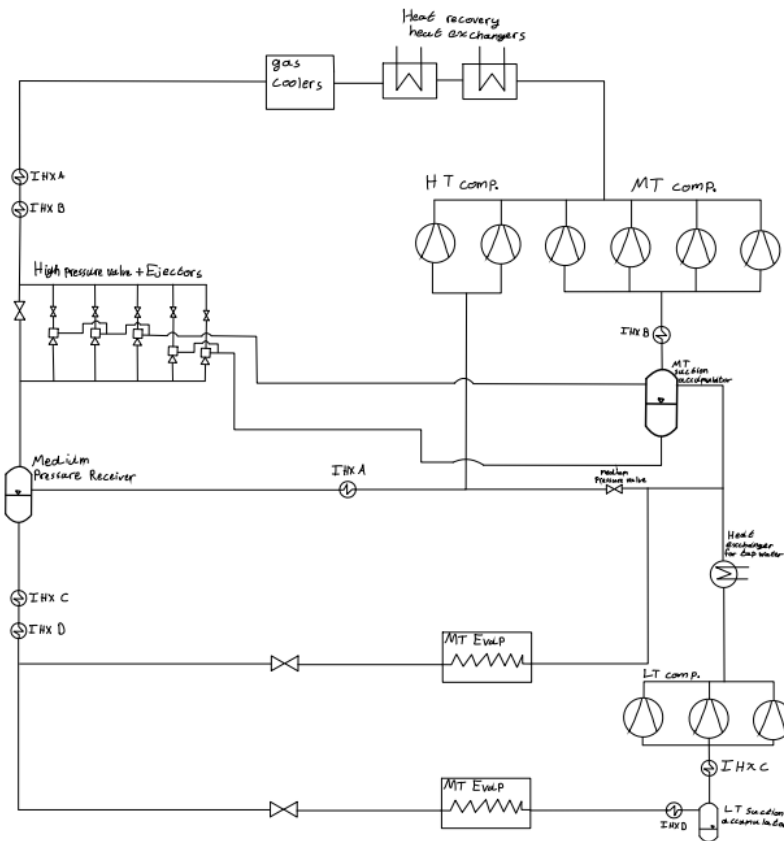
Figure 13: R744 multi-ejector system upgraded to the first multi-ejector system
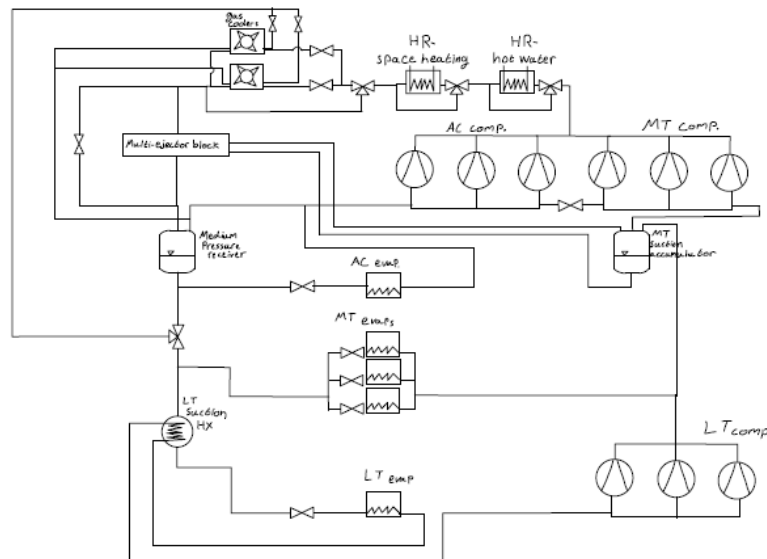
Figure 14: All in one R744 multi-ejector system, installed in Northern Italy

Cooling demands in the hot climate countries are significantly high as expected for both refrigeration and AC. With the increase of climate change and global warming, the environmental, economical and energetic effects are at utmost relevance. Since, the use of HFC refrigerants is most popular these days, since, CO_2 was not the most efficient refrigerant to use at the start before the technological advancements. It is only recently that emerging countries have been starting

16

to transition to environmentally friendly refrigerants. In fact, the first CO_2 system to be installed in the Middle-East was installed in 2018 in Jordan with the help of Abdin Industries, Enex and LU-VE. In a 2000m² supermarket. This system served as a benchmark for all emerging R744 system.

Ejector technology was also able to push the CO_2 equator down south, to enable the use of R744 systems to be much more efficient in high ambient temperatures, where the system will be run in transcritical mode almost all year round due to the fact of the low critical temperature of R744 at only 31.1^OC.

Figure 15 shows a strong R744 solution for hot climate areas to be installed in commercial supermarkets. This solution integrates the use of (1) two multi-ejector systems for both AC and refrigeration loads, (2) use of MT and LT overfed evaporators, (3) exterior heat exchanger which is used as an extra evaporator for recovering heat during heating mode and as a gas cooler during AC mode, (4) auxiliary heat sink up stream of the multi-ejector block to cool down the refrigerant and finally (6) integration of ice-water evaporators that are connected with the AC multi-ejector block. Done to increase the suction pressure of parallel compressor. Hence, decreasing the pressure ratio and increasing the isentropic efficiency of the compressor.
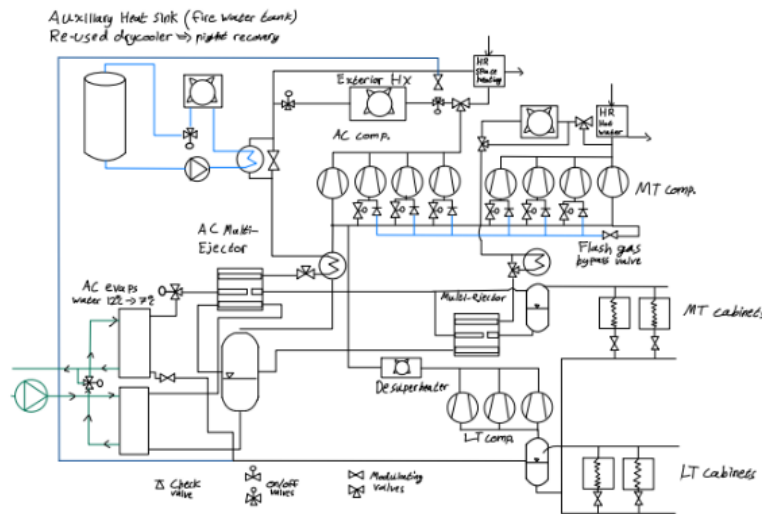
Figure 15: All in one R744 multi-ejector system for hot climates

Both all in one systems in figures 14 & 15, adopt the technology of pivoting principle. Which is a technique that is based on a wide interchangeability of the MT and AC compressors, where as can be seen in the figures; the compressors are joined together through their suction inlets by employing on/off valves up stream of their inlet, this technology was recommended by Krzysztof Banasiak et al. 2015; Hafner 2017; Hafner, Fredslund et al. 2015; Minetto, Girotto, Rossetti et al. 2015; Pardiñas et al. 2018. Based on Pardiñas et al. 2018, the pivoting principle will give the system great flexibility when it comes to achieving the actual system load profile, which can also mean less number of compressors in a system. Hafner 2017 added that the pivoting principle will create a gap free control of the refrigeration load, as well as lowering the cost of installation and increasing the compactness of the system.

Studies performed by Singh, Krzysztof Banasiak et al. 2018; Singh, Armin Hafner et al. 2018; Singh, Reddy et al. 2018 showed that (1) R744 ejector supported system will offer stable performances at high ambient conditions, (2) it also showed that a R744 system at operating conditions of AC evaporator temperatures from 7 to 11 degrees Celsius, MT and LT evaporation temperatures of -6 and -29 degrees Celsius respectively, and gas cooler outlet temperatures from 36 to 46 degrees Celsius with an intermediate pressure of 44 bar, the system can achieve a max total COP of 4.2, a max cooling COP of 2 and an exergy efficiency of 0.315 at 46 degrees. Where having the intermediate pressure at 44 to 48 bar will lead to a 10.7% reduction of parallel compression

consumption, the use of liquid ejectors will increase the MT evaporation pressure by 45% and decrease the compressor power requirement by 5.5%.(3) A R744 multi-ejector heat pump system in Indian climate, can achieve a total COP between 7.2 and 4, with cooling COP being between 4 and 2 at gas cooler outlet temperatures from 36 to 46 ^{O}C and evaporating temperatures ranging from 7 to 9 ^{O}C.

Research completed by Armin Hafner, Försterling et al. 2014; Armin Hafner, Poppi et al. 2012 showed that R744 systems with parallel compression as seen in figure 12, will result in approximately 11% energy savings when compared to the conventional booster system seen figure 1. Moreover, system in figure 12 proved to increase the COP by 17%, 16% and 5% in Athens, Frankfurt and Trondheim respectively during summertime, and during the winter time they showed an increase of COP between 20 to 30% when compared to the conventional booster system. The addition of a multi-ejector decreases the energy consumption further by 22.5% when compared to the first generation booster system as presented by Minetto, Girotto, Salvatore et al. 2014. Girotto 2017, also presented the yearly energy consumption reductions between a simple booster, booster with parallel compression, booster with liquid ejector, booster with parallel compression and liquid ejector, booster with parallel, liquid and vapor ejectors systems seen in figure 16. This shows how far technological advancements came through since the first generation booster system.
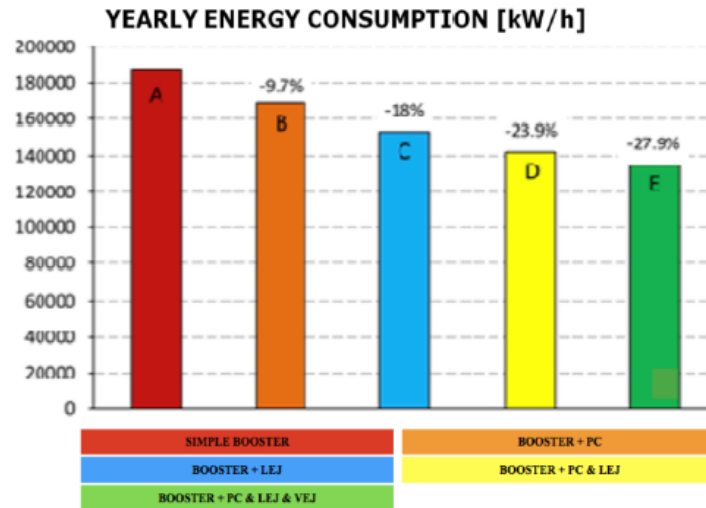
Figure 16: Energy Savings comparison between different booster systems in comparison to the first generation booster system Girotto 2017

2.3.4   Dedicated Mechanical Sub-Cooling

Another method to sufficiently increase the efficiency of a refrigeration systems in hot ambient conditions; is decreasing the vapor fraction of the refrigerant entering the evaporator. Which in return, increases the cooling effect. This is achieved by the use of a dedicated mechanical subcooling circuit(shown in figure 17). The use of such technology will not only increase the available cooling capacity of the evaporator, but it will also cause a decrease of the discharge pressure. Hence, decreasing the power required to run the compressor.
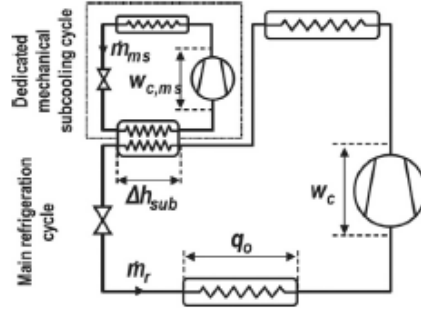
Figure 17: Mechanical subcooler Llopis et al. 2015

A dedicated mechanical subcooling circuit, is simply a self contained vapor compression refrigeration unit placed downstream of the gas cooler. Hence, it will be used to cool down the CO_2 refrigerant leaving the gas cooler. This is achieved by vaporizing the secondary refrigerant (usually propane) in the auxiliary circuit through a plate heat exchanger. This was proved by Gullo, Elmegaard et al. 2016, where an average reduction by 64% of the vapor fraction of R744 entering the high pressure valve in transcritical mode. Which led to an increase in the cooling effect and higher overall energy efficiency. Moreover, Gullo, Elmegaard et al. 2016 ensured that the use of the mechanical subcooler circuit will drop the optimal high side pressure (discussed in section 2.5.1) to a lower value at high ambient conditions, which will decrease the pressure ratio hence a decrease of the power required for compression.

Mazzola et al. 2016 took it a step further and compared three different subcooling technologies and derived their advantageous. The technologies were comprised of a dedicated chiller which was used as a mechanical subcooler, a water and CO_2 subcooler which integrated the CO_2 refrigeration system with the air conditioning unit, and the use of ground water so subcooling. The tests were run at ambient temperatures from 40 to 48^OC and the energy saving of the mentioned systems were compared to that of a conventional booster system. The results showed a 25, 36 and 30% increased energy savings respectively.

Moreover, Sánchez et al. 2016 was able to experimentally prove that the use of a dedicated R290 mechanical subcooler increased the cooling capacity and COP of the system by 27.2 to 42.8% and between 5.1 to 19.3% respectively. When compared to the increase of cooling capacity and COP of a suction internal heat exchanger which results in an increase of 1.9 to 11.7% in cooling capacity and 0.8 to 12.2% in COP.

It is also important to mention that the use of a mechanical subcooler also comes with its drawbacks as suggested by Girotto 2017. First the high investment cost, increase in complexity of the system as well as the complicated control strategy that comes with it. Moreover, depending on the auxiliary refrigerant used there would be a risk of flammability, chemical reaction and toxicity. Finally it will increase the difficulty of performing heat recovery such as water or space heating.

2.3.5   Double Stage Evaporation

The setup shown in figure 18 represents a gravity fed evaporator loop on one side (right side) of a plate heat exchanger, explained previously in section 2.3.2, and on the other of the plate heat exchanger is an ejector dependant evaporator circulation loop used in a CO_2 heat pump. Both stages of the heat exchangers are joined together in a sandwiched pattern. The use of such configuration; allows a larger temperate differences with less piping work and space required. This makes the system much more compact when compared to the previous heat exchanger models.

The investigation done by HAFNER et al. 2022 proved that the use of an ejector assisted double stage evaporation setup, will allow an increase in the compression suction level. Hence, improving the overall COP of the system. The working principle of the systems is as follows; first thing to note is that the secondary fluid passage is internally connected between both heat exchangers where

it first passes through the gravity fed evaporator then through the ejector assisted evaporator. It is important to note that the gravity fed evaporator operates on the separator pressure which equals to the compressor suction pressure. Whereas, the ejector supported evaporator flow rate and operating pressure, is based on the suction pressure of the ejector. Which is determined by the available expansion work and efficiency of ejector. This makes it possible to have a pressure difference of 5-10bar between the two stages.

Figure 18: Double stage evaporation system with gravity fed setup HAFNER et al. 2022

In the gravity fed evaporator the refrigerant flows back directly to the separator, where the ejector assisted evaporator returns to the suction nozzle of the ejector with a flow rate that is 50% lower than the motive flow rate. Then as explained in 2.3.3 the mixed refrigerant enters the separator, where the vapor and liquid refrigerant are separated and the liquid refrigerant is utilized by the evaporators, and the vapor is drawn by the compressor. After compression it is sent via the heat recovery circuits and gas cooler, then to the motive nozzle as seen in figure 18.

From figure 19a shows that the cooling capacity of the gravity fed evaporator is more affected by the change of water inlet temperatures, than it is by the water flow rates. As the water inlet temperature increases, the cooling capacity increases significantly unlike the increase of water flow rates which increased the capacity a little bit only. On the other hand, the cooling capacity of the ejector assisted evaporator increases significantly with the increase of water flow rate as well as the increase of the inlet water temperature which has a lesser effect seen in figure 19b. Hence, it can be determined that the ejector assisted evaporator's performance is directly affected by the performance of the gravity-fed evaporator.

This can be explained by the fact that as water inlet temperature increases the approach temperature for the gravity fed evaporator increases in return. This increases the cooling capacity as seen in figure 19a, and with low water flow rate then the temperature of water is going to decrease alot over the gravity fed evaporator, hence the approach temperature of water in the ejector assisted evaporator is going to be low, causing the cooling capacity of the ejector assisted evaporator to be low at small water flow rates. Hence, with the increase of the water flow rate the approach temperature in the ejector assisted evaporator is going to increase which means the cooling capacity of the evaporator is going to increase significantly as seen in figure 19b.

As presented by HAFNER et al. 2022, the pressure lift in the ejector was 4 bar at all operating conditions, this means that the pressure over the gravity fed evaporator is either 42 or 45 bar, as

seen in figure 20. Of course the cooling capacity at a lower evaporation pressure is higher than that when operating at a higher evaporation pressure. Due to the fact that, a refrigerant with a lower evaporating pressure has a lower evaporating temperature leading for a higher amount of cooling. This is also directly affected by the water inlet temperature as discussed earlier. As seen in figure 20a the cooling capacity increases significantly as the water inlet temperature increases then it reaches a plateau. This is due to, the shape of the isotherm when close to the saturated vapor state HAFNER et al. 2022. This affect the cooling capacity over the ejector assisted evaporator, seen in figure 20b, as explained earlier with the approach temperatures, the larger the temperature difference at inlet the higher the cooling capacity.
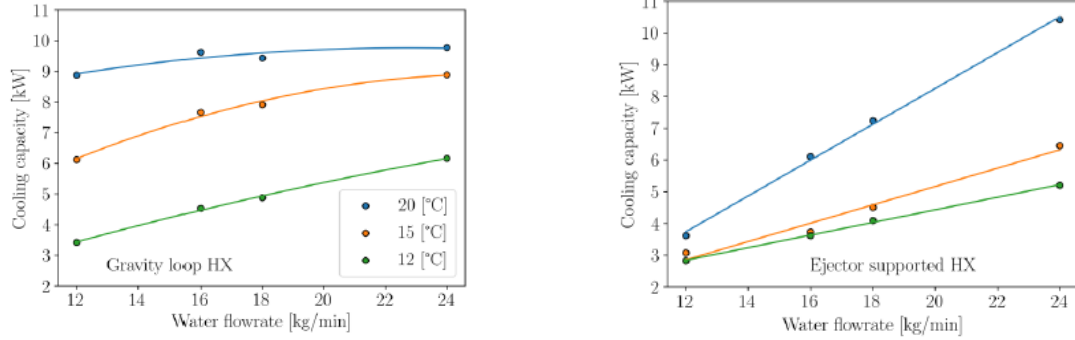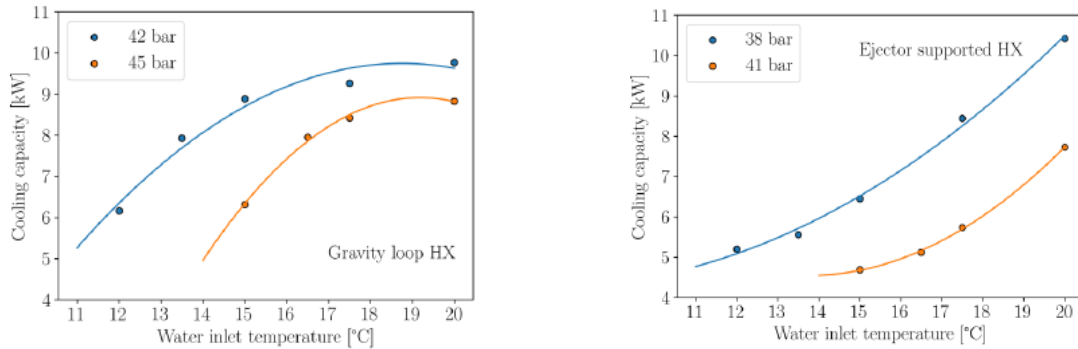

(a) Effect of water flowartes at different water inlet temperatures on cooling capacity of gravity fed evaporator HAFNER et al. 2022

(b) Effect of water flowartes at different water inlet temperatures on cooling capacity of ejector assisted evaporator HAFNER et al. 2022

Figure 19: Effect of water flowartes at different water inlet temperatures on cooling capacity of both evaporators HAFNER et al. 2022

(a) Effect of different water inlet temperatures on gravity fed evaporator cooling capacity at different operating pressures HAFNER et al. 2022

(b) Effect of different water inlet temperatures on ejector assisted evaporator cooling capacity at different operating pressures HAFNER et al. 2022

Figure 20: Effect of water inlet temperatures at different operating pressures on either of evaporators HAFNER et al. 2022

2.4   Thermal Energy Storage (TES)

Thermal energy storage is a technique that has been widely used since the beginning of time and been in development ever since. Basically, it is a technology that stores thermal energy by heating or cooling of a storage medium so that it can be used at a later time. TES, is very important to reduce energy consumption by storing heat that is normally wasted, or using the HP for heating or chilling during off peak hours. Hence, it can reshape electricity patterns that is used for heating or cooling. There are two main types of thermal energy storage sensible and latent heat storage. The types of TES can be seen in figure 21.
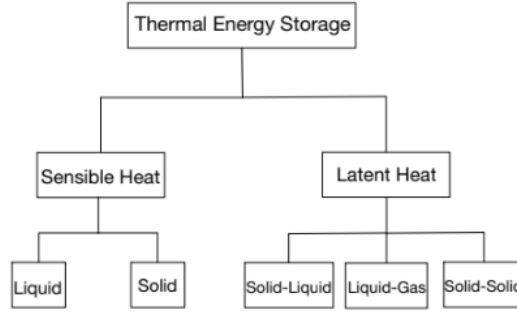
Figure 21: Thermal energy storage types

Heat and Cool storage systems can be applied in all most all types of buildings, where heating or cooling demands are significant, and electricity prices are high during peak hours making TES systems more favorable than conventional systems. Which will reduce the peak electrical demands by shifting the time of operation throughout the day.

2.4.1   Sensible Heat Storage

Sensible heat storage systems, is where the temperature of the storage material whether liquid or solid varies with the amount of energy stored SM Hasnain 1998a. Hence, it is effected by raising the temperature of the storage medium, as seen in figure 22 presented by Sarbu and Sebarchievici 2018. Therefore, it is of utmost importance that the storage medium has high specific heat capacity, stability over temperature cycling, compatibility with the heating/cooling refrigerant if direct contact is involved and finally a low cost. The sensible heat capacity can be calculated as seen in equation 6, where Q_s is the sensible heat capacity, m is the mass of the storage medium, c_p is the specific heat capacity of the storage medium, T_i and T_f are the initial and final temperatures of the storage medium respectively.
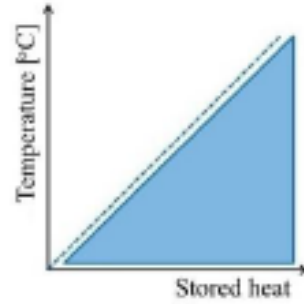
Figure 22: Sensible Heat Storage Sarbu and Sebarchievici 2018

$$Q_s = \int_{T_i}^{T_f} mc_p dt = mc_p(T_i - T_f) \tag{6}$$

Sensible heat storage can be split to two categories liquid (such as water, molten salts and oil based fluids) and solid (such as rocks and metals) medium temperatures. The liquid storage medium are much more used in these days as they are economically competitive. Water as a storage or transport medium is one of the best, as it has high specific heat capacities higher than any other liquid, available everywhere and cheap. However, water has a high vapor pressure, consequently this means that insulation costs will rack up as well as the need of materials that can withstand high pressure and temperatures are required.

22

When storing water maintaining thermal stratification in the tanks is very important, and this is achieved by using diffusers to eliminate the mixing between hot (top of the tank) and cold (bottom of the tank) water layers. These layers, hot on top and cold on bottom, is caused by the buoyancy forces. Stratification is important because; 1) it improves the efficiency of the system by delivering the heated/cooled water at the temperature it was collected rather than a higher/lower mixed storage temperature than required, depending if we are using the water for cooling or heating, 2) the amount of energy collected is easily increased if the tank's inlet temperature is lower/higher (based on operation) than the temperature of a mixed fluid.

In chilled water storage (CWS), the tank is charged with water from the bottom of the tank at low temperatures 4 to 6 degrees Celsius, and discharged from the bottom of the tank, with the return water entering from the top of the tank maintaining stratification. On the other hand, in hot water storage (HWS) water is charged at temperatures up to 90 degrees Celsius from the top of the tank, and discharged as well from the top of the tank, with the return water entering the bottom of the tank to maintain stratification. HWS system can be seen in figure 23. A cold water storage system would be similar to that of the HWS in figure 23 except that it would be connected to the evaporators rather than the gas coolers. In both systems the cooling or heating capacity will depend on the temperature difference over the stratified tanks, moreover both systems charging process will be during off-peak hours. This is usually during the night which not only favorable due to the low electricity prices, but also due to the low ambient temperatures which will improve the efficiency of heat rejection. The discharge process occurs at the highest thermal demand, which is during the day or the occupation time to accommodate the building requirements.

A lot of advantages arise from the use of CWS or HWS versus conventional systems, 1) the refrigeration plant heating and cooling capacity can be reduced since it is no longer operated during peak demands, 2) the plant will operate at a 100% of its rated capacity hence, no longer working in partial load throughout the charging process, hence, it will have the best efficiency, 3) the electricity load will be shifted during the night time, where electricity is cheaper than during the day due to the off peak hours.
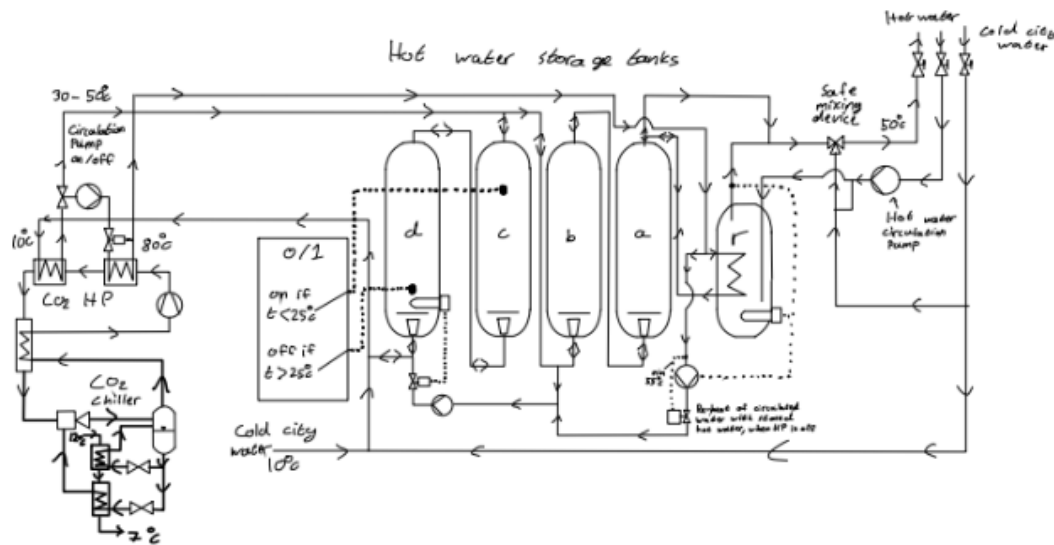
Figure 23: Hot water storage system

As discussed earlier other fluids can be used such as storage in salty water, or oil based fluids which are capable of reaching higher storing temperatures. Also the use of solid media is possible such as rocks, metals, concrete which have high thermal storage capabilities. Moreover, they can be stored at much higher or lower temperatures than water as they do not freeze nor boil. Hence, the drawbacks that arise from using water such as the high vapor pressure are eliminated. However, usually they are more costly than water, for example, the use of cast iron even though it has a higher energy density level than water storage Hasnain et al. 1996, it is much more expensive. So, the payback time is much longer. The use of such metals is justified when high thermal conductivity

is required and is primary and cost comes secondary.

2.4.2   Latent Heat Storage

Latent heat storage, is the storing of energy emitted by the storage medium when a phase change occurs (solid to liquid and vice versa, liquid to gas and vice versa, and solid to solid). Latent heat storage techniques are becoming more and more attractive, as they provide high energy storage and has the capacity to store heat through the latent heat of fusion at constant temperatures. This depends on the phase transition temperature of the storing medium SM Hasnain 1998a. Which can be seen in figure 24 (the blue area under the graph). The latent heat storage capacity can be calculated as seen in equations 7 and 8. Where t_m is the melting temperature, m is the mass of PCM medium, c_{ps} is the average specific heat of the solid phase between T_i and T_m, c_{pl} is the average specific heat of the liquid between T_m and T_f, f is the melt fraction, Δq is the latent heat of fusion Sarbu and Sebarchievici 2018.

One main advantage of latent heat storage over sensible heat storage is the fact much smaller weight and volume of a material is required to store energy. Due to the fact that, water for example, has 80 times more energy when melting 1kg of ice when compared to raising the temperature of 1kg of water by 1^OC. Liquid to gas phase change materials have high heat of transformations, however, they are usually looked down upon due to the fact that when the storing medium is in the gas phase it occupies large volume space, hence the use of solid to solid or solid to liquid is much more favorable.
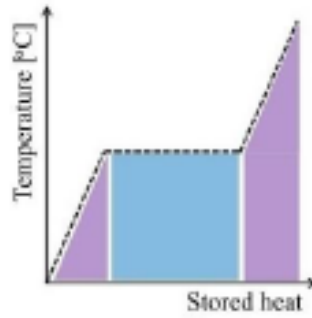
Figure 24: Latent Heat Storage Sarbu and Sebarchievici 2018

$$Q_s = \int_{T_i}^{T_m} mc_p dT + mf\Delta q + \int_{T_m}^{T_f} mc_p dT \tag{7}$$

$$Q_s = m[c_{ps}(T_m - T_i) + f\Delta q + c_{pl}(T_f - T_m)] \tag{8}$$

In a heat storage cycle, during the charging phase, a heated transport medium is circulated through tubes around the phase change material (PCM) which in return melts the PCM by storing the heat as both sensible and latent heat of fusion. During discharge phase when the heat is required, the circulation of a low temperature transport medium is used which would take the stored heat energy in the PCM and is then transported to cover the heat load. The same but opposite process takes places for cooling. Hence, in both methods the latent heat storage will use both the sensible heat in the solid and liquid phases as well as the latent heat due to the phase change at either melting or freezing SM Hasnain 1998a. PCMs can be categorized as inorganic compounds such as salt hydrates, organic compounds which are composed of paraffin's and non paraffin's such as water and eutectics of organic or inorganic compounds.

Ice storage systems are increasing in popularity, where water is used as a phase change storage medium. This is advantageous since water phase changes have high storage capacity. Due to, the latent heat of fusion either during the charging process; where water changes to ice. Or the discharging process; where ice melts to water SM Hasnain 1998b, such system can be seen in figure

25. The main working idea of the ice storage system is pretty simple. During the off-peak hours the system is operated to evaporate the refrigerant in water tank and the water around the coil will freeze. During the discharge process, the ice water is circulated to cool down a chilled water loop which is used to cool the incoming air in the building. The cooling capacity of the ice storage system, will depend on the rate at which ice is melted to water to satisfy the cooling requirements. Which is directly related to the heat of fusion available in the phase change of water.
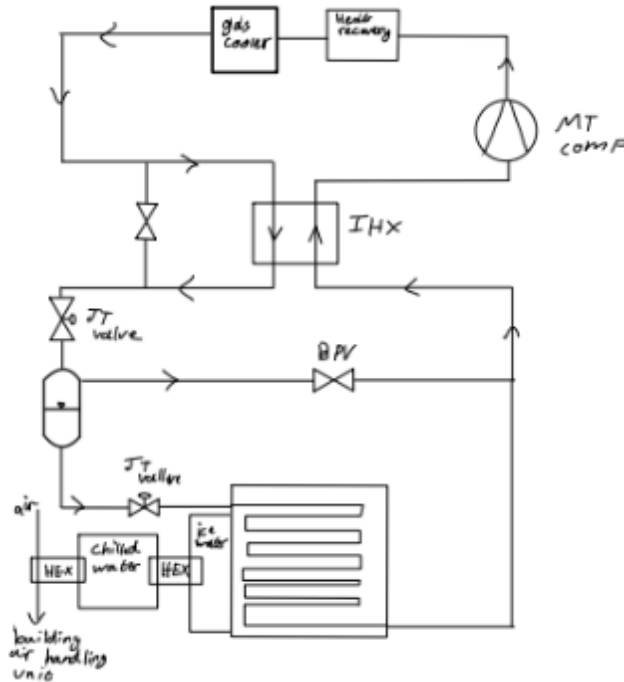
Figure 25: Latent Heat Ice Storage System

Some of the advantage of ice storage system over a chilled water system is; 1) the larger cooling capacity for a storage volume, 2) it requires less space making it more compact, 3)less thermal losses, 4) more reliable and easier design without many restrictions and 5) lower cost of maintenance SM Hasnain 1998b.

2.4.3   Operation Strategy

There are two main operating strategies that work for both the sensible and latent heat storage systems. 1)Full storage or 2)partial storage and is split into load leveling or demand limiting SM Hasnain 1998b. They simply mean, whether the storage will meat the full heat/cool load during peak hours as seen in figure 26 by SM Hasnain 1998b.
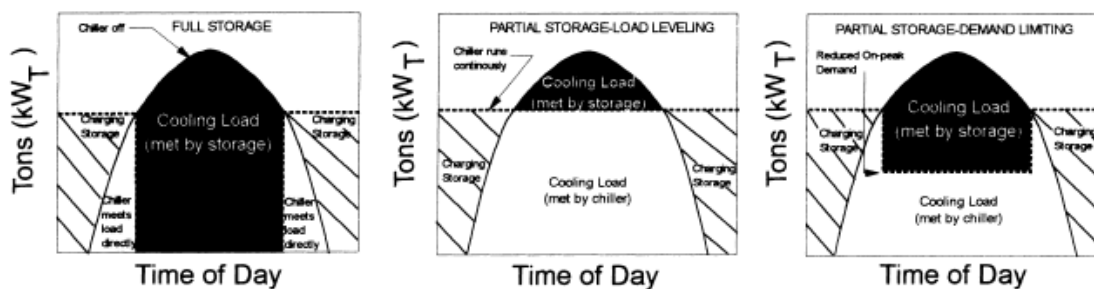
Figure 26: Operating strategies as presented by SM Hasnain 1998b

Full storage strategy, will minimize the cost of thermal load by shifting the operation time to off peak hours, while during on peak hours the TES system will cover the entirety of thermal demand, hence large refrigeration and storage capacities are required. This operation is favorable, when the on peak demand is significantly high or when the demand time is short similar to that of an office building where the occupation time is short.

On the other hand, partial storage operation will meet a portion of the peak thermal load via the storage and the rest is met through the operation of the heat pump or refrigeration system. In load leveling the system is designed to run the entire time 24hrs with a capacity that is lower than the peak demand capacity. The peak demand capacity will be met by the use of the storage system which will have the extra cooling/heating capacity required. Hence, allowing to downsize both the HP or refrigeration system as well as the storage capacity unit since the system will be running 24 hours. In demand limiting, the system is also run all day on full capacity except during max cooling/heating demand as can be seen in figure 26 (right side figure). Hence, the HP or refrigeration system will operate at partial capacity during the peak hours and the rest of the capacity will be met by the TES system. Such operation strategy is usually not used due to its high complication of control systems SM Hasnain 1998b.

2.5   Control Strategies

2.5.1   Optimal Heat Rejection Pressure

Theoretical

The cooling capacity and heat output of the system increases with the increase of pressure in the gas cooler and this can be seen in figure 27 as the gas cooler exit temperature (point b) is moved to the left. However, if the exit conditions from the gas cooler is close to the critical conditions then the process will have a significant low cooling capacity and COP. The relationship between pressure and temperature in the supercritical area is not clear, which makes the volume and amount of CO_2 in the gas cooler of utmost importance. Hence, to control the pressure in the gas cooler, adjusting the amount of CO_2 via the high pressure control valve will be required based on the operation requirements Eckert et al. 2022.

From figure 28 it is seen that a transcritical process has a higher cooling capacity when compared to the subcrtical operation at same temperatures. Similar to figure27, figure 28 also shows that in a transcritical operation close to critical conditions the cooling capacity drops significantly. Finally, as the temperature increase before the throttling valve the cooling capacity will drop as well due to the higher expansion losses.
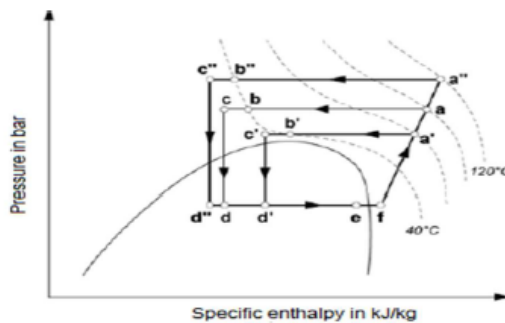
Figure 27: Effect of gas cooler pressure on cooling capacity Eckert et al. 2022
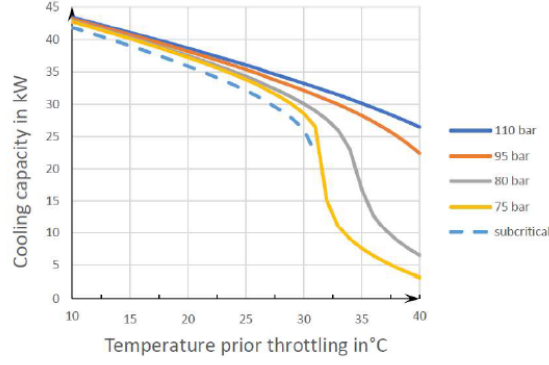
Figure 28: Change of cooling capacity depending on the temperature and pressure before throttling valve Eckert et al. 2022

As stated earlier as the pressure increases in transcritical operation the cooling capacity will increase, but also the compressor required work will increase as well, until the temperature curve is much steeper then the cooling capacity will start to decrease and the power required of the compressor will keep on increasing. This means that at a certain high pressure and above, the COP of the system will start to drop. Hence, for every operation conditions there will be an optimum high side pressure to give the max value of COP. This is seen in figures 29 a and b presented in Sawalha 2008 and book Eckert et al. 2022. It can be concluded that, operating at a higher pressure with subcooling is better than operating with low pressure without subcooling. Basically, reaching low refrigerant temperatures before expansion increases the effectiveness of the system. In figure 29a Sawalha 2008 presented the optimum pressure formula in the graph for the investigated system by connecting the point with max COP at different discharge pressures as a function of the ambient temperature. This is seen in equation 9 where $T_{gc,app}$ is the approach temperature as explained in section 2.5.2.
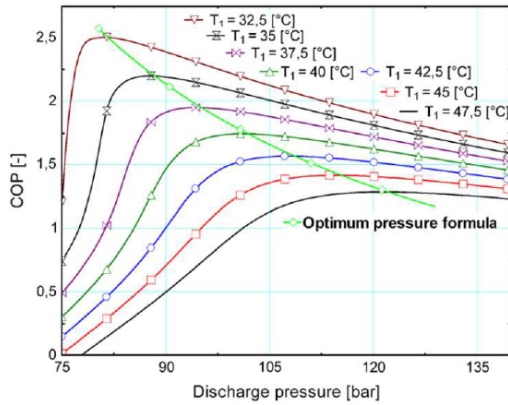
(a) Theoretical COP as a function of the discharge pressure with changing gas cooler outlet temperature Eckert et al. 2022; Sawalha 2008
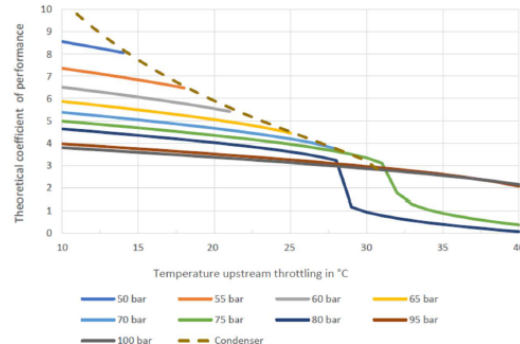
(b) Theoretical COP as a function of the gas cooler outlet temperature with changing gas cooler pressure Eckert et al. 2022

Figure 29: Effect of pressure and temperature of CO_2 in the high pressure side on the COP Eckert et al. 2022

$$P_{opt} = 2.7(T_{amb} + T_{gc,app}) - 6.1 \tag{9}$$

The main aim of controlling the pressure in the gas cooler is to have the most efficient system possible, which is achieved via a high side pressure control device (ejector or expansion valve).

In heat recovery case, where the cooling medium gas cooler inlet temperature is constant then the high side pressure can be fixed to one value, this pressure is decided based on the approach temperature and location of pinch point (explained in section 2.5.2). On the other hand, when the cooling medium temperature is varying, the pressure will be dependent on the temperature of CO_2 in the gas cooler according to the pressure temperature curve which can be seen in figure 30. This is accomplished via an electronic controller and a motor operated throttle device.

To further explain this strategy, in subcritical mode the high side pressure is controlled through the amount of subcooling, in the transcritical mode, the pressure will be controlled as explained earlier in figure 29a. The connection that occurs between transcritical and subcritical as seen in figure 30 occurs below the critical point and in transition the subcooling is increased with the increase of pressure. Other control strategies are, control of gas cooler fan (for example, decrease fan speed when less cooling demand is required), control of airflow. Another method, is the use of the heating system in heat recovery to send signals to control the pressure Eckert et al. 2022.
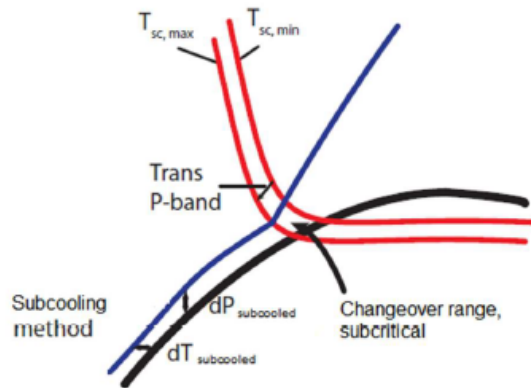
Figure 30: Controller characteristic for optimal gas cooler pressure Eckert et al. 2022

Experimental

Trough experimental work Cabello et al. 2008, investigated the effect of gas cooler pressure, and CO_2 temperature before throttling on the COP, cooling capacity, mass flow rate and compressor power. The investigated system was a single stage CO_2 refrigeration plant. Figure 31, presents the experimental data for the listed parameters, at evaporating and gas cooler outlet temperatures of -10 ^{O}C and 40.2 ^{O}C. It can be observed that the mass flow rate and the power consumption have a linear relationship with the varying of the discharge pressure. While the cooling capacity significantly drops at low discharge pressures. Figure 32 presents the values of COP at three different evaporating pressures at varying gas cooler outlet temperatures and wide range of discharge pressures. As discussed earlier, the optimal gas cooler pressure depends on the gas cooler outlet temperature, where the optimal discharge pressure is increased if the refrigerant outlet temperature also increase.

From figure 32a, b and c it is observed that the optimum pressure value also depends on the evaporating temperature, the lower the evaporating temperature the higher the optimal discharge pressure is going to be Cabello et al. 2008. As stated by Cabello et al. 2008, a high decrease in COP occurred when the outlet temperature of the gas cooler was close to the critical temperature of CO_2 which is 31.1 ^{O}C, as well as when the gas cooler pressure was below the optimal point.
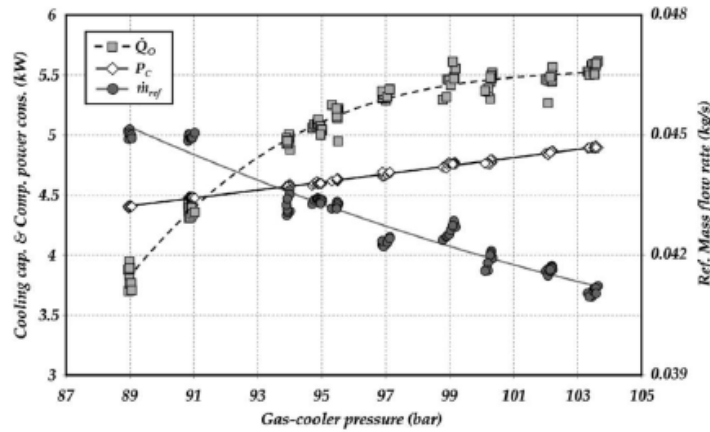
Figure 31: Compressor power consumption, mass flow rate, and cooling capacity at constant evaporating and gas cooler outlet temperatures while varying the discharge pressure Cabello et al. 2008
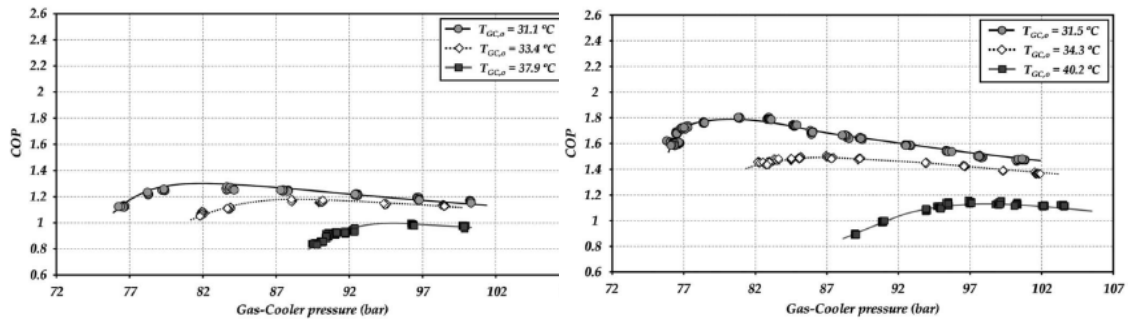
(a) COP at evaporating temperature of -18.1 ^{O}C Cabello et al. 2008

(b) COP at evaporating temperature of -10.1 ^{O}C Cabello et al. 2008
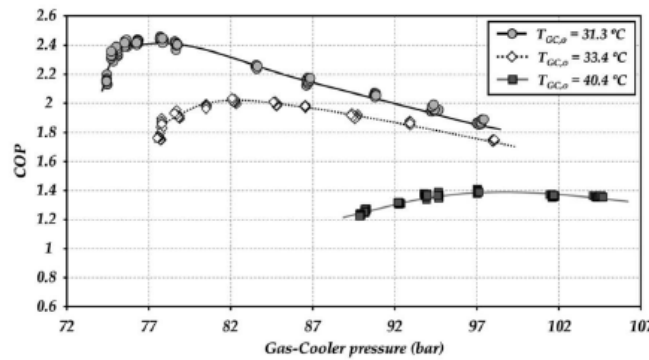
(c) COP at evaporating temperature of -0.9 ^{O}C Cabello et al. 2008

Figure 32: Effect of different gas cooler pressures at varying evaporation and gas cooler outlet temperatures Cabello et al. 2008

Elbel and Hrnjak 2008 investigated the effect of different gas cooler pressures with varying internal heat exchanger efficiencies, on the COP and cooling capacity between an ejector technology and expansion valve technology. The graphs in figure 33 were gathered at an ambient temperature of 45 ^{O}C, indoor temperature of 27 ^{O}C at 30% relative humidity. Figure 33c, was developed so the systems had a constant cooling capacity. Achieved by varying the compressor frequency. It can be

29

noticed that between 11 and 12 bar the COP curves reach their maximum value for both systems, the ejector and expansion valve. When the IHX effectiveness is constant whether in the ejector or expansion valve system, the max COP occurred at approximately the same value of discharge pressure. In both cases of IHX effectiveness the ejector system will have a higher COP than the expansion valve system regardless of its IHX effectiveness. IHX effectiveness in Elbel and Hrnjak 2008 was calculated as seen in equation 10.

$$\varepsilon_{IHX} = \frac{\dot{Q}_{act}}{C_{min} \cdot \Delta T_{max}} \tag{10}$$

33 a & b shows the cooling capacity and COP as a function of the discharge pressure experimentally, which are in accordance with the prediction from 33c, and can be maximised by optimising the discharge pressure. The experiment also proved that the ejector in collaboration with the highest efficiency of an IHX will provide the highest COP and cooling capacity Elbel and Hrnjak 2008.
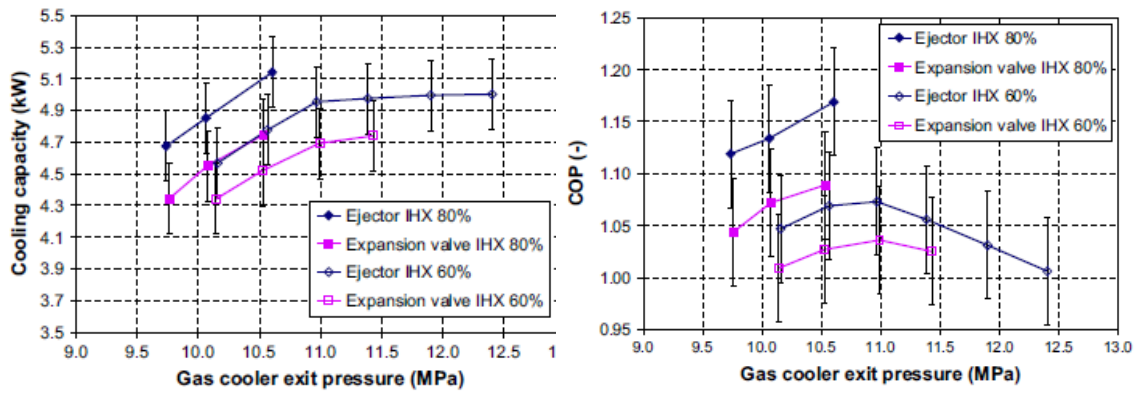
(a) Experimental cooling capacity of R744 ejector and expansion valve systems as a function of discharge pressure at varying IHX effectiveness Elbel and Hrnjak 2008.

(b) Experimental COP of R744 ejector and expansion valve systems as a function of discharge pressure at varying IHX effectiveness Elbel and Hrnjak 2008.
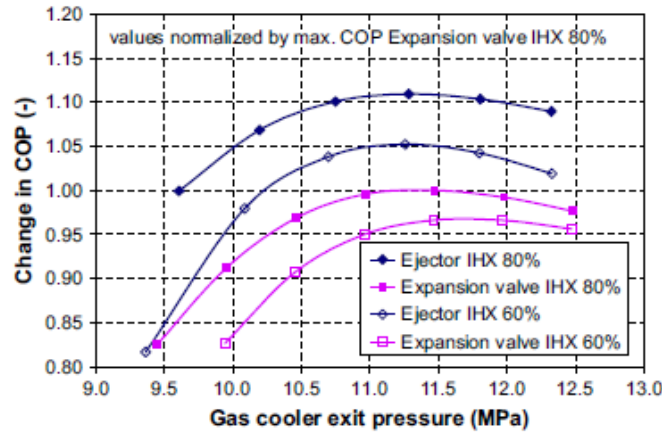
(c) Predicted discharge pressure optimization for maximum COP at different IHX effectiveness Elbel and Hrnjak 2008.

Figure 33: Effect of different gas cooler pressures at varying IHX effectiveness on COP and cooling capacity Elbel and Hrnjak 2008

2.5.2   Heat Recovery

Heat recovery is the utilization of waste heat, usually rejected to the ambient, for heating processes such as heating water, space heating and snow melting, as seen in figure 34. The snow melting circuit (3rd circuit) could be used for preheating water, from low to medium temperature and the first hot water circuit would be used for reheating to higher temperatures.
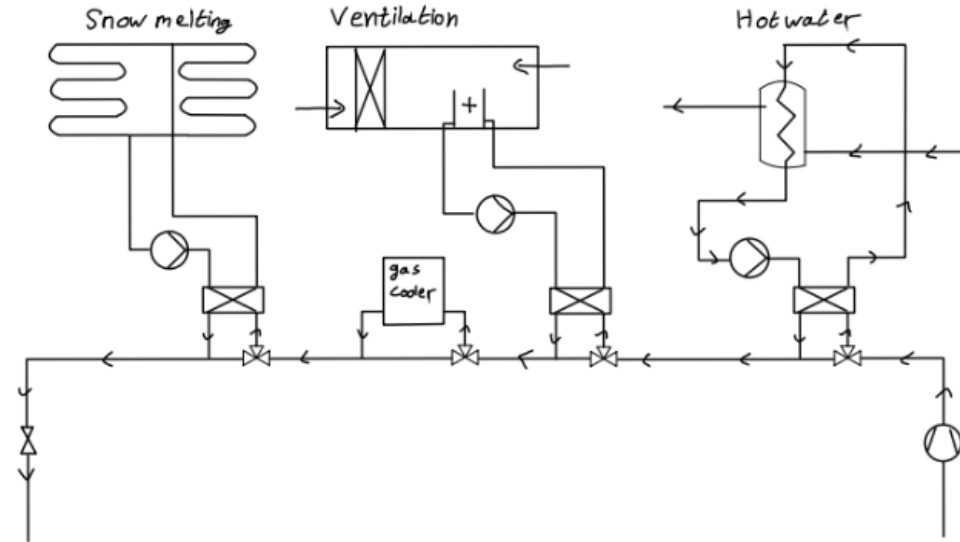
Figure 34: High side pressure with heat recovery circuits

Optimizing the system for the optimal discharge pressure for the highest efficiency with heat recovery, the pinch point and approach temperatures must be discussed. The pinch point is the smallest temperature difference between the refrigerant and the cooling media. The pinch point can be at the inlet of gas cooler, the outlet of gas cooler or in between. At high discharge pressures it is best to have the pinch point at the outlet of the gas cooler (the cold end). The position of the pinch point over a gas cooler can be affected by the size of the gas cooler, discharge pressure and the mass flow of the cooling medium. The higher the mass flow is, the smaller the slope of the heating curve which in return increases the chance that the pinch point is going to be at the cold end of the gas cooler. This can be checked by developing a temperature curve similar to the one seen in figure 35.

As previously mentioned, it is of utmost importance for the refrigerant temperature to be as low as possible before expansion. By using heat recovery this is possible to achieve, because of the temperature glide in CO_2 is easily utilized. Hence, at the outlet of the gas cooler the CO_2 can reach temperatures very close to that of the inlet cooling media temperature. Which justifies the importance for the cooling media to have as low temperature as possible, as long as the discharge pressure and gas cooler sizing are designed properly. The temperature difference between the temperature of CO_2 at outlet and the inlet cooling media temperature is called the designated temperature approach (Δt_A). This will measure how well the system is adapted for the transcritical mode Eckert et al. 2022. The lower the temperature approach value the more efficient the system is, it is designed to be $\Delta t_A = 1$ to 4 K.
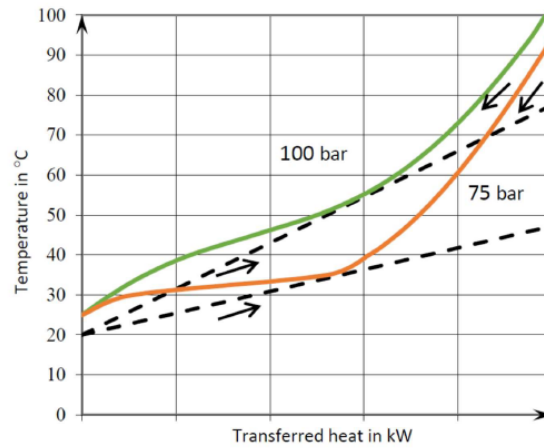
Figure 35: Temperature curve with pinch effect at different discharge pressures and cooling media flow rates Eckert et al. 2022.

Figure 36a represents a temperature curve in a gas cooler for heating water. The discharge pressure is somewhat low at 85bar, as a consequence the pinch point is located in the middle of the heat exchnager. Hence, the temperature difference at the outlet will be limited, even though the water inlet temperature is 5 ^{O}C, the outlet temperature of CO_2 is 32 ^{O}C. This means that (Δt_A) is high(27K). Meaning, high throttle losses, low cooling capacity and low COP. In the same conditions of the cooling media but with an increase in the discharge pressure to 100bar, the operation will become much more efficient as seen in figure 36b where the (Δt_A) is now low at 3K and the pinch point is now at the outlet of the heat exchanger, in this case the COP of the system is much higher than the first case. As seen in figure 36c the discharge pressure directly affects the (Δt_A), hence when designing the system the high side pressure could be controlled based on the approach temperature, where the pressure increases when the system reads that the approach temperature is increasing in the case of cooling media temperature is not always constant.
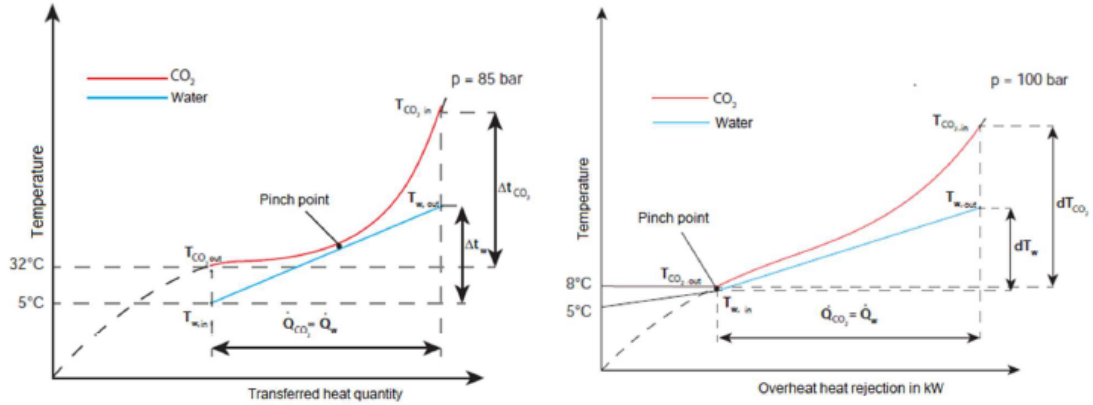
(a) Low discharge pressure affect on pinch point Eckert et al. 2022.

(b) High discharge pressure affect on pinch point Eckert et al. 2022.
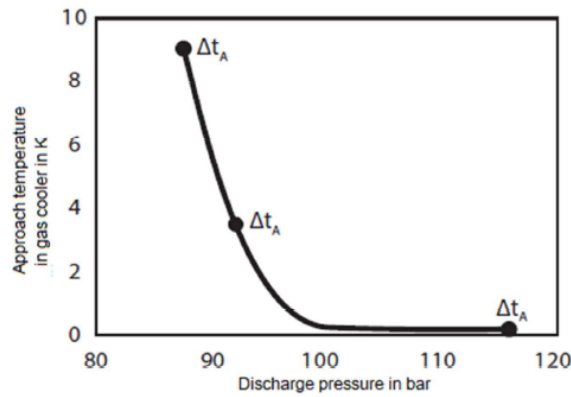
(c) Dependency of approach temperature on the discharge pressure Eckert et al. 2022.

Figure 36: Approach temperatures, pinch point locations based on discharge pressure Eckert et al. 2022.

In the case where heat recovery is applied on multiple temperature levels as seen in figure 34. Three gas coolers placed in series and for example in the coldest gas cooler (left gas cooler) water is preheated to about 30 degrees Celsius and then sent to the hottest gas cooler (first one on the right) to heat the water up to 70 degrees Celsius, while the middle gas cooler is utilized to for space heating the temperature curve will look like in figure 37. Such configuration can be challenging to design, however if designed correctly based on the explanations in section 2.5 the all in one or heat pump system will have high operating efficiencies and COP Eckert et al. 2022.
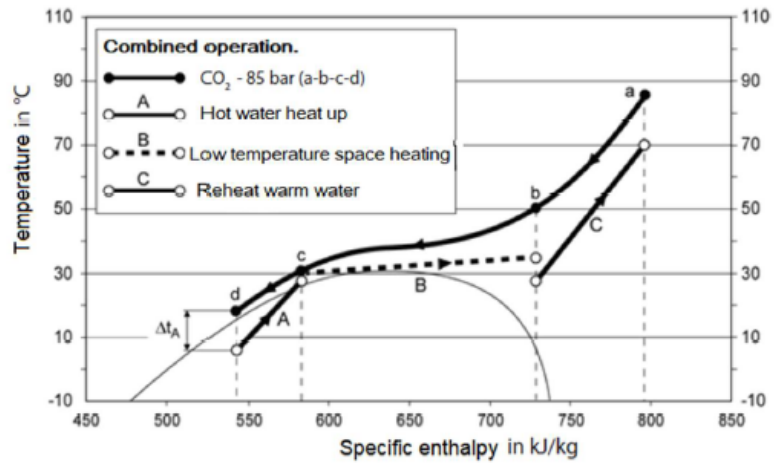
Figure 37: Heat recovery at three different temperature levels Eckert et al. 2022.

3   System Design

3.1   System Description

The heat pump system was designed to supply a hotel in Goa, India with domestic hot water for its visitors, as well as cooling for air conditioning use. The entire system can be seen in figure 38. The heat pump system working fluid is CO_2, whereas the secondary fluid is water for both hot and cold loops. CO_2 as working fluid was chosen for the fact that its properties allows for large temperature glide on the water side, which enables the heat pump to lift the temperature of cold city water at around 25 to 30 degrees Celsius up to 70 degrees which is the set point for this system on the hot water side, whereas on the cold water side decrease the temperature from 12 degrees Celsius down to 7 degrees Celsius. Large temperature glides as was discussed in the chapter 2.5.2 will increase the overall energy efficiency of the system. Water was used as a heat source over the evaporators to achieve the cooling demands of the building due to its low cost and wide availability in all countries as the proposed system is highly adaptable to all regions and can be used as a standard system for building applications in the future. The following subsections 3.2.1-3.2.3 are going to dissect each section of the entire system to further describe its operation modes and control strategies.
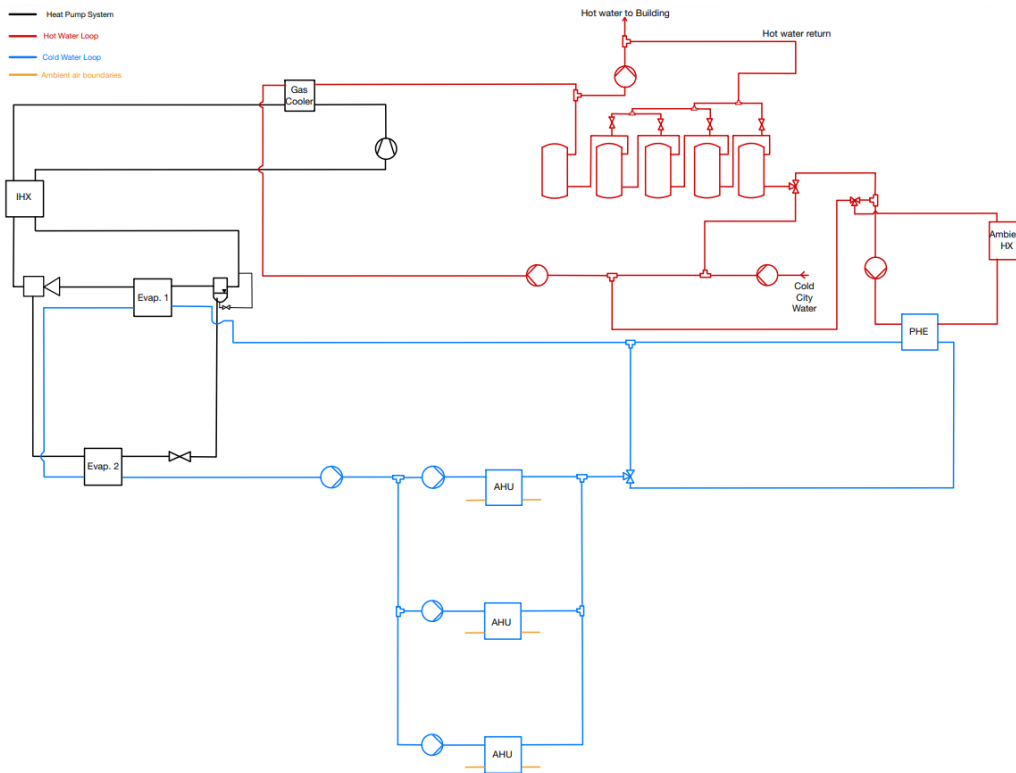
Figure 38: Heat Pump system with hot and cold water loops

3.2   Operation Modes and Control Strategies

3.2.1   CO$_2$ Heat Pump System

The CO_2 heat pump consists of inverter compressor, meaning that the its frequency can be controlled to achieve the required capacity of the system. In the model only one compressor can be seen however, in real life system another on/off compressor can be added, to work during peak hours to supply extra capacity required. Hence, the main compressor can operate at its design

point for higher efficiencies. The compressor frequency is controlled via a PI controller which is directly linked to the exit temperature of the water after the second evaporator. This is done to achieve the required cooling capacity to bring the water temperature to 7°C which is the setpoint. An oil return separator would be placed after the compressor to separate the oil from the CO_2 after compression and return it to the suction line of the compressor. This cannot be seen in the schematic diagram as it was not added to the model in modelica as can be seen in the upcoming chapter 4. It is then followed with the gas cooler, which is used as a heat sink device to supply heat for the cold city water and lift its temperature to 70 ^{O}C for domestic use. An important addition to the system is the internal heat exchanger (IHX) to further cool the CO_2 before expansion, as well as superheat the CO_2 in the suction line of the compressor to ensure no liquid CO_2 return to the compressor. By further cooling the CO_2 via the IHX before expansion will result in a larger cooling capacity hence, a higher COP and less expansion losses.

In addition, the expansion device used is a multi-ejector, which is used to control the high pressure side of the system at 100 bar to achieve the pinch point at the end of the gas cooler. To use the entire area of the gas cooler in return increase the system's efficiencies, this was further explained in chapter 2.5. Moreover, via the suction nozzle of the ejector, the pressure of the CO_2 over the second evaporator (low pressure) will be lifted to the pressure of the liquid receiver, hence free work recovery which reduces the expansion losses, as explained in sub-section 2.3.3. The ejector's discharge nozzle is then connected to the first evaporator in the modeled case, the reason for this is discussed in section 4.2. However, in the real system it would be directly connected to the liquid separator, and the first evaporator will operate in gravity fed operation, as discussed in section 2.3.2.
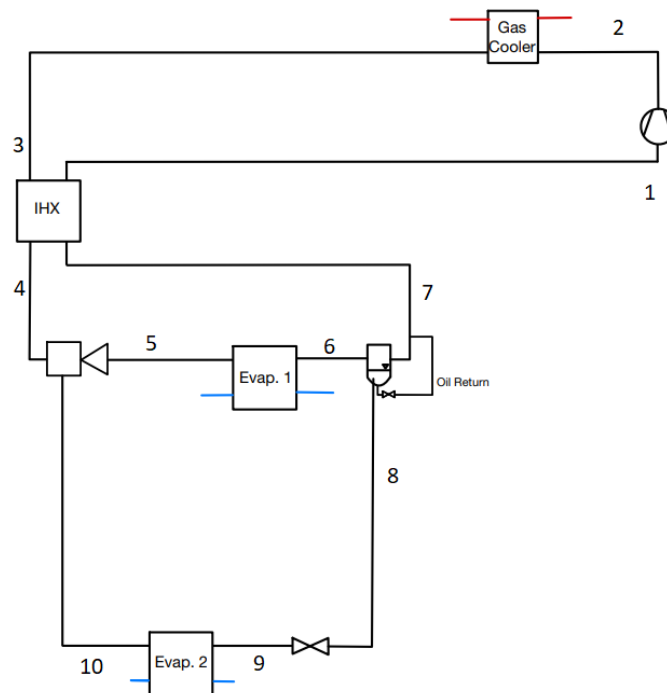
Figure 39: CO_2 Heat Pump system

The liquid separator aims to separate the liquid CO_2 from the vapor CO_2, where the liquid CO_2 is sent to the expansion valve to further expand the CO_2, which will flow through the second evaporator for the second stage cooling, whereas the vapor CO_2 is sucked by the compressor via the suction line. In gravity fed operation, where the first stage evaporation will take place. The liquid CO_2 will be supplied via the separator to achieve natural circulation for flooded evaporation as discussed in section 2.3.2. Moreover, the separator serves as a storage tank for the CO_2 during stand-still conditions hence, it should be sized to be able to host the entire CO_2 charge. The separator will also be used to charge the system with CO_2, until the pressure in the system is over the triple point pressure. In the bottom of the liquid receiver, is an oil return line to the suction line

of the compressor as seen in figure 39. The expansion valve prior to the second stage evaporation controls the quality/vapor fraction of the CO_2 at the outlet of the evaporator, to ensure flooded evaporation for all its benefits as presented earlier in section 2.3.2.

3.2.2 Hot Water Loop

The hot water loop seen in figure 40 consists of 4 controlled water pumps, where pump number 1 mass flow rate is equal to the hot water demand by the building. This pump is what controls the amount of cold city water entering the loop. Whereas, pump number 2 is controlled so that the exit temperature of the water after the gas cooler is equal to the setpoint temperature. Pump number 3 is what sends the hot water to the building and its mass flow rate is equal to the building demand plus a constant small demand. This simulates the fact that there will always be hot water in the hotel's piping system hence, the last room of the corridor will not require to wait a long time before hot water reaches the room. Pump number 4 controls the mass flow rate in the extended loop, based on the active operation which will be seen later on. The hot water loop also consists of 5 hot water tanks each with a capacity of 4000L. These tanks are used to supply the hot water demand during peak hours when the hot water production is not enough to meet the demand. As can be seen in figure 40, the water returned from the building has 4 different valve entry points to the tanks, the valve opens depending on the water return temperature to maintain stratification within the tanks. This will be explained further in this section. Finally the extended loop and one of the novelties of this system, serves to keep the system running in case, there is not enough hot water demand, and available cooling demands when the tanks are fully charged. Or, when there is not enough cold water demand, and the exit temperature of water from the air handling units (AHU) is low while there is hot water demand. This will be explained further when talking about the different operations.
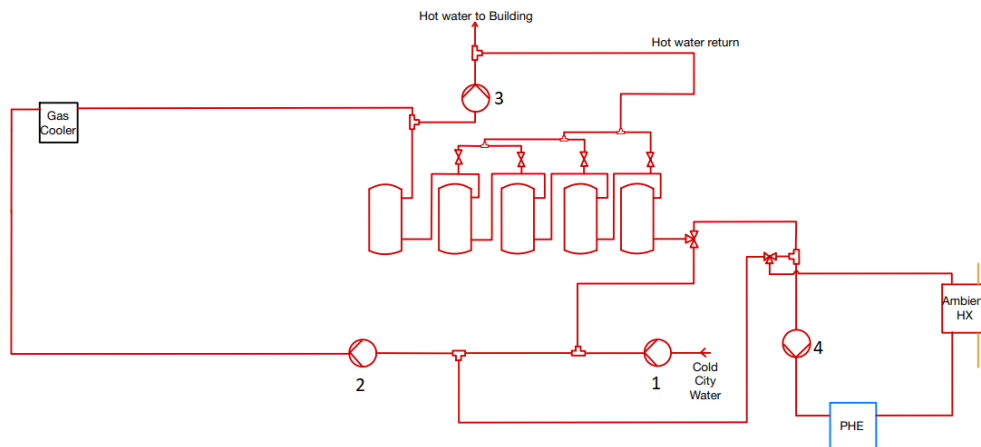
Figure 40: Hot Water Loop

For the hot water loop, there are three different possible operations as can be seen in figure 41. During the charging process in figure 41a, the hot water demand by the building is less than the hot water production hence, the heat pump system will be able to provide the entire demand. Hence, the extra hot water production will start to charge the tanks with hot water. Starting with tank 1 and ending in tank 5, this is true to maintain stratification within the tanks. Simultaneously, while tank 1 is being charged, colder water from tank 5 will be sent to pump number 2 to be pumped to the gas cooler and heated. Based on the temperature of the return water from the building, the corresponding valve will open and filled in its correlated tank which is true for all operational cases. For better operation the valve for the return water from the building should not open only based on the return temperature, but also the water temperature in the tank at that specific moment. This however, was not applied in the modelica, the reason for this is explained in section 4.2.
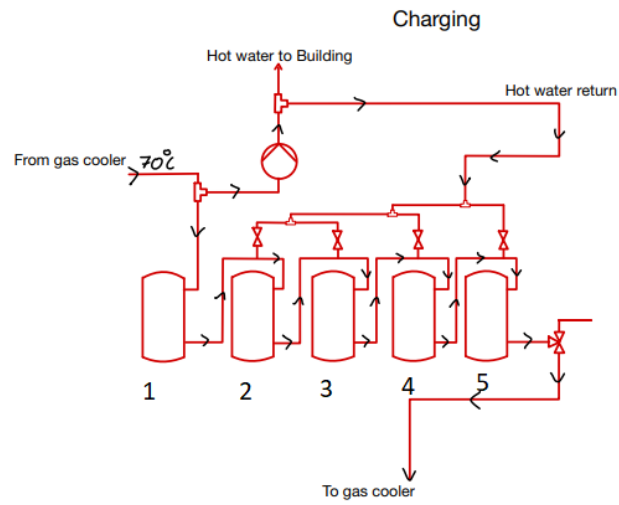
Charging

Hot water to Building

Hot water return

From gas cooler $70°C$

1 2 3 4 5

To gas cooler

(a) Hot water charging operation.

Discharging

Hot water to Building

Hot water return

From gas cooler $70°C$

$70°C$

$25°C$

Cold City Water

(b) Hot water discharging operation.

Fully Charged, Rejecting Heat to Ambient

Hot water to Building

Hot water return

From gas cooler $70°C$

$40°C$

$30°C$

To gas cooler

Ambient HX

PHE
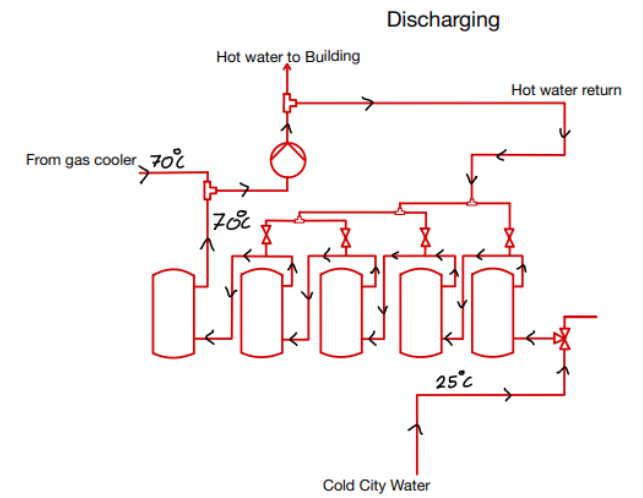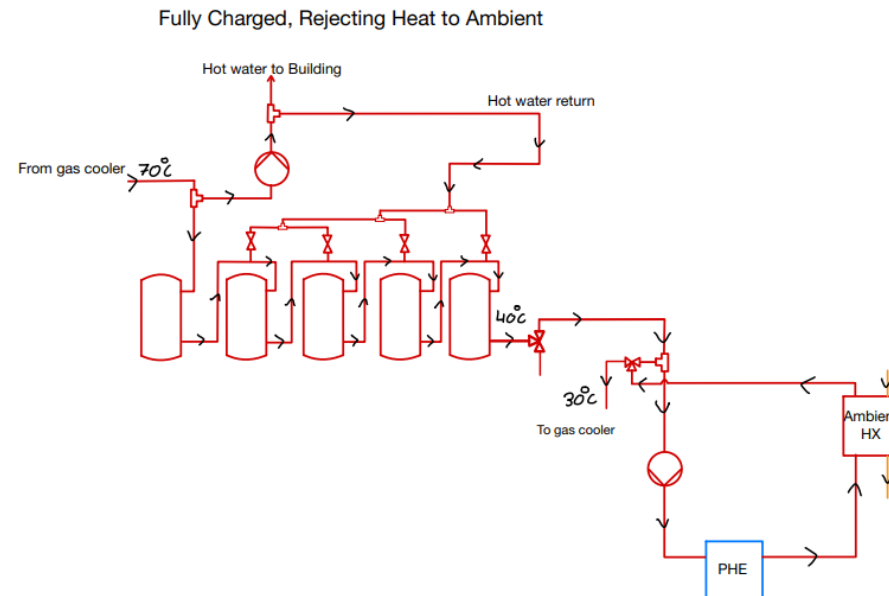
(c) Fully charged with low hot water demand.

Figure 41: Hot water loop operations.

During discharging process, as seen in figure 41b, the hot water demand is larger than the hot water production, hence, the hot water stored in the tanks combined with the hot water production by the heat pump will be combined to provide the total hot water demand by the hotel. The hot water stored in the tanks will be first sucked from tank number 1. Simultaneously, cold city water will enter tank number 5 this maintains stratification within the tanks, and the returned hot water from the building will follow the rule of the charging process. Finally, the third operation occurs when the hot water tanks are fully charged and the hot water demand is lower than the hot water production. The tanks are considered fully charged when the exit water temperature from the fifth tank is 40 degrees Celsius or above.

Rather than sending the hot water exiting the fifth tank directly to the gas cooler, as in the charging process, the directional three way valve will switch directions as seen in figure 41c, where the hot water will enter the extended loop and will reject heat to the ambient to cool down, before being sent back to the gas cooler. This is done because, if the hot water is sent back directly to the gas cooler at 40 ^{O}C or more, it will ruin the entire efficiency of the heat pump system. Since, the exit temperature of the CO_2 after the gas cooler is going to be high. The mass flow rate of pump 4, (inside the extended loop) is determined by the subtraction of the hot water production and hot water demand. Achieved, to maintain a balanced mass flow rate of the water in the entire loop. Otherwise, cold city water be stuck in the piping between pump 1 and 2 which will increase the system's pressure immensely, and fails the simulation. More about the control of this pump will be discussed in the upcoming chapter 4. The water temperature after rejecting heat to the ambient, will of course, depend on the ambient temperature, which will then be mixed with the cold city water before it is pumped to the gas cooler again.

3.2.3 Cold Water Loop

The cold water loop, seen in figure 42, consists of one main pump and 3 pumps that distribute chilled water to the different air handling units (AHU). As, it can be seen, the water is cooled in two stages, where the first stage of cooling occurs over the first evaporator and the second stage cooling occurs over the second evaporator. The water mass flow rate of the chilled water via the main pump is constant, and the total mass flow rate in the loop is equally divided by three for each of the three pumps. In a more advanced simulated system the total mass flow rate of the chilled water will not be equally divided among the three pumps, but tailored based on the cooling demand required by each AHU. There are three AHU, each unit represents a different cooling demand, one unit covers the cooling for the hotel bedrooms, one for the lobby and ball rooms, and the last unit represents the cooling required for the kitchen and dining area. There is one directional control valve, and one plate heat exchanger (PHE) which is connected to the extended loop in the hot water loop. The reason for the connection and PHE will be explained when looking at the different operation of the cold water loop system.
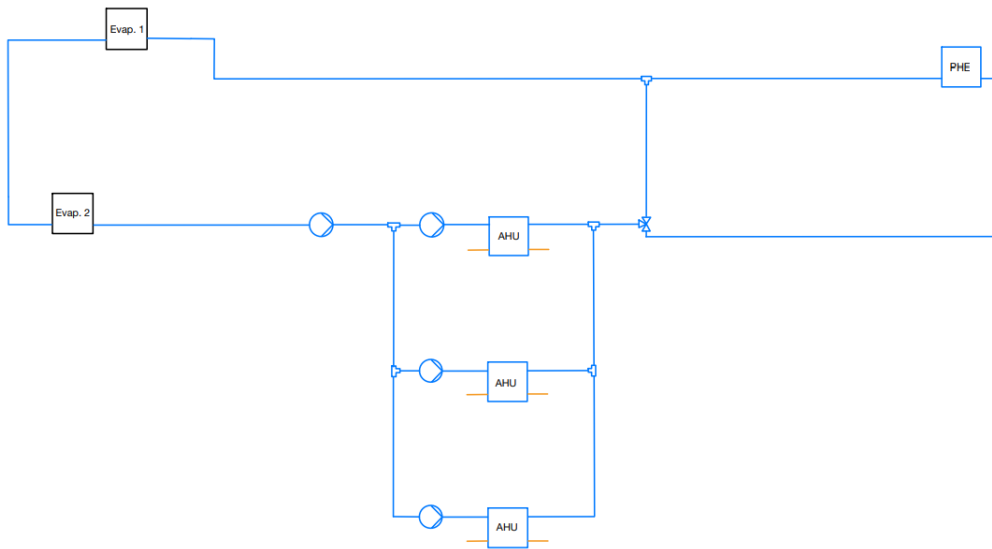
Figure 42: Cold water loop.
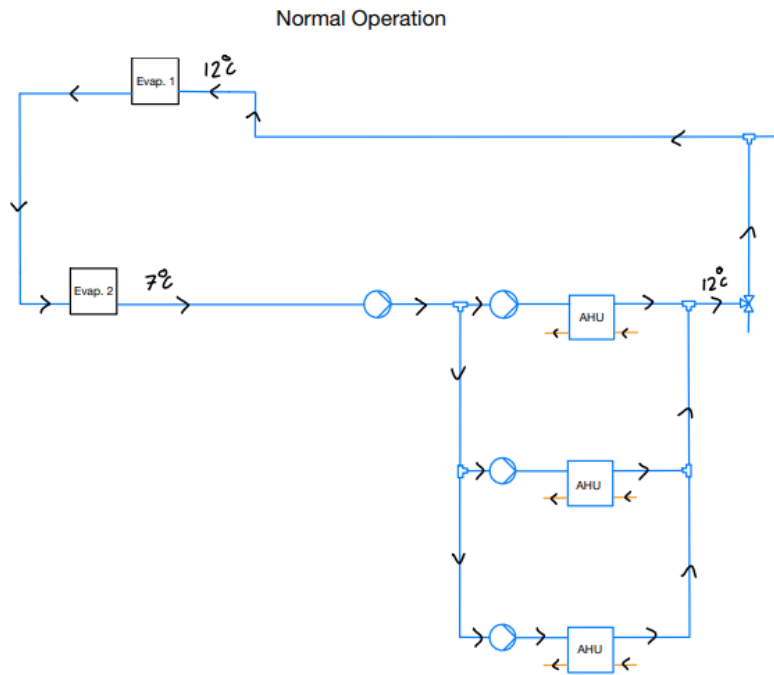
(a) Normal cold water loop operation.
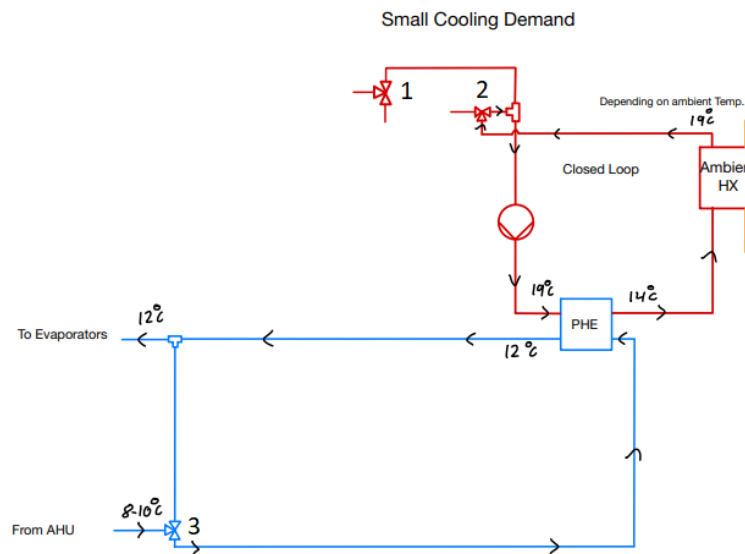
(b) Low cooling demand operation.

Figure 43: Cold water loop operations

For the cold water loop there are two different possible operations, as can be seen in figure 43. Where figure 43a represents the normal operation of the cold water loop, cooling water from 12^OC to 7^OC over both evaporators and sending the chilled water to the AHU. However, in the case when there is not enough cold water demand and the exit water temperature from the AHUs is low, for example 9^OC. While simultaneously, there is hot water demand, and hot water production is required. Hence, the heat pump system should stay in operation. This is when low cooling mode is activated, shown in figure 43b. In this operation, the directional three way valve (valve number 3) after the AHUs switches direction so that the chilled water is sent towards the PHE, rather than directly back to the evaporators. This will create a fake load, which will increase the

cold water temperature back to 12^OC,. This is acquired thanks to the extended loop of the hot water loop. As it can be seen in the figure, the extended loop is now a closed loop, so the water in the pipes is just constantly circulating via the pump. The pump's mass flow rate, is controlled to achieve the 12^OC water in the cold water loop. So it works as follows, as directional control valve 3 switches direction, directional control valve 1 will operate switch so that no hot water is sent into the loop, and directional control valve 2 switches direction so that the water in the extended loop is not sent back to the gas cooler but kept circulating in the loop. The pump's mass flow rate in that loop is no longer zero or equal to the subtraction of the hot water production from the hot water demand. But now, it is controlled to achieve the temperature setpoint for the chilled water, before being sent back to the evaporator. Creating a fake load. The warm water in the hot water loop cools down, as it heats the cold water in the PHE to the set point. It regains its temperature as it warms up again, from the ambient heat via the ambient heat exchanger. In figure 43, one can see as the warm water cools from 19^OC to 14^OC then back to 19^OC over the ambient HX, and the cold water goes from 9^OC to 12^OC over the PHE. This operation, can also be used in the case where there is high hot water demand, and the tanks are no longer charged, and hot water production is not enough to supply the entirety of the hot water demand. Hence, this operation takes place in order to heat the water in the cold loop further to increase the cooling demand. In return, the mass flow rate of CO_2 in the heat pump will increase. Leading to higher hot water production to cover the hot water demand.

4   Methodologies

The model data was given by the research group INDEE+ which included the capacities of the gas cooler, both evaporators and internal heat exchanger. This data can be found in appendix B. However, the design of the system, components sizing, building the modelica model, and control strategies were all developed from scratch and the methods to achieve the results shown in section 5 are described below in subsection 4.1. This master thesis is a continuation of the project development work done earlier this year in which the modelica model of the heat pump system alone was developed, hence subsection 4.1.1 is referenced to the project assignment Abdin 2022.

4.1   System Development

Figure 44, shows the final working iteration of the full heat pump system. It includes, the heat pump circuit, hot water loop and cold water loop. In the following subsections, the method to reach the final iteration of the working model in this master thesis is presented. Taking each section individually. The development of the system, started from scratch for each of the circuits. The heat pump system was built during the project development work and was sized and edited during the master thesis to serve the required capacities. The hot water and cold water loops were developed during the master thesis work. Developing the hot water loop was the most demanding out of all circuits. The final working iteration took around 5 months worth of work.
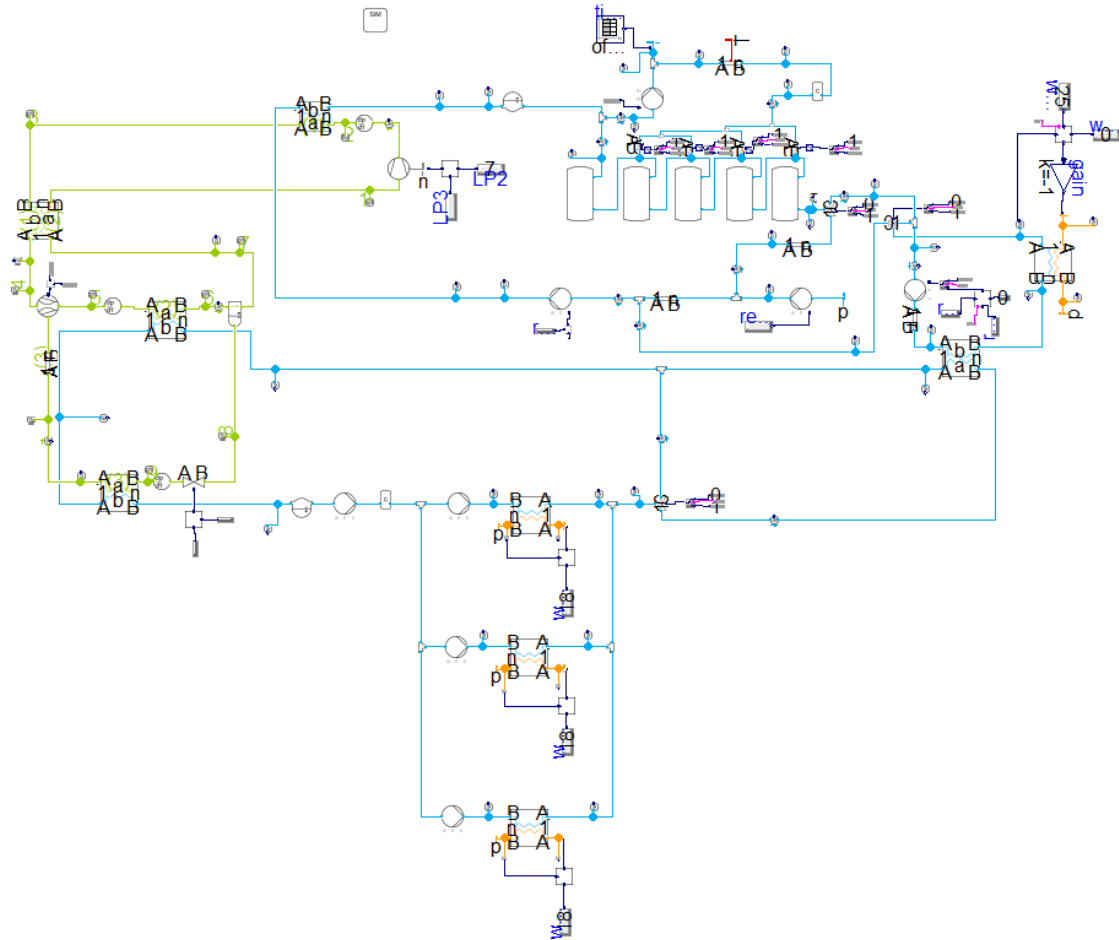
Figure 44: Final iteration of the working Modelica model.

4.1.1   Heat Pump system

In order to build the modelica model of the heat pump system, some data and boundaries are required to be found and set. This is shown below. The model presented, is a heat pump system developed for an Indian hotel in Goa, that requires water heating and space chilling through a double stage evaporation as seen in section 2.3.5. The hotel requires a cooling capacity of 130kW, gas cooler capacity of 160kW, with a compression power input of 30kW. Where the high stage circuit has a refrigerant mass flow rate of approximately 2627 kgh^{-1} (0.73 kgs^{-1}) and the medium and low stage circuits have refrigerant mass flow rate of approximately 1314 kgh^{-1} (0.365kgs^{-1}). Where the discharge pressure is at 100 bar, medium pressure is at 45 to 47 bar and low pressure is at 40 to 41 bar, this pressure lift from 40 bar to the medium pressure will be supplied via the ejector.

Figure 45, shows the assumed Ph diagram of the presented schematic diagram in figure 39, the Ph diagram represents the state point based on the data given by the INDEE+ group.
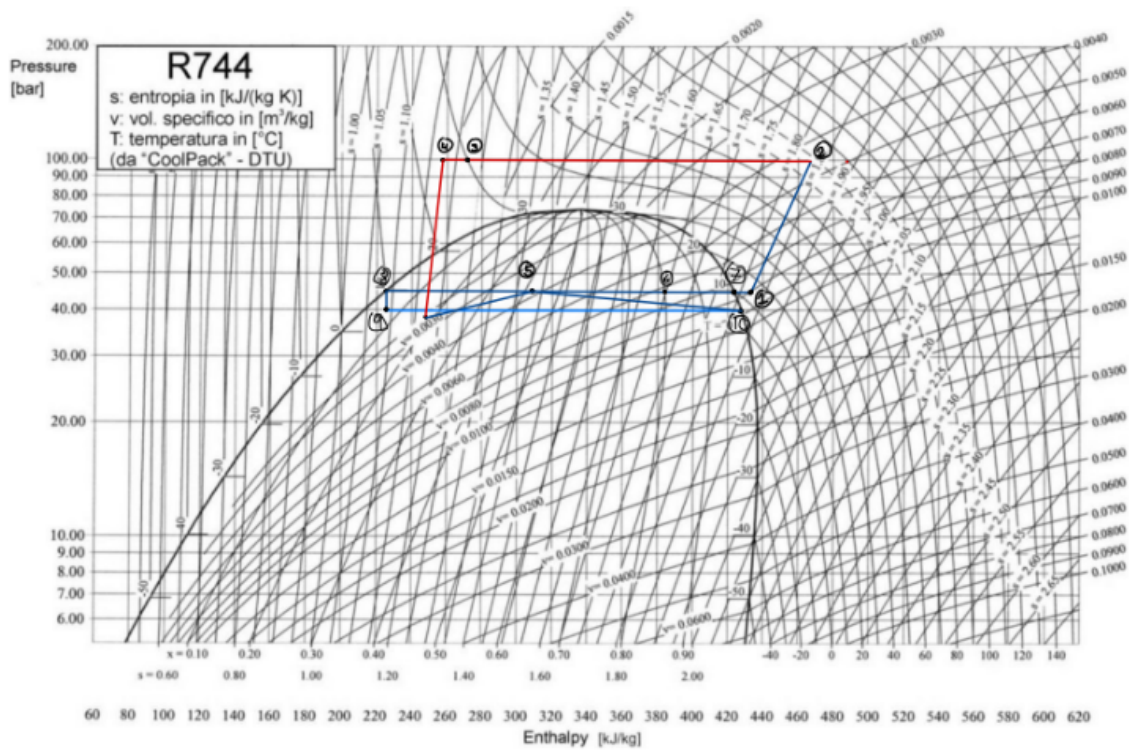
Figure 45: Ph diagram of the heat pump system for Goa Hotel

The separator was required to be designed and sent for the INDEE+ group to manufacture it. The manufacturer at first, placed a limit on the size of separator they can manufacture. Which had a height of 700mm and diameter of 150mm. So, based on these values and the other given data seen in appendix B, the design and size of the separator is calculated. To check whether the charge can be filled in one separator or more. Keep in mind that one difference occurred between the schematic diagram shown in figure 39 and the actual system to be installed. Which is the utilization of gravity fed evaporation over first evaporator as seen in figure 46 with its respective Ph diagram in figure 47, where as in figure 39 the method of gravity fed evaporation was not utilised. The reason will be discussed later in section 4.2. The design of the separator however, was designed based on the actual system to be installed.
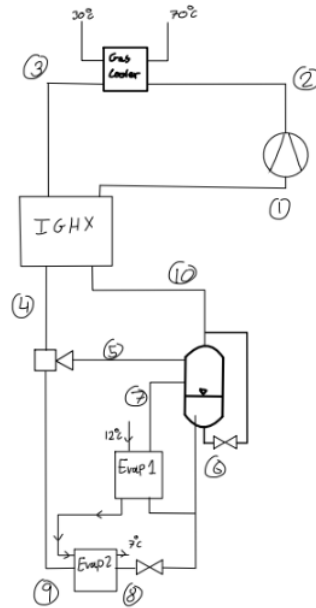
Figure 46: Schematic diagram of the actual to be installed system for Goa Hotel
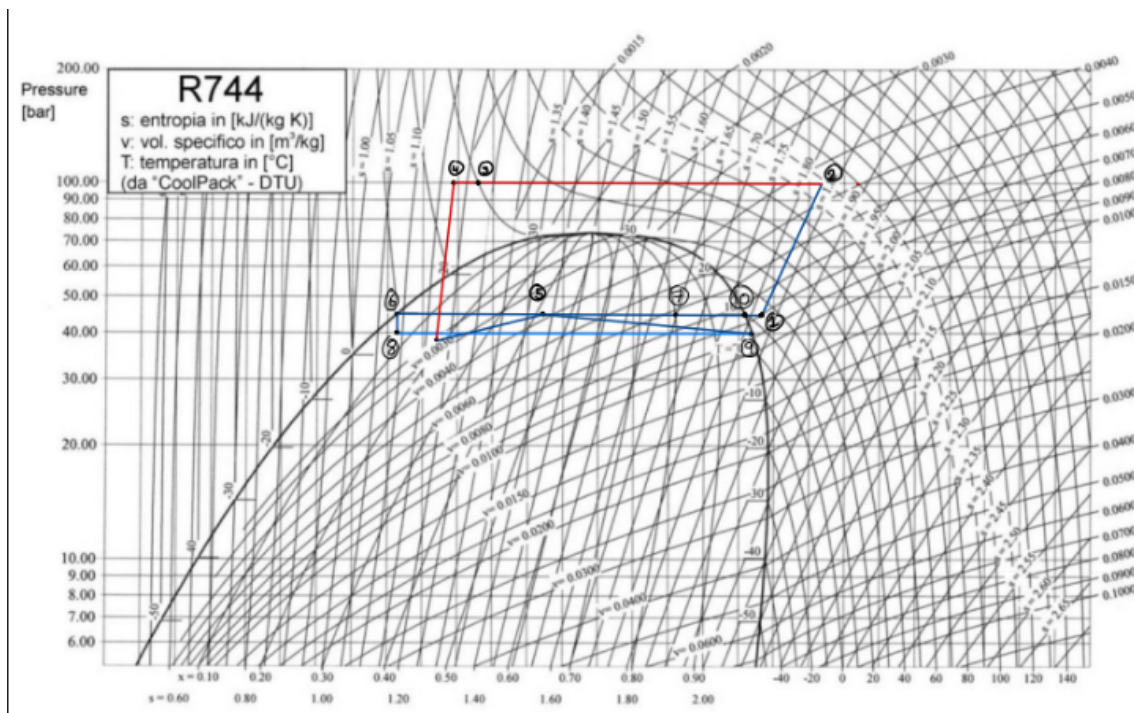
Figure 47: Ph diagram of the actual to be installed system for Goa Hotel

First the total charge of the system must be calculated, to do so;

$$=!PropSSI("H";"T";293;"P";4500000;"CARBONDIOXIDE") \tag{11}$$

The volume over the compressor, gas cooler, internal heat exchanger, both evaporators and ejector were given, hence what is left is the volume of the pipes. Which was found by choosing a suitable diameter for each section based on the velocity of the refrigerant in said pipe. The recommended velocities for each section are seen in figure 48, which was supplied through lecture

45

material Armin Hafner 2022. The available pipe diameters from the manufacturer are presented in table 1. To find the velocities in each pipe to determine the chosen pipe diameter. The flow rate in said pipe was divided by the multiplication of density by the pipe area(all the diameters were used for each pipe to get all possible velocities) to get the velocity in m/s, as seen in equation 12.

Then the area of each pipe section based on the chosen diameter to fulfill the recommended velocities requirements was found. Using equation 13, where d is the diameter if the chosen pipe in meters. What follows was, finding the volume of each of the pipe by multiplying the area by the length of the pipe, which was approximated for each section to be 1 meter for all pipes except pipe number 5 seen in figure 46 (between ejector and separator) to be 0.5 meters. Equation 14 was used to find the volume of the pipes where L is the length in meters.

$$u = \frac{\dot{m}_{ref}}{\rho_{ref} \cdot A_{pipe}} \tag{12}$$

$$A_{pipe} = \frac{1}{4} \cdot \pi \cdot d^2 \tag{13}$$

$$V_{pipe} = A_{pipe} \cdot L \tag{14}$$

Recomended velocities

Discharge pipe: 5-12 m/s

Suction MT pipes: 3-12 m/s

Suction LT pipes: 5-15 m/s

Return liquid line from gascooler: 2-4 m/s

Liquid line to cabinets: 1-2 m/s

Figure 48: Recommended Velocities for each section Armin Hafner 2022

Table 1: Available Diameters by manufacturer in mm

available pipe diameters mm
9,52
12,7
15,87
19,05
22,23
28,57
34,92
41,27
53,97

To find the total charge the density of the refrigerant in each component was multiplied by the volume of each section which will give the charge in kg for said section, the sum of all the charges in all of the components will equal to the total charge. Equations 15 & 16 were used to find the charge in each section and the total charge in the entire system respectively.

$$Charge_{section} = \rho_{ref} \cdot V_{section} \tag{15}$$

$$Charge_{total} = \sum^{z} charge_{section_z} \tag{16}$$

Finally, to find whether the separator volume is enough to collect all the refrigerant in standstill conditions, the total volume was found by summing the volume of refrigerant in each component,

then was divided by the total charge to find the specific volume of the refrigerant (m³kg⁻¹), as seen in equations 17 and 18. Then using the specific volume calculated, the vapor fraction (x) at 3 standstill temperatures were found using COOLPROP, the temperatures used were 20, 25 and 27.71 ^{O}C. Using equation 19, to find the liquid amount in kg at said temperature, which was then multiplied by the specific volume to find the liquid volume in m³ as seen in equation 20. Which was then used to find the liquid volume in L, as seen in equation 21, at each temperature. And liquid height in the separator at each temperature, as seen in equation22, where d_{sep} is the diameter of the separator. The liquid height in the separator, was found in order to know the height placement of the inlet and return pipes coming from the ejector and evaporator, to avoid back flow. To decide whether the tank size is applicable the total volume of the tank/s (seen in equation 23 where H_{sep} is the separator height) should be bigger than the total volume of refrigerant.

$$V_{total} = \sum^{z} V_{section_z} \tag{17}$$

$$v = \frac{V_{total}}{Charge_{total}} \tag{18}$$

$$Liq_{kg} = (1 - x) \cdot charge_{total} \tag{19}$$

$$Liq_{m³} = Liq_{kg} \cdot v \tag{20}$$

$$Liq_L = Liq_{m³} \cdot 1000 \tag{21}$$

$$Height_{liq} = \frac{Liq_{m³}}{\frac{1}{4} \cdot \pi \cdot d_{sep}^2} \tag{22}$$

$$V_{sep} = \frac{1}{4} \cdot \pi \cdot d_{sep}^2 \cdot H_{sep} \tag{23}$$

Due to the restriction by the separator manufacturer the volume of separator will be smaller than the total volume of refrigerant as seen in results section 5.1.1. Hence, two separators will be required. Figure 49, represents how the connection between the separators will be achieved and figure 50, shows the 2-D dimensional side cut, top and bottom view of the separator.
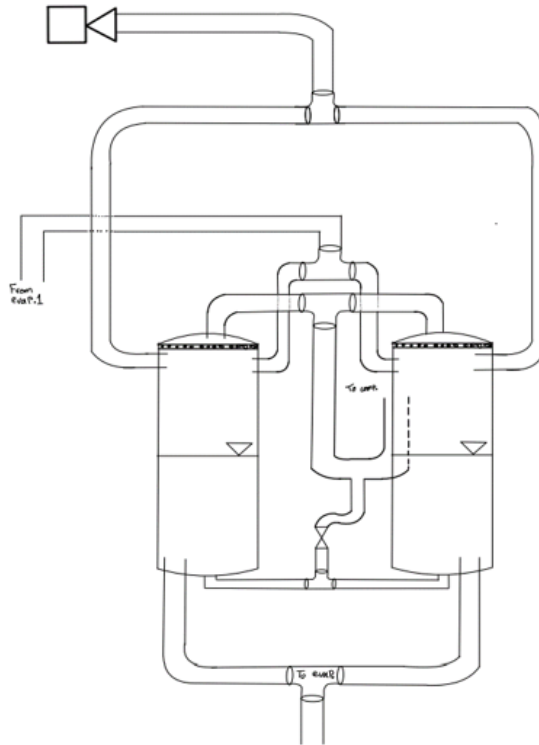
Figure 49: Two separators connection
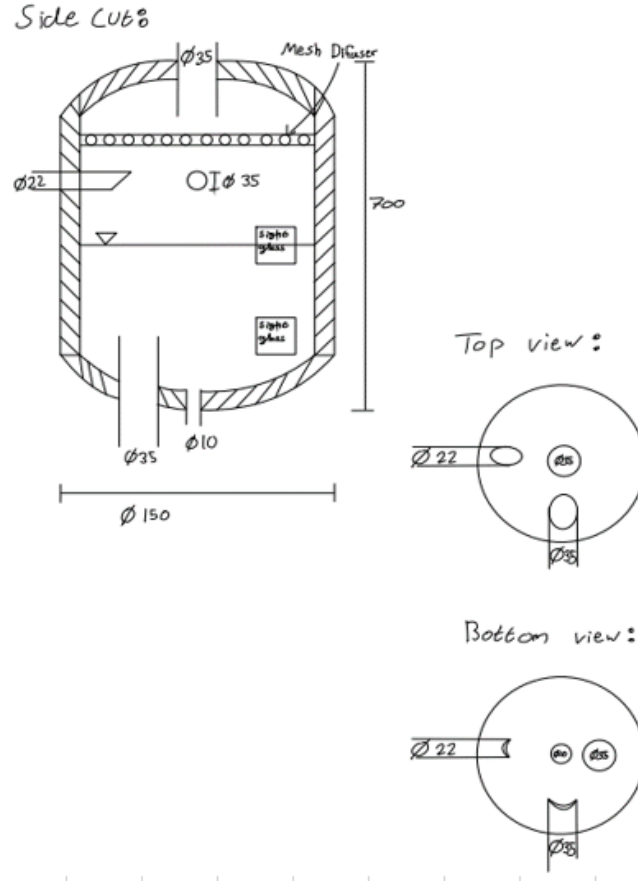
Figure 50: Side cut, top and bottom view of the separator

After designing the separator, the ejector was designed next. To find the state point of the refrigerant at the ejector outlet, an energy balance shown in equation 24 is required. Where subscript 1 is for the flow coming from high side through the motive nozzle, subscript 2 is for the flow coming from the evaporator drawn by the ejector through the suction channel and subscript 3 is the outlet flow from ejector. $\dot{m}$ is the mass flow rate and h is the enthalpy of refrigerant at that point.

$$0 = \dot{m}_1 h_1 + \dot{m}_2 h_2 - \dot{m}_3 h_3 \tag{24}$$

To find the efficiency of the ejector, equations 25, 26, 27, and 28 presented and explained earlier in section 2.3.3 are used. Also seen below:

$$\omega = \frac{\dot{m}_{suction\ nozzle}}{\dot{m}_{motive\ nozzle}} \tag{25}$$

$$\prod = \frac{P_{diffuser\ outlet}}{P_{suction\ nozzle\ inlet}} \tag{26}$$

$$P_{lift} = P_{diffuser\ outlet} - P_{suction\ nozzle\ inlet} \tag{27}$$

$$\eta_{ejector} = \omega \cdot \frac{h(P_{diffuser\ outler}, s_{suction\ nozzle\ inlet}) - h_{suction\ nozzle\ inlet}}{h_{motive\ nozzle\ inlet} - h(P_{diffuser\ outler}, s_{motive\ nozzle\ inlet})} \tag{28}$$

After defining the entire system's boundaries and components' sizing, the modelica model can be built. The modelica model was created, in order to see the system's performance in a dynamic simulation, rather than static conditions, before building and installing the real system in India.

48

The model was created on the programming language Modelica, in the programming environment Dymola, which is capable of simulating dynamic systems with changing conditions. For example, heating and cooling loads which are implemented via dynamic controllers, or as simple as the change of temperature profile over a year. The components used in the model were derived from the component library for thermodynamic systems named TIL-Suite Library. Developed by TLK-Thermo GmbH and Institute *für* Thermodynamik in Braunschweig Tegethoff et al. 2011 as presented in Armin Hafner, Försterling et al. 2014. TIL Suite library was developed based on years of experience and high level of understanding and knowledge in thermal science, simulation procedures and software design. This what makes the TIL-Suite an advanced library in the modelling language Modelica for simulation of transient fluid systems, such as refrigeration, air conditioning, heat pumping and chilling systems. The library provides all the components needed to build any of the previously mentioned systems in the literature review. Such as, ejectors, heat exchangers, compressors, pumps, tubes and valves. It also includes the fluid property data for many different refrigerants and fluids such as CO_2, water, and moist air, since it is embedded with REFPROP an add on similar to COOLPROP for the use in the simulation. For the visualisation aspect of the simulation, results such as the Ph and Ts diagrams, Dave software was used for the direct visualisation as it is directly connected with modelica and TIL-Suite library.

To start building the modelica model, the components were placed and connected as seen in figure 51. Figure 51, shows a screenshot of the heat pump modelica block. The process that went into building the heat pump system: 1)First the fluids used in the system were defined in SIM, where the working refrigerant is R744, the cooling/heating media used is water for the hot and cold water loops and moist air over the ambient heat exchanger and air handling units. 2)The components were then placed and connected, compressor used is the efficiency based compressor representing a piston compressor which has variable speed to achieve the required capacity of the system. The efficiencies were all set to 80%, with mechanical port option was placed as true in order to connect the mechanical boundary to it, which through it combined with a PI controller the frequency of the compressor is controlled. The displacement for the compressor chosen was $2e^{-4}m^3$, which is sized larger than the required capacity which will be noticed in the results section. The reasoning behind this will be discussed in section 6. 3) pressure states components were used to define the initial common pressure in that circuit, high pressure state at 100 bar initial pressure, medium pressure state at 45 bar initial pressure, low pressure state at 40 bar initial pressure.

After the high pressure state component the gas cooler was placed, the gas cooler chosen is a plate heat exchanger with its main dimensions given by INDEE+ as seen in B, with the CO_2 and water coefficient of heat transfer set to 4000 W/(m^{2}K). It is then followed by an internal plate heat exchanger. Following the procedures done for the gas cooler, except the heat exchange rate was set at 2000 W/(m^{2}K) on the high pressure side and 3500 W/(m^{2}K) on the suction line, same goes for both plate heat exchange evaporators with a heat exchange rate of 2500W/K each. What comes after the first evaporator is the separator that has an initial filling level of 70%, the gas is drawn by the compressor via the internal heat exchanger and the liquid R744 is sent through the expansion valve to the low pressure evaporator, which the exit of the evaporator is drawn by the ejector to lift its pressure back to the separator pressure level.

3)The gas cooler was sized so it is capable of lifting the water temperature from a temperature of 30 degrees Celsius to 70 degrees Celsius setpoint. Where the pressure in the circuit is controlled via the ejector. Whereas, the IHX was sized so that it achieves good amount of subcooling before expansion, and to control of superheat before inlet to compressor. The evaporators were also sized to achieve cooling from 12 degrees Celsius to 7 degrees Celsius, with the pressures at the low stage is controlled via the frequency of the compressor.

4) There are 3 different PI controllers used, one to control the compressor speed to maintain an exit water temperature of 7 degrees Celsius. The ejector PI controller, was used to maintain the high side pressure of the system at a 100 bar, by changing the effective flow area of the motive nozzle in the ejector. Finally, the PI controller over the expansion valve was used to maintain an outlet vapor fraction of 0.8 after the evaporator to maintain a flooded operation for maximum efficiency, as discussed in section 2.3.2. Hence, the changing variable was the flow area of the expansion valve.
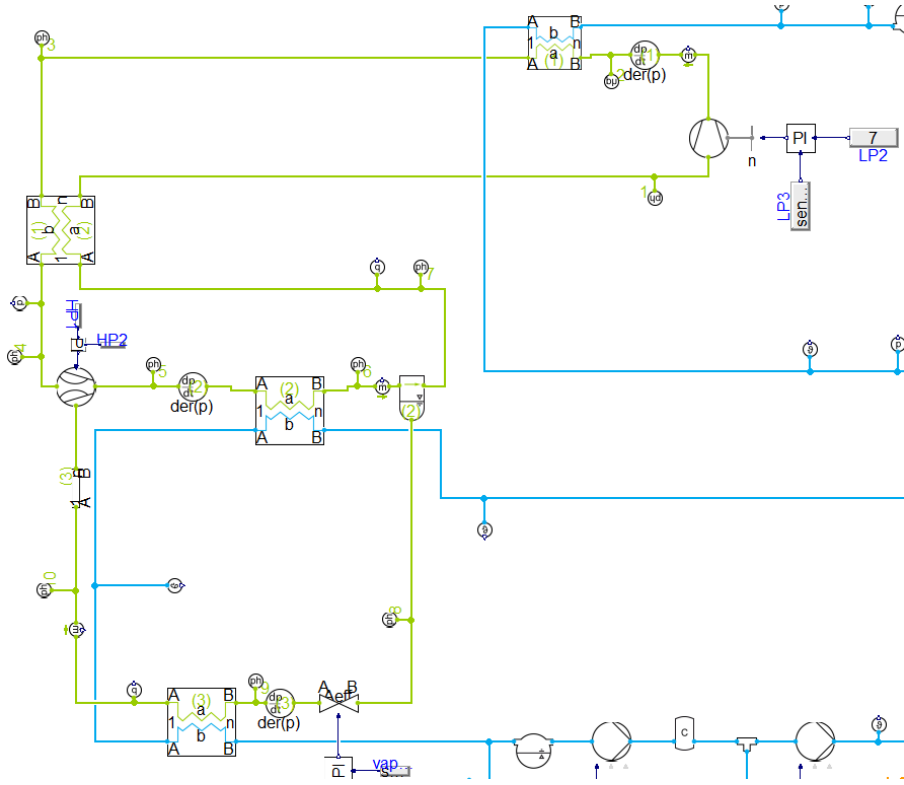
Figure 51: Modelica model of the heat pump system for Goa hotel.

To configure the PI controller there are a couple of parameters need to be given. Looking at the compressor PI controller for an example, it has the setpoint signal which basically is the outlet water temperature from the second evaporator to be 7^OC, this is given via real expression block in TIL library, there is also the measured signal which is the live reading of the system and it would be connected to a temperature sensor in the cold water loop in this case. Finally, there is the output signal which in this case is controlling the speed of the compressor. Inside the PI controller as seen in figure 52, the k parameter is the proportional gain of controller, in other words how quick will the controller reach the set point value, this parameter value is different for each component and to a certain extent, the correct value is found through trial and error for a beginner user.

Ti parameter, is the time constant of the integrator block, and it basically controls the amount of deviations till the measured value reaches the set point steady state condition. The yMax and yMin dictates the max and minimum value out of the output signal in this case the speed of the compressor, finally yInitial is the initial output signal of the PI controller, in this case the speed of the compressor at start of simulation. The invertfeedback basically changes the operating direction of the controller by inverting the input difference. Hence, if the temperature goes below 7^OC the frequency of the compressor will decrease and if it goes above the setpoint the frequency will increase. If the inverfeedback was set to false then the opposite of what is explained occurs. The three parameters seen in figure 52 are connected through equation 29.

Figure 52: PI controller settings in Modelica

$$ki = \frac{k}{Ti} \tag{29}$$

Through Modelica, one can also calculate the capacities of each of the heat exchangers as well as the total COP and the COP for cooling and heating. This is done by using the real value block in modelica, where one inputs the variables to be seen. The cooling capacities are easy and that is done by inputting the Q-flow for said heat exchanger in the real value block as seen in figure 53. To find the COP the equation must be placed in the number tab as seen in figure 54 which represents the heating COP in this case. The COP equations are shown in equations 30, 31, 32 for the total, heating and cooling COP respectively. Where, $P_{compressor\ shaft}$ is the shaft power input for the compressor. Must note that the correct way to find the COP is also by including the power inputs of the fans, pumps and any auxiliary components, however in this investigation only the power input for the compressor was used.

$$COP_{total} = \frac{Q_{evap1} + Q_{evap2} + Q_{gascooler}}{P_{compressor\ shaft}} \tag{30}$$

$$COP_{heating} = \frac{Q_{gascooler}}{P_{compressor\ shaft}} \tag{31}$$

$$COP_{cooling} = \frac{Q_{evap1} + Q_{evap2}}{P_{compressor\ shaft}} \tag{32}$$

Figure 53: Capacity of first evaporator (evap1.summary.Q$_{flow}$)

Figure 54: COP for heating of system

Finally, to draw the Ph diagram diagram of the system, state point sensors were placed around the system as seen in figure 51. The sensors locations were placed at every point where there is a change in the state of the refrigerant. After placing the state points in the correct locations, Dave software was used. To use the software, the cycle from modelica was imported into Dave, then the selection of the graph type was chosen based on what it represents a Ph or Ts diagram or temperature distribution over a heat exchanger. For the case of the Ph or Ts diagrams, the cycle is drawn based on the state point sensors positioned in modelica. Then the refrigerant Ph diagram is chosen in this case it was R744. After applying the cycles the Ph diagram is drawn.

4.1.2 Hot and Cold Water Loops

To reach the final working iteration of the hot and cold water loop shown in figure 44 a total of 66 different iterations and trials were created. This subsection will summarize the main milestones which lead to the successful simulation. Figures 55 and 56 shows a close up screenshots of the final iteration, to give an idea of the final system compared with how it started.
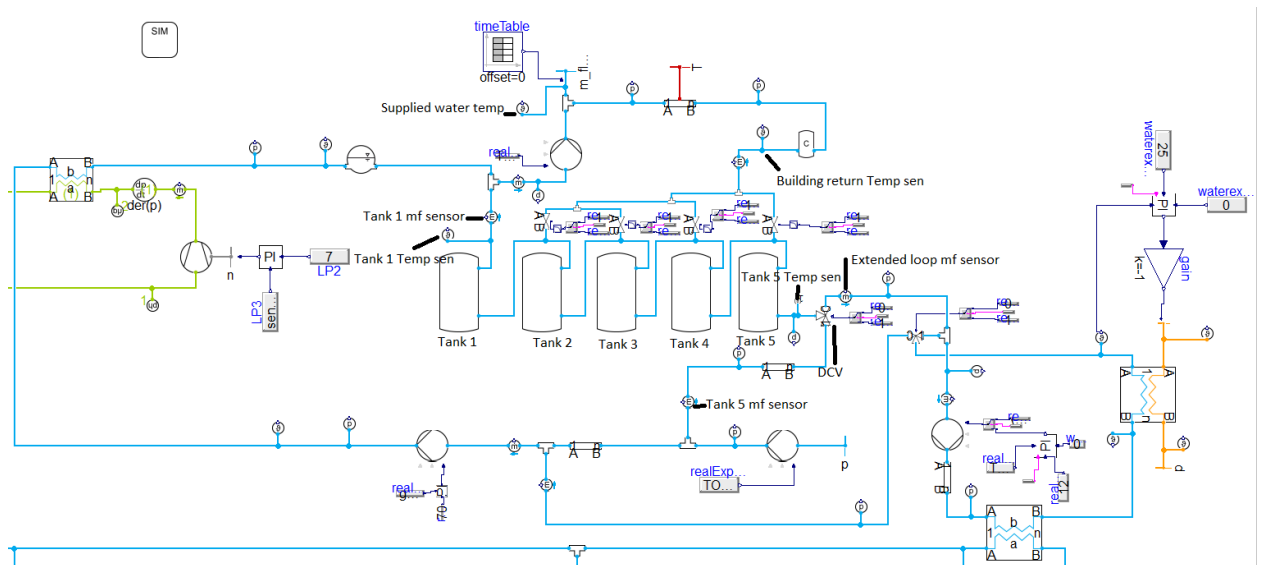
Figure 55: Final iteration of the working hot water loop.
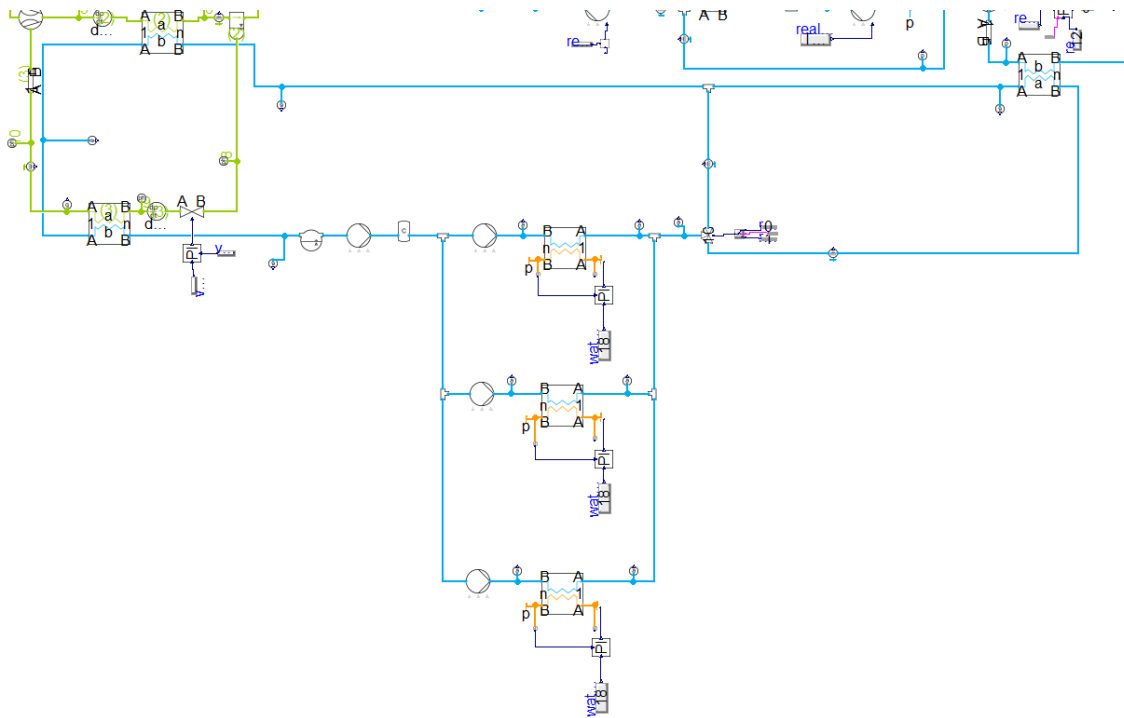
Figure 56: Final iteration of the working cold water loop.

Before presenting the main developing iterations of the system, an explanation of how each of the final working water loops models work is required. Including, its controls and how the system is dynamically connected. A continuation to section 3.2; as can be seen in figure 55, there is a table connected to the boundary representing the hot water demand. Three different cases of hot water demands were investigated in this simulation to show the tanks behaviour and storage capacity at different demands. Where the simulation is done over 1 full day with each hour reflecting real life data on the typical demand of hot water at that time. Done to have a better understanding of how the system will work in real life and the relationship between the peak power demand, and the hot water production compared to how much hot water is in the tank. This will show how to size the hot water tanks to best suit each case.

That being said, based on the hot water demand by the hour, cold city water is pumped via pump number 1 seen in figure 40, accomplished by connecting the pump to a real expression which controls the input mass flow-rate to equal the amount of hot water demand. Next is pump number 2, which is connected to a PI controller which controls the pump's flow rate in order to achieve an exit water temperature from the gas cooler at 70^OC. Moving to pump number 3, similarly to pump number 1, it is also connected to a real expression. It is defined as the mass flow rate of the hot water demand plus 0.3kgs^{-1}. This ensures that there is always hot water running through the buildings pipes. In the hot water return line, there is a tube which represents the pipes in the building. It is connected to a heat port which represents the heat loss of the hot water, in the building, due to ambient losses. Moving to the valves that are connected above each of the tanks, each valve is connected to a switch which determines whether the valve is open or closed; based on the return temperature of the hot water. The far right valve, opens if the return temperature is between 20 and 40^OC, the next switch opens when the return temperature is between 40 and 50^OC, the one after is when the temperature is between 50 and 60^OC and finally the last switch opens when the return temperature is over 60^OC. The three way directional control valve position is also controlled via a switch. Which is defined by the value of the exit water temperature from tank 5, as defined in figure 41, and when the hot water production is larger than the hot water demand. Hence, when these two boundaries are achieved, the three way valve changes directions to send the hot water via the extended loop to reject heat to the ambient. As can be seen in figure 55, there is a PI controller that controls the flow rate of air intake into the heat exchanger so that the exit water temperature is 25-30°C depending on the ambient temperature. That PI controller

is also connected to the mass flow rate sensor, in the extended loop, which determines whether the extended loop is in operation or not. If it is, then the fans of the heat exchanger are on, if not the ambient air flow rate will equal to zero.

Inside the extended loop, is a pump that has a switch which is connected to a real expression and a PI controller, by far it has the most control complication out of all the other pumps. First what determines the switch's location is the position of the directional three way valve. If the position of the three way valve is open and the hot water is entering the extended loop, then the pump is controlled via the real expression. Which has a mass flow rate value that is equal to the subtraction of the hot water production minus the hot water demand. To ensure a mass flow rate balance and no extra water is stuck in a section of the system. On the other hand if the directional three way valve is in the other position then the switch will switch to the PI controller. The expression that controls the PI controller, depends on the mass flow rate sensor in the extended cold water loop. The hot and cold water loops are connected via a plate heat exchanger seen in figure 56. If the value of the sensor is above zero, then the PI controller will control the pump's flow rate so that the cold water leaving the PHE has a temperature of 12^OC. Otherwise, the PI controller will signal to the pump to have a mass flow rate of zero. Finally, the last switch position connected to the second directional three way valve in the extended hot water loop, is determined based on the position of the directional three way valve number 1. If it is activated, then directional control valve number 2 will also activate to send the hot water back to the gas cooler, otherwise the extended loop will now be a closed loop to operate as explained earlier in section 3.2.3.

Moving to the cold water loop's control, which is much simpler than that of the hot water loop, includes three PI controllers each connected to one of the air boundaries of the AHU. They control the mass flow rate of the air so that the exit temperature of the air is 18^OC to cool down the rooms, and other sections of the hotel.

Figure 57, shows the main milestones of creating the modelica model, where the first and second iteration took place to understand how the storage tank model works. Starting from the 3rd milestone is where a very simple hot water loop was developed. At this point the model was a static simulation. There is a constant circulation of water and the CO_2 side of the gas cooler was only set boundaries. After getting the system to work, the addition of the extended loop was added as well as the development of the cold water loop was created. At this step the simulation was still a static simulation, to reach this point many iterations of the system took place. From this milestone, it was found that the air handling units must be adjusted to work in parallel rather than in series; for easier control and to achieve the required cooling. A couple iterations later, once the hot water loop and the cold water loop were successful, the addition of the plate heat exchanger and extended cold water loop were added. The 5th milestone, to get the hot water and cold water loops to work together. At this point, the hot water production was no longer constant, but controlled via a PI controller to achieve the heating of 70 degrees Celsius, and in the cold water loop the AHU are now set in parallel. However, at this milestone the control of the cold water loop went into errors as it was over controlled and the mass balance was no longer existent as well as the water circulation is no longer constant and it was not possible to achieve the cooling required. Hence, after fixing these issues through many trials and errors to get the required result, the addition of the entire heat pump system was added. From the sixth milestone until the final working model, no major changes within the system were done, however, it was all about control and properly sizing the components. The control of the system which also included making sure that there is a mass flow rate balance in the entire system was the hardest to achieve. Taking a deeper look at the milestones one will find, the main changes comes in the PI controllers, real expressions of the pumps, addition of expansion tanks and hydraulic capacitors to maintain a constant pressure in the cold and hot water loops.
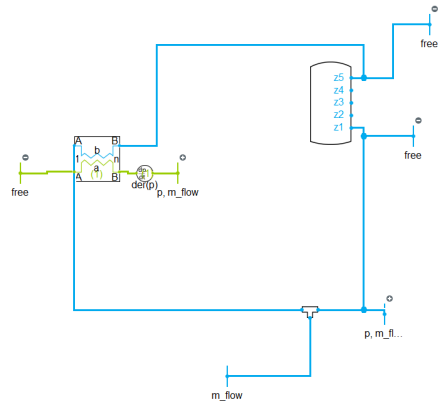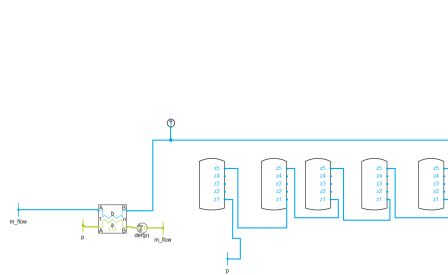
(a) 1st Milestone   (b) 2nd Milestone   (c) 3rd Milestone   (d) 4th Milestone
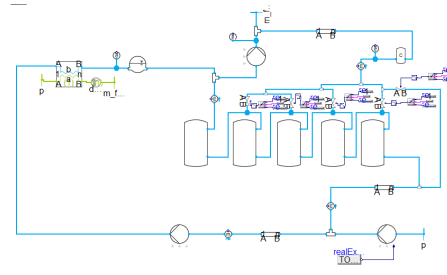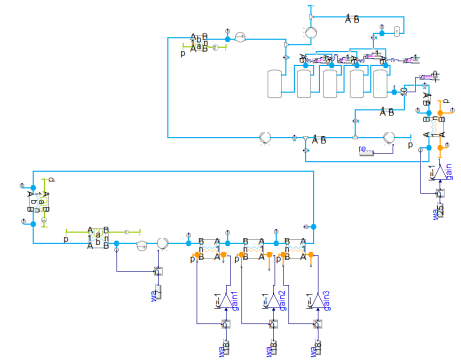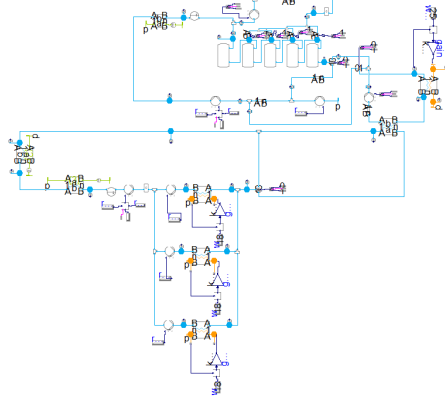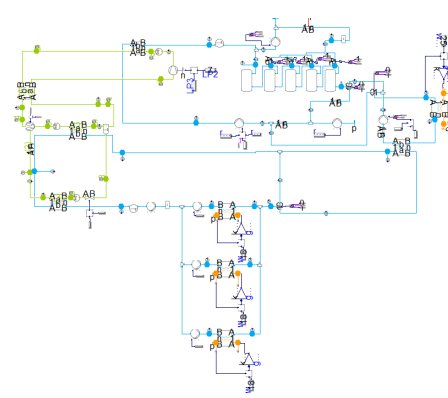
(e) 5th Milestone   (f) 6th Milestone   (g) 7th Iteration   (h) 8th Milestone
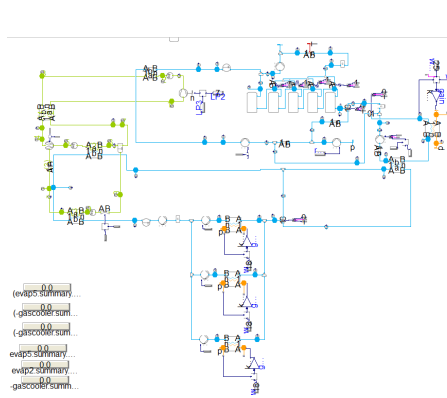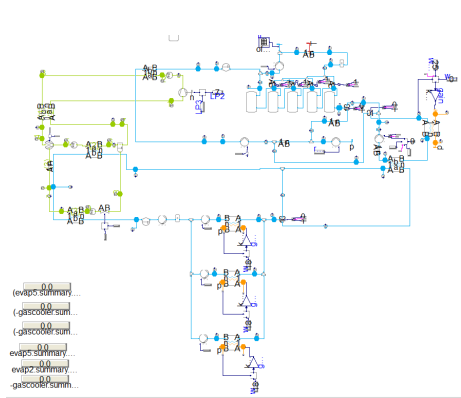
Figure 57: Main milestones of creating modelica model

4.2   Difficulties and Errors

While building the modelica model, the complexity level increases. With that, comes errors and difficulties. First things first, the main difference between the original system to be installed in Goa and the simulated system is the fact that in the original system the medium pressure evaporator utilizes the concept of gravity fed as can be seen in figure 46. Whereas, the simulated system has the medium evaporator inlet directly after the ejector as seen in figure 39. Either systems have their advantages and disadvantages. Starting with why the gravity fed evaporator would be better, one the inlet refrigerant is going to be 100% liquid, hence, a higher heat exchange coefficient and consequently a more efficient heat exchanger. As well as, the size of the evaporator can be decreased, since the cooling capacity of the exchanger is going to be higher. Because, the entirety of the heat exchange area is going to be utilised. If the temperature of the supercritical CO_2 before expansion is high or near the critical temperature, then the expanded CO_2 in the 2 phase region is going to have a high vapor fraction, hence the cooling capacity of the evaporator is going to be decreased. So, if the system is not running in gravity fed mode, then it is of extreme importance to cool down the CO_2 as much as possible before expansion, which was done in this case.

On the other hand, having the evaporator not operated in gravity fed evaporation then the entirety of the expanded refrigerant mass flow rate will be used, and the capacity of the system is increased. The reason for not simulating the original system of gravity fed evaporation, is due to the fact that it requires really complex simulation methods; and not much experience was developed in modelica to be able to achieve such complex simulation. Hence, gravity fed was not applied.

Another difficulty, that was faced and could have been done better, is the fact that the return hot water from building will enter the hot water tanks only based on the return temperature of the water and not taking in consideration the water temperature of the tank at that instant, hence stratification can be destroyed. For example, the valve that is connected to tank number 4 seen in figure 41, opens when the return temperature is from 40 to 50^OC. So, if the tanks are fully charged meaning that the water in tank 4 is over 60^OC, and the return water is 40^OC. Then, the return water will enter tank number 4, rather than entering tank 5 and this will unbalance the stratification of water in this case. Hence, to fix this the valves opening should be based on both the temperature of the water inside the tanks and the return water temperature from the building simultaneously to maintain stratification throughout the entirety of the simulation.

Finally, it is must be said that the cooling demand is constant through the entire period of the simulation and not changing like the hot water demand, as well as the size of the air handling units are very over sized. When trying to add a changing cooling demands or further fixing the size of the air handling units an error kept occurring which would fail the simulation. Where, for an unknown reason the pressure inside the hot water loop would jump to at least 400 bars when any value in the cold loop was changed. 2 weeks of trials and errors were used to try and find the reason behind the cause of this error however, nothing done helped fix the simulation. So, this is the reason behind the constant cooling demand. Also, the fact that the air handling units are over sized the exit temperature of the water is equal to the inlet temperature of air which is equal to the ambient room temperature, hence the temperature of water in the cold loop was never below 10 degrees Celsius. This means that the extended loop in the cold water loop discussed in subsection 3.2.3 was never used in the simulation, since the switch was never activated because, the water temperature did not reach the boundary required.

5   Results

5.1   Heat Pump Circuit

In this sub-section 5.1 the results relative to the heat pump circuit are presented.

5.1.1   Separator Results

Following the steps of the methodology for sizing the separator these results were achieved. Table 2 presents the state points data in coordination with the points in figure 46. The pipe diameter column was chosen based on the calculations achieved in table 3, with the pipes points presented in the figure on the right of the table. As seen pipes 2, 4, 5, 7 have recommended velocities that are half of pipes 1, 3, 6, and 8 respectively, due to the fact that the mass flow rate is halved as it is sent to two symmetrical separators.

Table 2: Defining the State Points' Data

POINT	pressure Pa	temp K	density kg/m^3	enthalpy J/kg	flowrate kg/s	vapour fraction x	Pipe diameter m
State point Data							
point 1	4500000	293	117	443363	0,73	1	0,035
point 2	10000000	365	200	491342	0,73	1	0,029
point 3	10000000	300	802	261796	0,73	1	0,022
point 4	10000000	294	850	244943	0,73	1	0,022
point 5	4500000	283,15	778	229621	0,73	0,02	0,022
point 6	4500000	284	861	225676	0,37	0	0,019
point 7	4500000	286	330	284845	0,37	0,3	0,035
point 8	4000000	280	379	256495	0,37	0,2	0,029
point 9	4000000	282	110	434411	0,37	1	0,035
point 10	4500000	285	131	427433	0,73	1	0,035

Table 3: Choosing Diameter Calculations

Constants			
pipe number	Density	Flowrate	Recommended Velocity
1	778	0,73	2-4m/s
2	778	0,36	1-2m/s
3	330	0,37	1-2m/s
4	330	0,18	0.5-1m/s
5	131	0,36	1.5-6m/s
6	131	0,73	3-12m/s
7	861	0,18	0.5-1m/s
8	861	0,37	1-2m/s

Diameter Dependent

Pipe1					Pipe5			
Diamter	Area	Den*Area	Velocity		Diamter	Area	Den*Area	Velocity
0,010	7,12E-05	0,055	13,2		0,010	7,12E-05	0,009	39,2
0,013	1,27E-04	0,099	7,4		0,013	1,27E-04	0,017	22,0
0,016	1,98E-04	0,154	4,7		0,016	1,98E-04	0,026	14,1
0,019	2,85E-04	0,222	3,3		0,019	2,85E-04	0,037	9,8
0,022	3,88E-04	0,302	2,4		0,022	3,88E-04	0,051	7,2
0,029	6,41E-04	0,499	1,5		0,029	6,41E-04	0,084	4,4
0,035	9,58E-04	0,745	1,0		0,035	9,58E-04	0,125	2,9
0,041	1,34E-03	1,040	0,7		0,041	1,34E-03	0,175	2,1
0,054	2,29E-03	1,779	0,4		0,054	2,29E-03	0,299	1,2

Pipe2					Pipe6			
Diamter	Area	Den*Area	Velocity		Diamter	Area	Den*Area	Velocity
0,010	7,12E-05	0,055	6,6		0,010	7,12E-05	0,009	78,5
0,013	1,27E-04	0,099	3,7		0,013	1,27E-04	0,017	44,1
0,016	1,98E-04	0,154	2,4		0,016	1,98E-04	0,026	28,2
0,019	2,85E-04	0,222	1,6		0,019	2,85E-04	0,037	19,6
0,022	3,88E-04	0,302	1,2		0,022	3,88E-04	0,051	14,4
0,029	6,41E-04	0,499	0,7		0,029	6,41E-04	0,084	8,7
0,035	9,58E-04	0,745	0,5		0,035	9,58E-04	0,125	5,8
0,041	1,34E-03	1,040	0,4		0,041	1,34E-03	0,175	4,2
0,054	2,29E-03	1,779	0,2		0,054	2,29E-03	0,299	2,4

Pipe3					Pipe7			
Diamter	Area	Den*Area	Velocity		Diamter	Area	Den*Area	Velocity
0,010	7,12E-05	0,023	15,6		0,010	7,12E-05	0,061	3,0
0,013	1,27E-04	0,042	8,7		0,013	1,27E-04	0,109	1,7
0,016	1,98E-04	0,065	5,6		0,016	1,98E-04	0,170	1,1
0,019	2,85E-04	0,094	3,9		0,019	2,85E-04	0,245	0,7
0,022	3,88E-04	0,128	2,9		0,022	3,88E-04	0,334	0,5
0,029	6,41E-04	0,211	1,7		0,029	6,41E-04	0,552	0,3
0,035	9,58E-04	0,316	1,2		0,035	9,58E-04	0,825	0,2
0,041	1,34E-03	0,441	0,8		0,041	1,34E-03	1,152	0,2
0,054	2,29E-03	0,754	0,5		0,054	2,29E-03	1,970	0,1

Pipe4					Pipe8			
Diamter	Area	Den*Area	Velocity		Diamter	Area	Den*Area	Velocity
0,010	7,12E-05	0,023	7,8		0,010	7,12E-05	0,061	6,0
0,013	1,27E-04	0,042	4,4		0,013	1,27E-04	0,109	3,3
0,016	1,98E-04	0,065	2,8		0,016	1,98E-04	0,170	2,1
0,019	2,85E-04	0,094	1,9		0,019	2,85E-04	0,245	1,5
0,022	3,88E-04	0,128	1,4		0,022	3,88E-04	0,334	1,1
0,029	6,41E-04	0,211	0,9		0,029	6,41E-04	0,552	0,7
0,035	9,58E-04	0,316	0,6		0,035	9,58E-04	0,825	0,4
0,041	1,34E-03	0,441	0,4		0,041	1,34E-03	1,152	0,3
0,054	2,29E-03	0,754	0,2		0,054	2,29E-03	1,970	0,2

Table 4, shows the calculation results to find the total charge of the refrigerant and the total volume of the system. After finding the charge and volume, the values were used to find whether one or more separator are required based on the manufacturer available sizing. As seen in table 5, the results show that one separator with a height and diameter of 700mm and 150mm respectively will not be enough to host all of the refrigerant, hence two separators were used and the connections between the separators was presented earlier in figure 49. The results also show that the 700mm height is enough but the inlet pipes must be placed above 680mm since that would be liquid level if the all the refrigerant in the system is hosted in the separator.

Table 4: Charge Calculation

component	Density kg/m^3	length m	area m^2	volume m^3	Charge kg	D*A (kg/m)	flowrate kg/s	flowrate/(D*A) (m/s)	recommended value
compressor suction	117			0,0050	0,59				
compressor high pressure	200			0,0004	0,08				
Gas cooler	501			0,0083	4,16				
IGHX high pressure	826			0,0021	1,71				
IGHX suction	124			0,0021	0,26				
Ejector	579			0,0002	0,12				
Evap 1	595			0,0028	1,68				
Evap 2	245			0,0044	1,08				
suction line	117	1	9,58E-04	0,0010	0,11	0,11	0,73	6,5	3-12m/s
discharge line -GC	200	1	6,41E-04	0,0006	0,13	0,13	0,73	5,7	5-12 m/s
discharge line -IGHX	802	1	3,88E-04	0,0004	0,31	0,31	0,73	2,3	2-4m/s
IGHX-Ejector line	850	1	3,88E-04	0,0004	0,33	0,33	0,73	2,2	2-4m/s
ejector - seperator line	778	0,5	3,88E-04	0,0002	0,15	0,30	0,73	2,4	2-4m/s
liquid line - evap 1+exp valve	861	1	2,85E-04	0,0003	0,25	0,25	0,37	1,5	1-2m/s
liquid line - exp to evap 2	379	1	6,41E-04	0,0006	0,24	0,24	0,37	1,5	1-2m/s
evap 1- seperator line	330	1	9,58E-04	0,0010	0,32	0,32	0,37	1,2	1-2m/s
evap 2- ejector line	110	1	9,58E-04	0,0010	0,11	0,11	0,37	3,5	3-12m/s
seperator - IGHX suction line	131	1	9,58E-04	0,0010	0,13	0,13	0,73	5,8	3-12m/s
seperator 1	861			0,0124	2,13				
seperator 2	861			0,0124	2,13				
SUM				0,056448404	16,00				

Table 5: Stand Still Calculations

Stand Still Calculations

Specific volume m^3/kg								
0,0035								

	Temperature (C)	Temperature (K)	Pressure (Pa)	Pressure (bar)	Density (kg/m^3)	Vapor Fraction		
	20,00	293,15	5729052,58	57,29	283,45	0,58		
	25,00	298,15	6434244,25	64,34	283,45	0,78		
Max temp before transcritical	27,71	300,86	6846091,61	68,46	283,45	1,00		

Assuming that the seperator tank is 1K lower than rest of system to ensure that all the liquid CO2 is in tank	Temperature (C)	Vapor Fraction	Charge (kg)	Liquid Amount (kg)	Seperator design	Height (m)	Diameter (m)	Volume (m^3)	Volume (L)
	20	0,58	16,15	6,79		0,7	0,15	0,012	12,37
	25	0,78	16,15	3,52		0,7	0,15	0,012	12,37
	27,71	1,00	16,15	0,00				Total volume available	24,74

Check if the total liquid will fit in seperator	Liquid Volume (m^3)	Liquid Volume (L)	Liquid Height (m)	Liquid Height per seperator (m)	Liquid Volume per seperator (L)	Fits in Seperator?
	0,024	23,96	1,36	0,68	11,98	yes
	0,012	12,43	0,70	0,35	6,22	yes
	0,000	0,00	0,00	0,00	0	yes

It was later decided by the manufacturer that a separator with a height of 867mm and a diameter of 219mm is possible to achieve, hence the new volume of the separator will around 32.6 liters and since, the total charge of the refrigerant is 24 liters one separator will suffice and the calculations for choosing the diameters with pipe numbering are shown in table 6. The final separator design with the dimensions sent to the manufacturer is shown in figure 58

Table 6: One Separator Pipe Diameter Calculations

Constants

pipe number	Density	Flowrate	Recommended Velocity
1	778	0,73	2-4m/s
2	131	0,73	3-12m/s
3	330	0,37	1-2m/s
4	861	0,37	1-2m/s

Diameter Dependent

Pipe1

Diamter	Area	Den*Area	Velocity
0,010	7,12E-05	0,055	13,2
0,013	1,27E-04	0,099	7,4
0,016	1,98E-04	0,154	4,7
0,019	2,85E-04	0,222	3,3
0,022	**3,88E-04**	**0,302**	**2,4**
0,029	6,41E-04	0,499	1,5
0,035	9,58E-04	0,745	1,0
0,041	1,34E-03	1,040	0,7
0,054	2,29E-03	1,779	0,4

Pipe3

Diamter	Area	Den*Area	Velocity
0,010	7,12E-05	0,023	15,6
0,013	1,27E-04	0,042	8,7
0,016	1,98E-04	0,065	5,6
0,019	2,85E-04	0,094	3,9
0,022	3,88E-04	0,128	2,9
0,029	6,41E-04	0,211	1,7
0,035	9,58E-04	0,316	1,2
0,041	1,34E-03	0,441	0,8
0,054	2,29E-03	0,754	0,5

Pipe2

Diamter	Area	Den*Area	Velocity
0,010	7,12E-05	0,009	78,5
0,013	1,27E-04	0,017	44,1
0,016	1,98E-04	0,026	28,2
0,019	2,85E-04	0,037	19,6
0,022	3,88E-04	0,051	14,4
0,029	6,41E-04	0,084	8,7
0,035	9,58E-04	0,125	5,8
0,041	1,34E-03	0,175	4,2
0,054	2,29E-03	0,299	2,4

Pipe4

Diamter	Area	Den*Area	Velocity
0,010	7,12E-05	0,061	6,0
0,013	1,27E-04	0,109	3,3
0,016	1,98E-04	0,170	2,1
0,019	2,85E-04	0,245	1,5
0,022	3,88E-04	0,334	1,1
0,029	6,41E-04	0,552	0,7
0,035	9,58E-04	0,825	0,4
0,041	1,34E-03	1,152	0,3
0,054	2,29E-03	1,970	0,2

Figure 58: Final Separator Dimensions done by INDEE+

5.1.2   Modelica Results

After running the simulation, the heat pump results gathered from modelica are presented below. Starting with the Ph diagram of the system, which was produced via the use of Dave software. The state points presented in the diagram 59 are relative to the points seen in figure 39. Based on the state point values, the calculated pressure lift by the ejector is 7 bars.
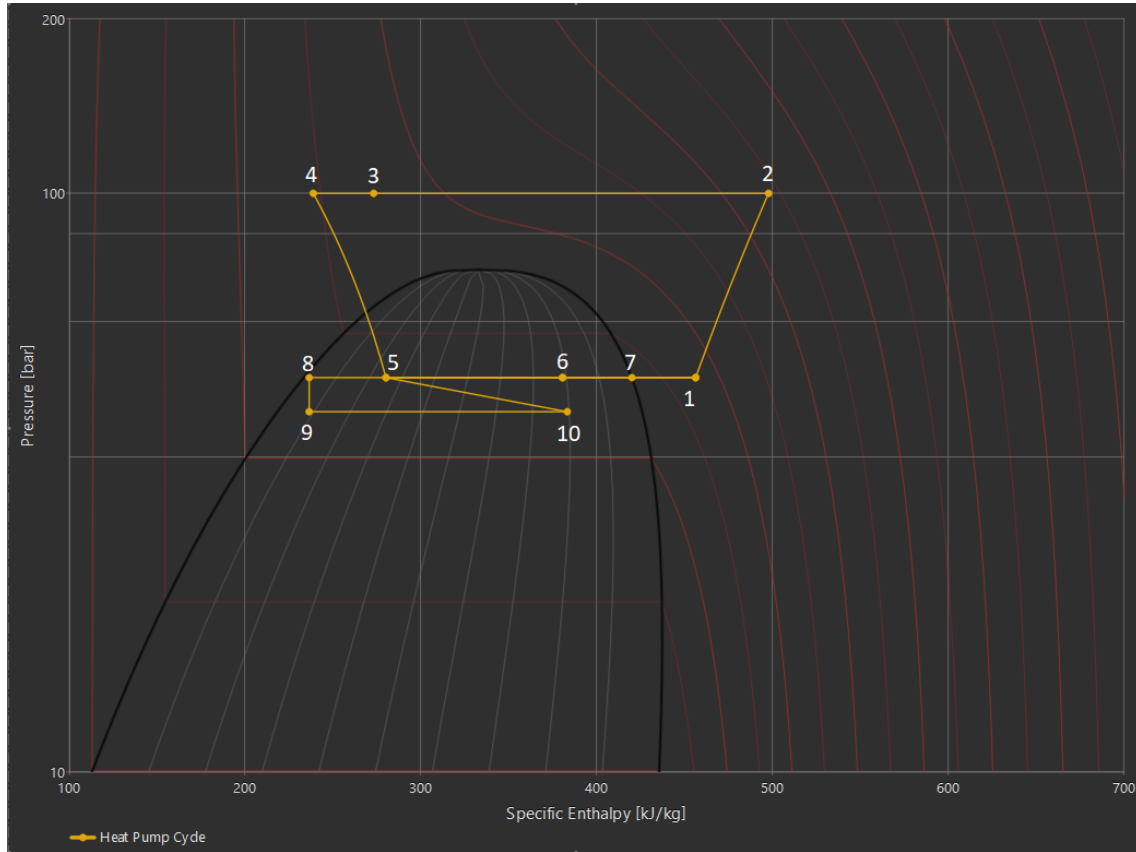
Figure 59: Ph diagram of simulated Heat Pump system

Via the use of modelica, the average cooling, heating and total COPs are 4.5, 5.4 and 9.9 respectively. With the average total cooling capacity is 133kW with the capacity of the first evaporator is 88kW and second evaporator 45kW and the heating capacity (gas cooler capacity) 160kW. This is shown in figure 60.
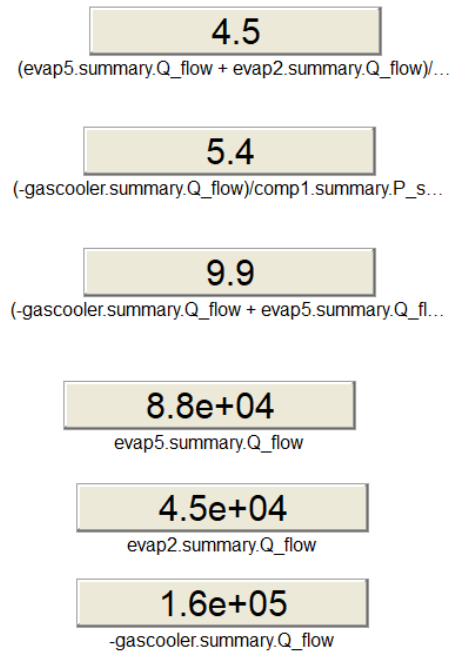
Figure 60: Calculated average COP and cooling capacities

Via the ejector PI controller, the high side pressure is controlled to be at 100 bars as seen in figure 61. As described in section 2.5.2 earlier, this is to achieve a low approach temperature at the exit of the gas cooler. Figure 62, shows the approach temperature over the entire duration of the simulation, with the average approach temperature between the outlet CO_2 temperature from gas cooler and the inlet water temperature to the gas cooler is 4.43^OC.
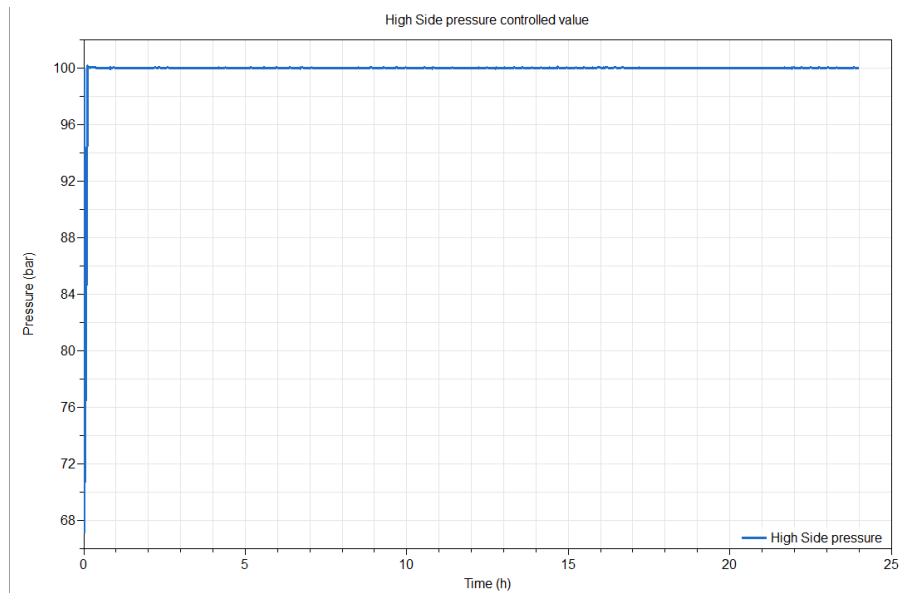
Figure 61: High side pressure value
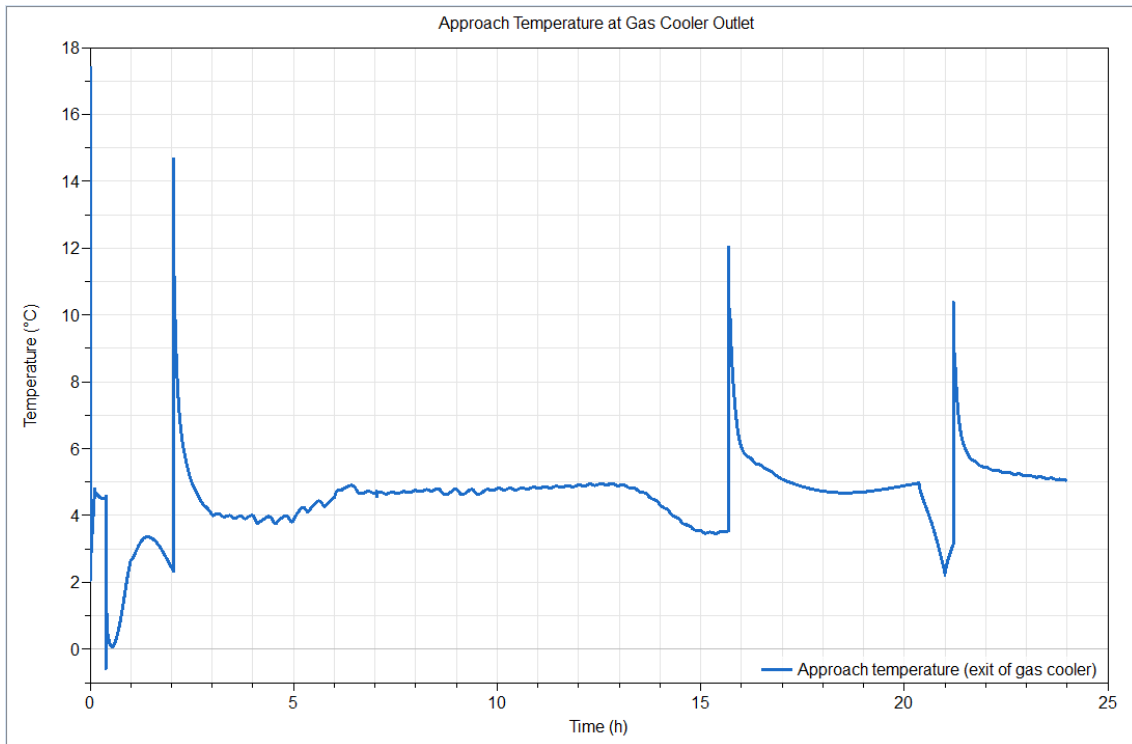
Figure 62: Approach temperature at the exit of gas cooler.

From data collected from modelica, a Th diagram was produced to show the location of the pinch point for the gas cooler, this is shown in figure 63.
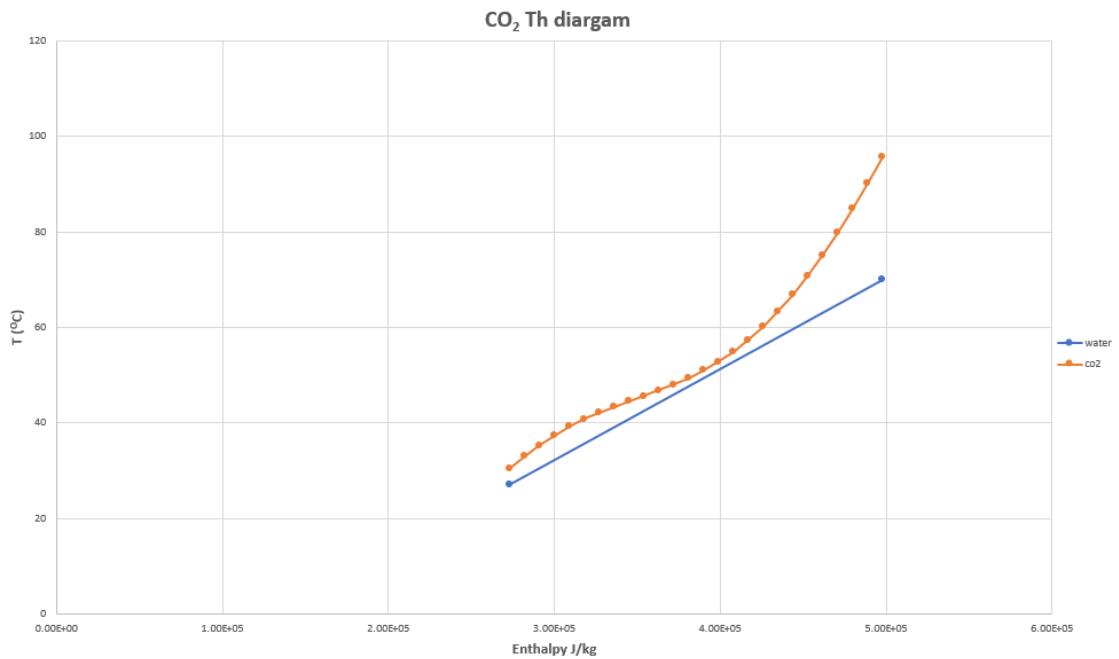
Figure 63: Th diagram to show the pinch point in the gas cooler.

Finally the heat pump's energy demand is shown in figure 64. The figure shows both the shaft power in W and frequency in Hz. The average shaft power input is 30.5kW and the average energy demand per day is 731.5kWh.

63
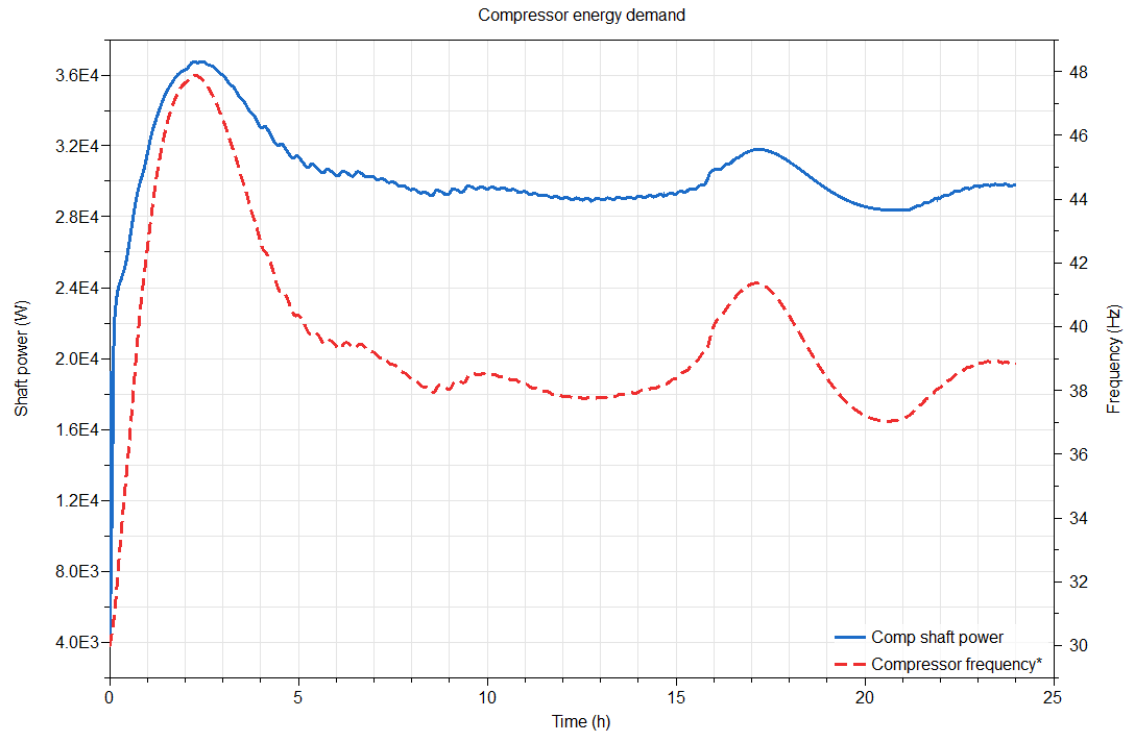
Figure 64: Compressor's shaft power input and frequency.

5.2 Hot and Cold water loops results

In this subsection 5.2, data produced by modelica that is relative to the hot and cold water loops have been collected and processed by modelica to produce the required diagrams. To start, the amount of hot water produced has been investigated with three different cases of hot water demands, as can be seen in Figure 65. Where case 1, has the least hot water demand of 37500L (an average of 0.43kg/s) over a 24 hour period. Case 1 resembles the real hotel's demand. Case 2, has 1.5 times more hot water demand when compared to case 1. Which is equal to 56250L (an average of 0.65kg/s) over a 24hr period. Finally, case 3, which has the highest hot water demand at 75000L (an average of 0.87kg/s) per day. These 3 different cases were investigated to test the system, and see what it can handle. As well as, the affect of increasing the hot water demand on the behaviour of tanks and system as a whole. The hot water produced per day is 77400L, which means an average 0.9kg of hot water is produced every second.

The amount of hot water demand per hour throughout the day was depicted based on real data of similar hotels, that show the hot water demand divided throughout the day. This is shown in figure 65. The figure will be further discussed in section 6.

64
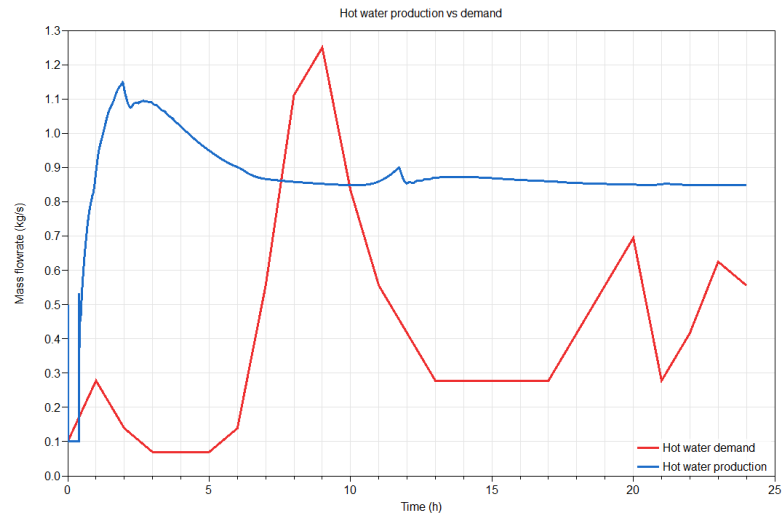
(a) Case 1: Lowest HWD
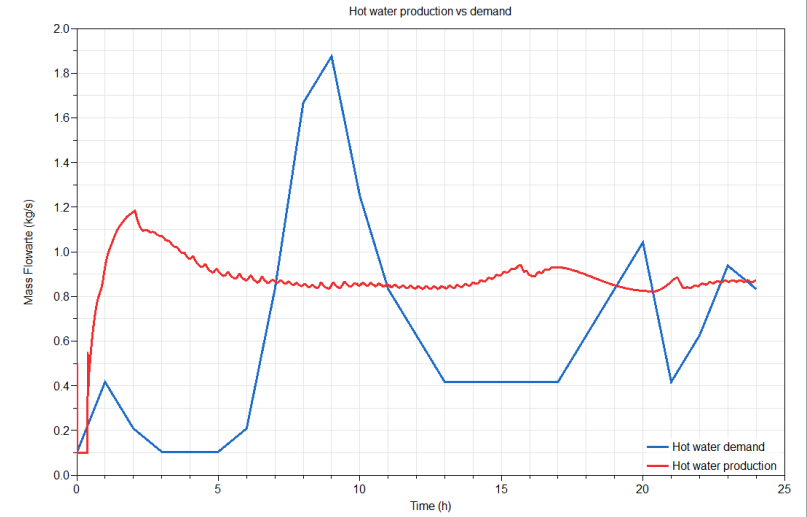
(b) Case 2: Middle HWD.
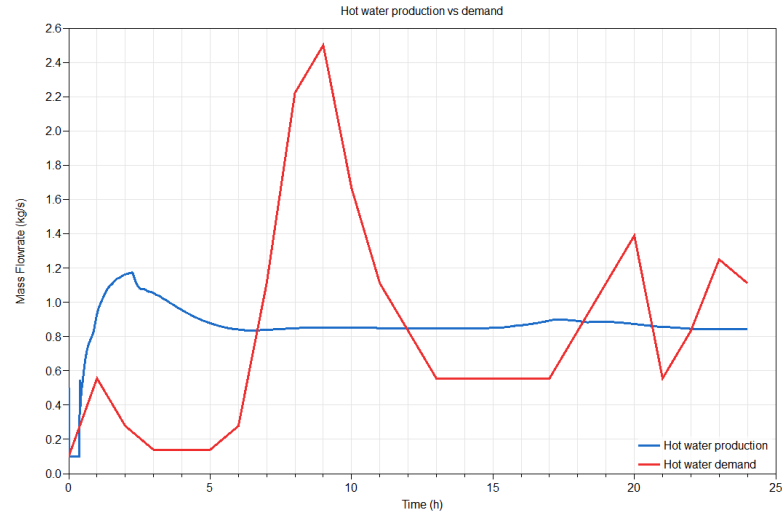
(c) Case 3: Highest HWD

Figure 65: 3 Cases of HWD vs HWP

Figure 66, shows the effect of the hot water demand on the hot water loop operation, and show that the control strategies for charging, discharging and fully charged operations are successful. This will be depicted in section 6.

Figure 67, shows the temperature at the bottom of tank 5 and its direct effect on the position of the three directional valve. When its position value is 0 then the direction is towards the extended loop when it is 1 the direction directly towards the pump to the gas cooler.

Figure 68, shows the effect of hot water demand on the temperature of the supplied water as well as exploring how the charging and discharging of tanks occur and what that tells us about the system.

Figure 69, represents the average temperature of water inside each one of the tanks over the period of simulation, which is used to analyze the tank behaviour in three different cases and whether stratification was maintained or not.

Figure 70, shows the control operation of the switches connected to the tanks for the return water of the building. If the value of the switch position is 1 then it is open. There can be only one switch open at a time and that depends on the return water temperature from building. These figures also make it easier to understand figure 69 regarding the temperature inside the tank.

Figure 71, shows the temperature of water at the inlet and outlet of the gas cooler, as well as the supplied water temperature. From these figures, the effect of increasing hot water demand on the inlet temperature of the gas cooler and supplied temperature of water can be depicted. As well as, showing that no matter the inlet temperature is the outlet temperature of water from the gas cooler is always 70^OC.

All figures presented in this section are further discussed in the section 6.
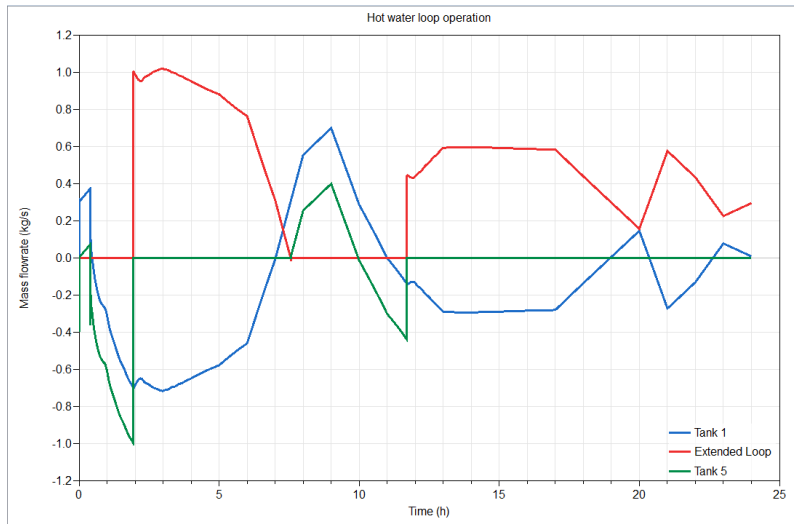
(a) Case 1: Lowest HWD
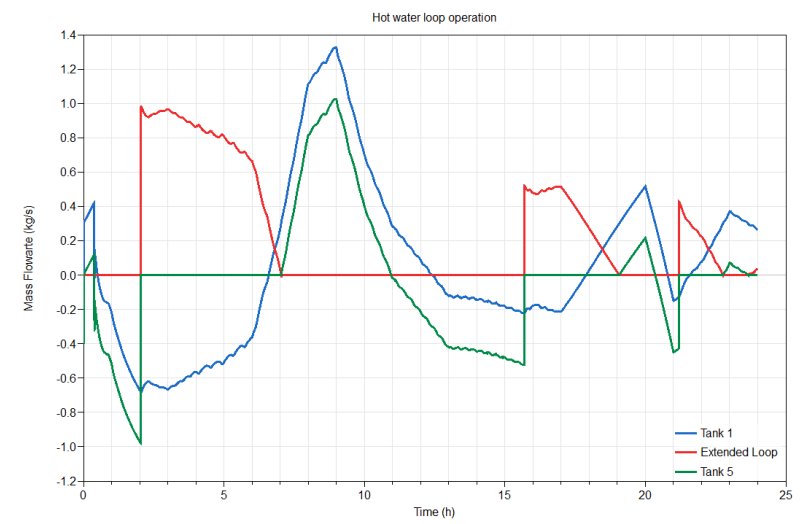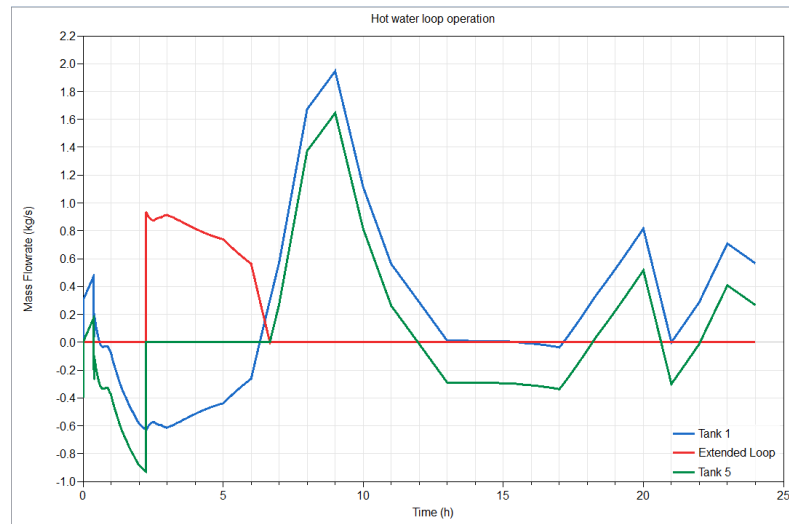
(b) Case 2: Middle HWD.

(c) Case 3: Highest HWD

Figure 66: Hot water operation.
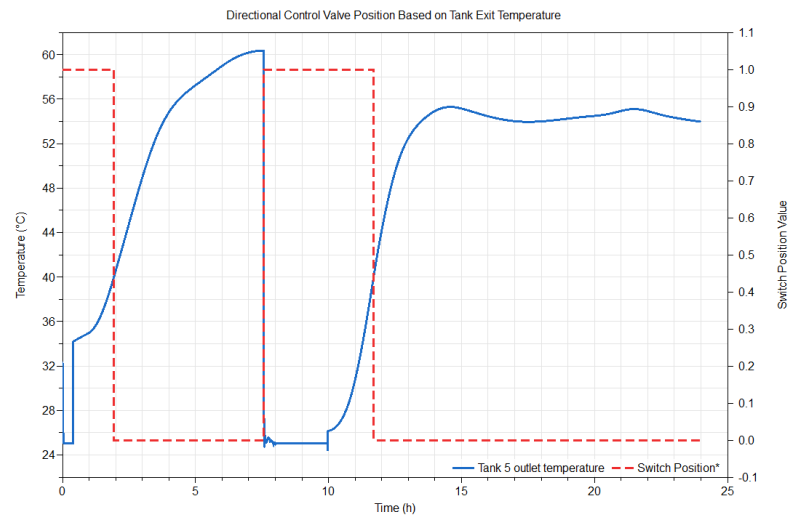
(a) Case 1: Lowest HWD
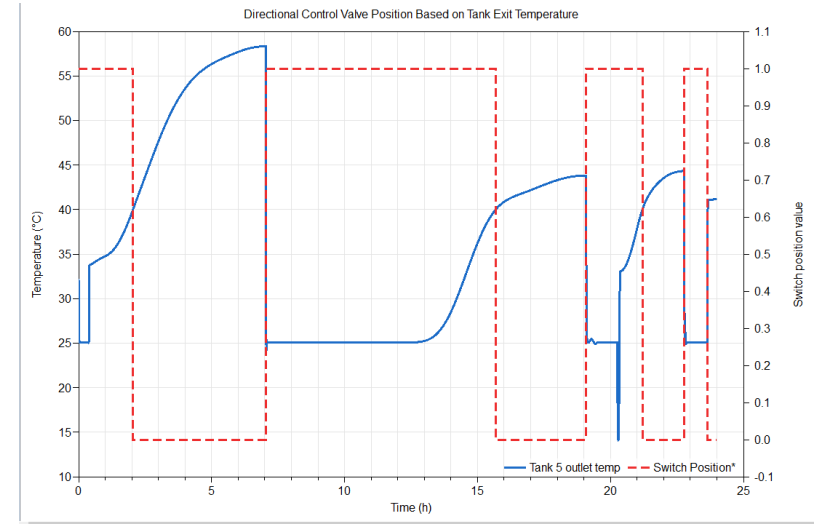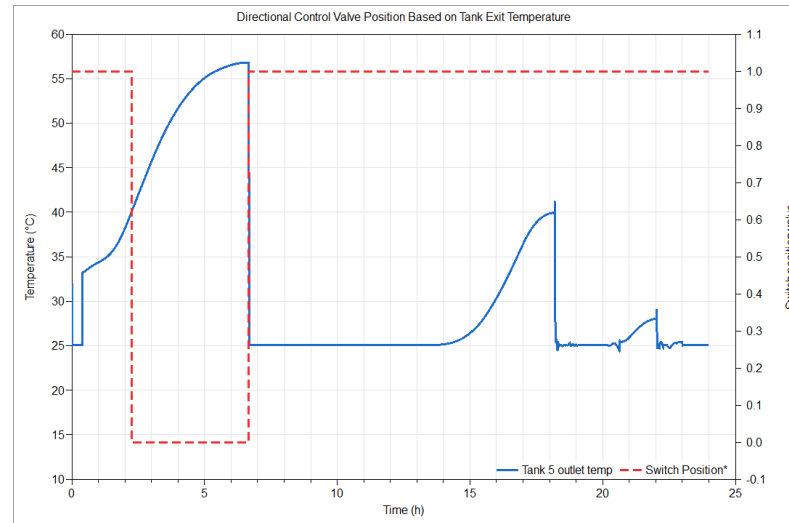
(b) Case 2: Middle HWD.

(c) Case 3: Highest HWD

Figure 67: Operation of directional control valve.
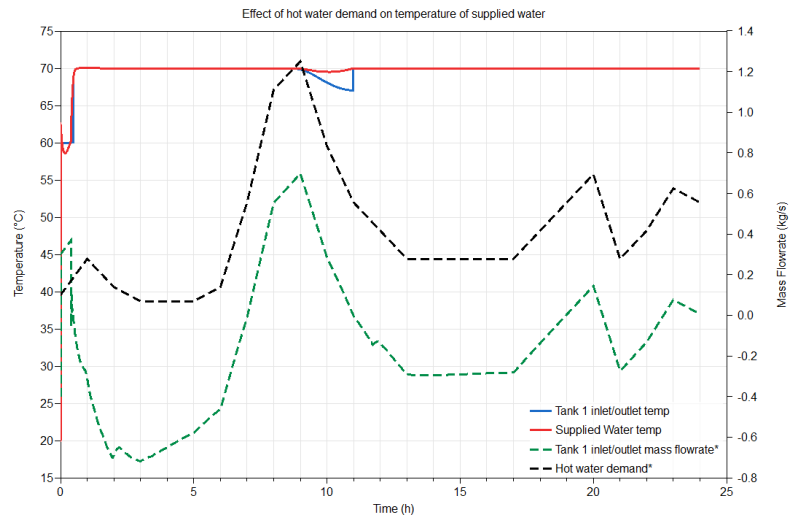
(a) Case 1: Lowest HWD
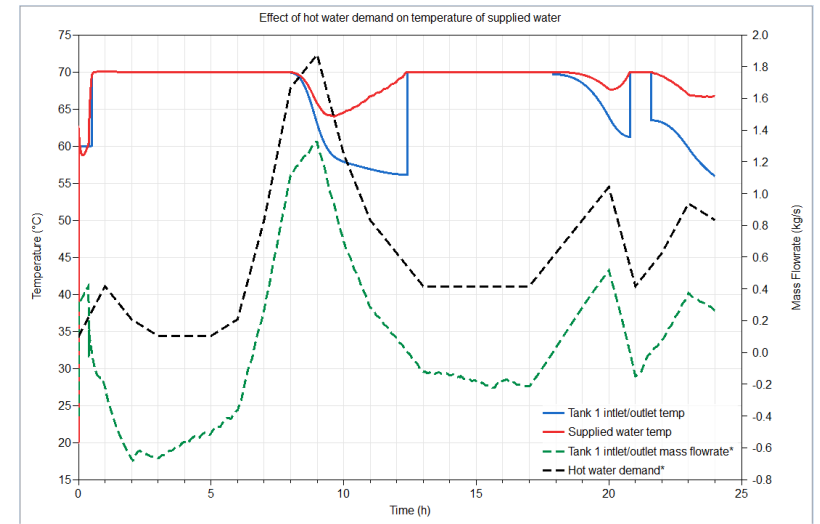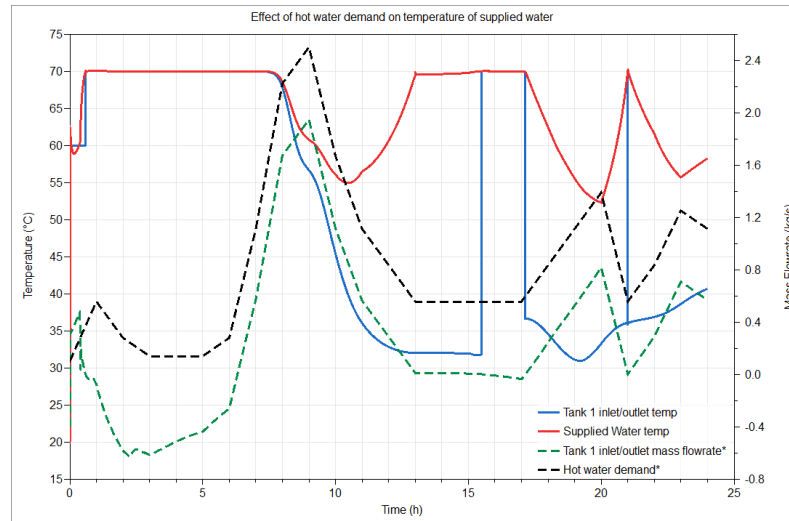
(b) Case 2: Middle HWD.

(c) Case 3: Highest HWD

Figure 68: Hot water demand vs temperature of hot water supplied
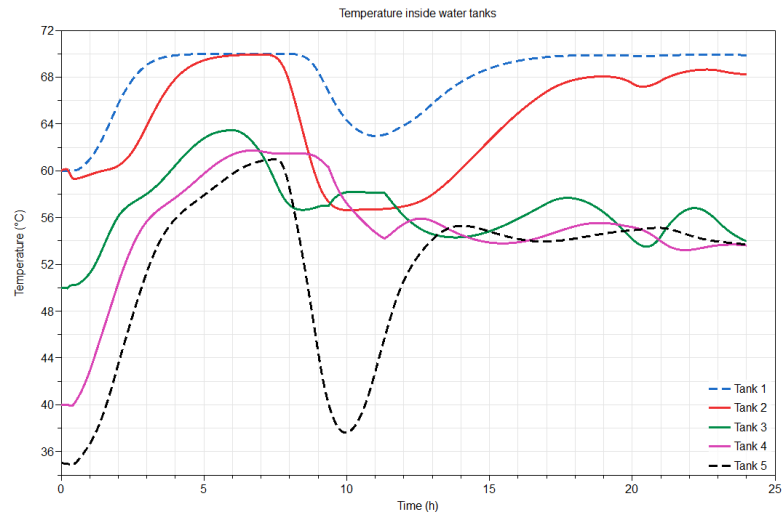
(a) Case 1: Lowest HWD
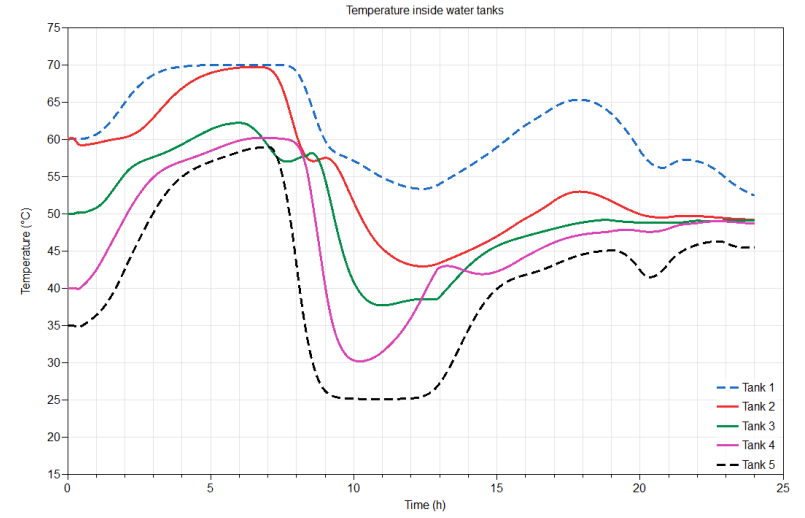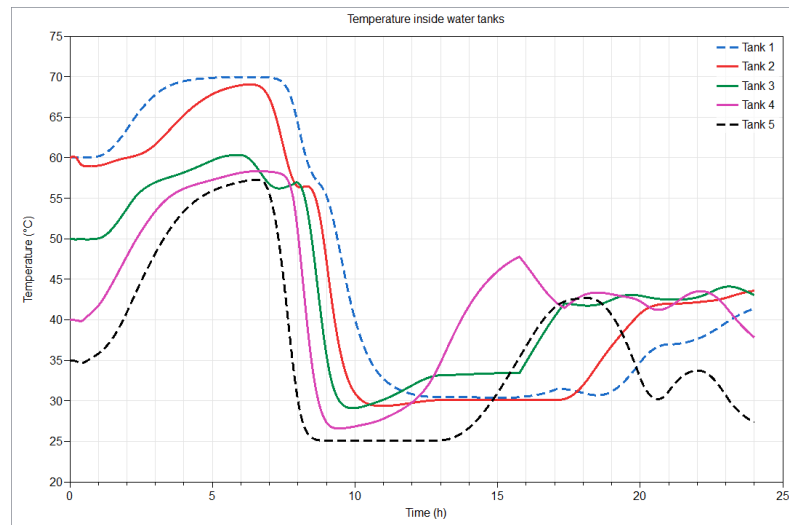
(b) Case 2: Middle HWD.

(c) Case 3: Highest HWD

Figure 69: Temperature of water inside each of the tanks
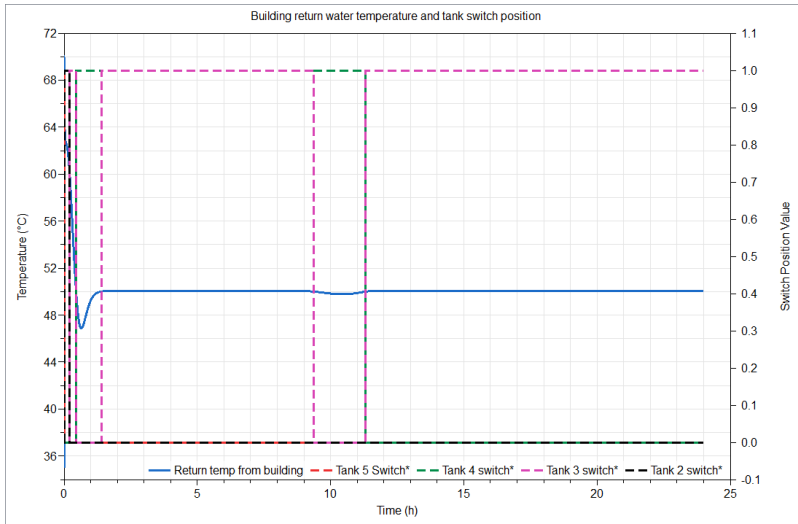
(a) Case 1: Lowest HWD
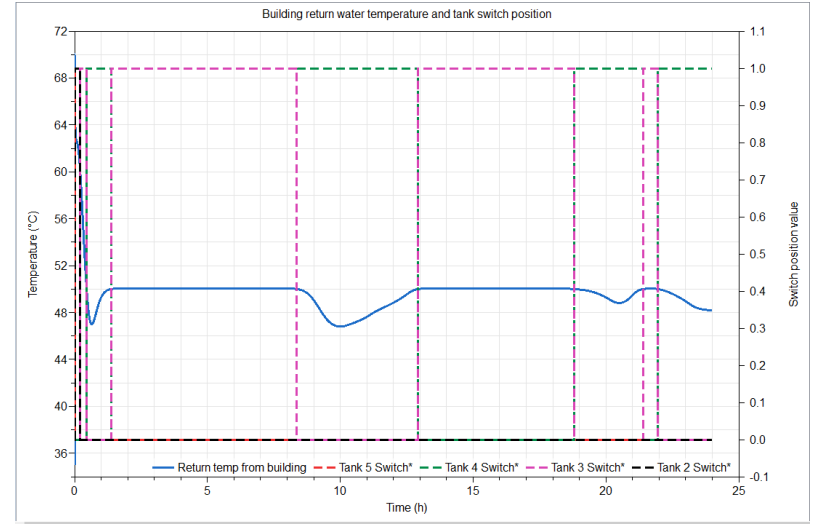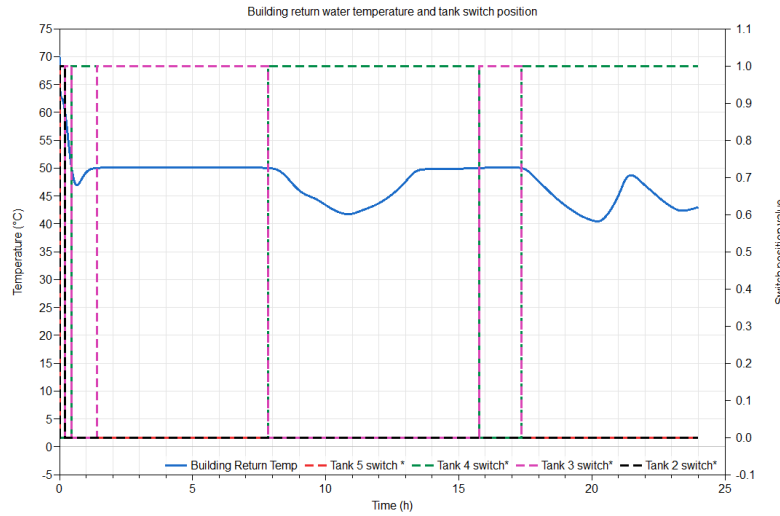
(b) Case 2: Middle HWD.

(c) Case 3: Highest HWD

Figure 70: Building water return temperature and tank switches activation
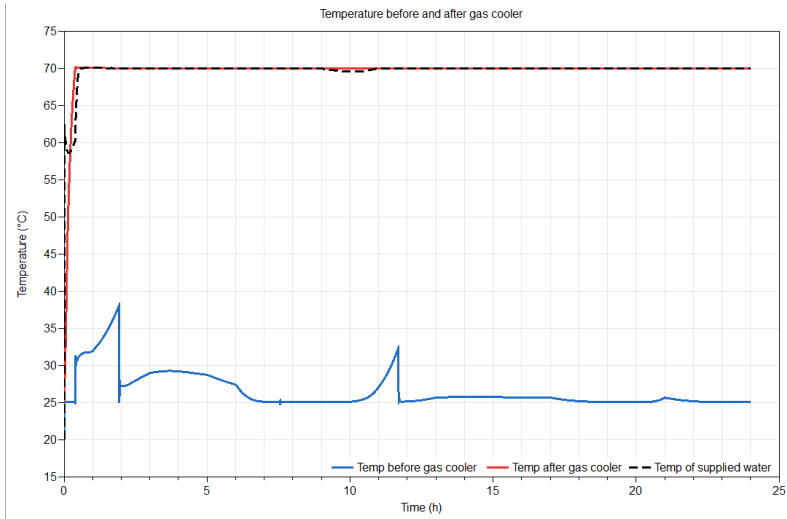
(a) Case 1: Lowest HWD
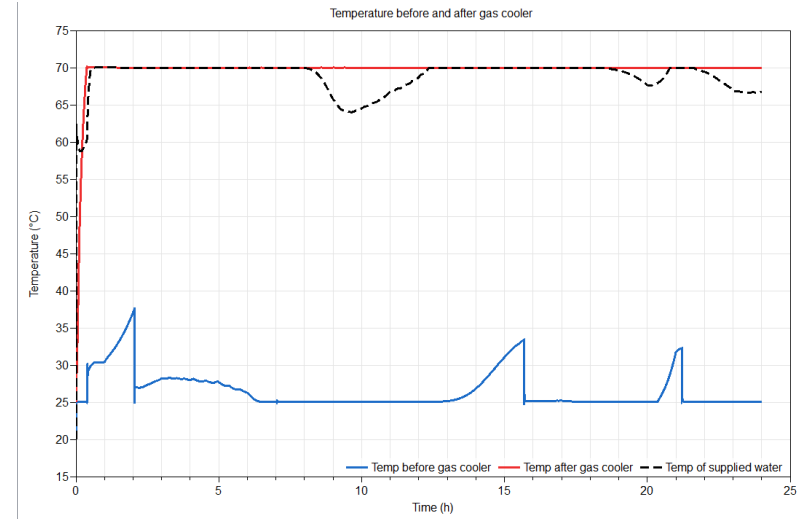
(b) Case 2: Middle HWD.
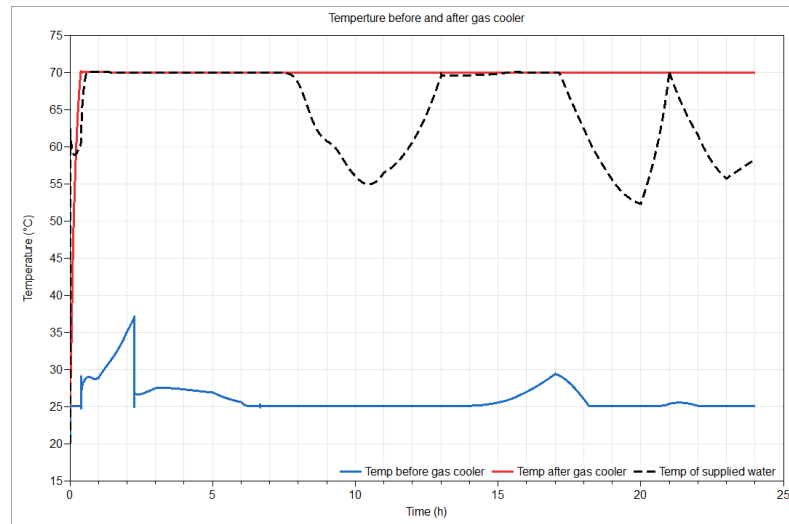
(c) Case 3: Highest HWD

Figure 71: Temperature before and after gas cooler

6 Discussion

6.1 Separator

In both separator design setups, the two separators in figure 49 and the single separator in figure 58 use a diffuser. This ensures no liquid is drawn through the suction line to compressor which is of extreme importance. However, if that occurred at small amounts for any reason the internal heat exchanger on the suction line will be able to evaporate the accidental drawn liquid. Hence, no liquid refrigerant will ever enter the compressor. The use of view visors is also a great addition to the separator, this will allow the technician to view the liquid level of the refrigerant in the separator. As seen in figure 50, the cut in the inlet pipes is important to direct the refrigerant to enter the separator in a downward angle, this was used also to prevent the liquid particles of being sucked into the compressor suction line. The position and placement of the pipes connected to the separator is also of utmost importance. The inlet pipe from ejector, and inlet pipe from the medium pressure evaporator should both be placed at a height that is will be above the liquid level in the separator in both operating and standstill conditions so no flow back occurs. As seen in figure 50, the pipes should not be placed in front of each other but at perpendicular angles to each other to avoid fluid flowing into the opposite pipe.

The suction pipe should be placed at the top of the separator, to significantly decrease the chance of any liquid being sucked to the compressor, and on the top for the obvious reason that the vapor will be accumulating in that region. The oil pipe return line is placed at the lowest point of the separator, (bottom middle) due to the fact that the oil has a higher density than the refrigerant. So, it will be accumulating in that region, as it is easier to return the oil to the suction line of the compressor. The liquid line pipe to the evaporator is positioned a bit to the side of the center, with the pipe length continuing to the inside of the separator just above the oil accumulation area. This is done to be sure that the refrigerant going to the evaporator has the least amount of oil as possible. Since, oil will decrease the efficiency of the evaporator significantly and by canceling this drawback the efficiency of the system will improve.

As presented in the results table 6, the green highlighted lines are the recommended diameters, for pipe 1 and pipe 4 as seen the highlighted cells do not fall within the recommended velocities and there are reasons for that. For pipe 1 the chosen diameter is 35mm, which will result in a lower velocity for the inlet of the separator. This is advantageous for the fact that at lower velocities the gas and liquid refrigerant is much easier to separate. In pipe 4 the lower velocity, is advantageous for easier control, moreover having it at 35mm means that there will not be any workmanship errors when placing the pipes (all same size) and it would be much easier to manufacture.

6.2 Modelica

From the Ph diagram seen in figure 59, it is possible to see the state of the CO_2 refrigerant in the high side pressure, medium side pressure and low side pressure. From this a lot of information can be gathered, such as the capacity of each of the heat exchanger in the circuit. Where the outlet temperature of CO_2 from the gas cooler is around 30^OC, in addition extra subcooling via the internal heat exchanger to reach a temperature of around 20^OC before expansion. The use of the internal heat exchanger is of utmost importance, as the cooler the CO_2 is before throttling via the ejector, the less expansion losses are to occur. As well as, resulting in a higher cooling capacity. The internal heat exchanger was also used to superheat the CO_2 in the suction line in order to evaporate any liquid CO_2 sucked accidentally into the suction line of the compressor. It can also be seen that both evaporators are run in overfed operation, as the outlet of CO_2 refrigerant in the two phase region is at a vapor fraction less than 1, about 0.7 to 0.8 vapor fraction. Moreover, the state of CO_2 at the exit of ejector as well as the amount of pressure lift.

From the results seen in figure 60, the system has achieved its required capacities, with a high COP especially for a country with very warm climate. CO_2 as a refrigerant proves to be very effective in this system which makes it a successful system. With a total COP of 9.9, heating and cooling COPs of 5.4 and 4.4 respectively. This heat pump system is very efficient.

Following the theory in section 2.5.2, the heat pump system's high side pressure was designed in order to achieve a low approach temperature constantly during operation. This was achieved but not totally successfully, due to the fact that there are outlying peaks where the water inlet temperature is higher than 30 degrees for a really short time. But an average approach temperature over the 24 hour period was 4K more or less. Which is, still great as the outlet CO_2 temperature from the gas cooler will have lowest temperature possible depending on the inlet temperature of water. This also mean the characteristic of the high temperature glide of CO_2 in supercritical region was utilised to the fullest. Even though, the approach temperature is quite low the pinch point in the gas cooler is more towards the middle rather the end. This not very favorable as it means not the entire area of the gas cooler was used to the fullest. By lifting up the high side pressure to 110bars for example the pinch point would have been at the outlet of the gas cooler as seen in figure 72. Which means the high side pressure control can be further optimised and controlled dynamically for a better result. Section 7 presents how this can be achieved.

From figure 64, the shaft power input and the frequency of the compressor can be depicted. From the shaft power line, the average energy demand can be found. This is done by finding the average shaft power over the 24 hour period then multiplying it by 24 to see the energy demand per day over each hour. Which was calculated to be 731.5kWh with an average of 30.5kW per hour. The figure, also shows the frequency (speed) of the compressor, where the minimum frequency possible is 30Hz and max is 70Hz. Hence, from the figure it can be seen that the compressor never reaches a frequency over 45Hz; which means that the compressor never ran on full capacity. The displacement of the compressor was over-sized purposefully, for different scenarios. For example, if more hot water production is required to supply the hot water demand, the cooling capacity can be increased by utilising the extended loop to warm up the chilled water more than 12^OC. By doing that the compressor used capacity is going to increase, since more cooling is required. Hence, a higher frequency will occur. The higher compressor capacity, is also used for the case, if the city water is supplied at a lower temperature than 25^OC for example 20^OC then the system can automatically increase the capacity, to be still capable of lifting the temperature to 70^OC. Or in the opposite case, if the water in the cold loop reached a temperature higher than 12^OC at the inlet of the first evaporator then the pressure in the medium and low pressure circuits is going to decrease to still be able to achieve an outlet temperature of 7^OC, hence the used capacity of the compressor is going to increase to keep the system running to achieve the set point values.
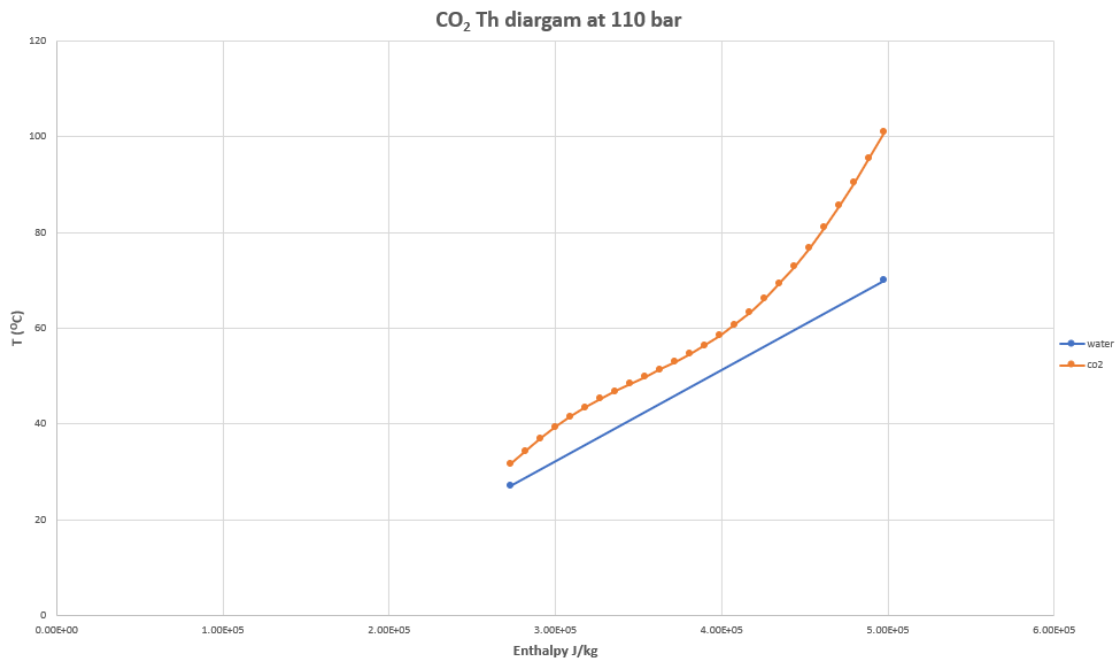
Figure 72: Th diagram to show the pinch point in the gas cooler at 110bar.

6.3   Hot and Cold water loops

Starting with figure 65, it can be seen that in all three cases the hot water production amount is identical. The hot water demand profile was also the same in all cases, as seen, the profile suggest the water demand increases slightly at 01:00hr then decreases again until 03:00hr and levels off until 05:00hr. Then the demand increases dramatically from 06:00hr till 09:00hr which is when the demand is at its peak of the day. This resembles when the guests are getting ready in the morning. Then it starts to decrease until 13:00hr where it levels off until 17:00hr. Then it increases until 20:00hr, where it reaches its second highest peak point and the third highest peak point is at hour 23:00hr. The highest hot water production occurs at 02:00hr in all cases.

After understanding the temperature profile, it can be seen that in case 1 the hot water demand was higher than the hot water production between 07:30hr and 10:00hr. Which is the only time the system is going to be run in discharging operation, since the hot water production is lower than that of the demand. Applying this understanding to the two other cases, in case 2 the system is going to run in discharging operation three times from 07:00hr till 11:00hr, 19:00hr till 20:30hr and from 22:50hr till 23:30hr. Finally, the final case, similar to case 2 there are three peaks where the hot water demand is higher than hot water production, however, unlike case 2, for much longer periods under discharging operation.

From figure 66, the hot water loop operation can be analysed. Hence, the type of operation can be depicted. The figures follow the mass flow rates in the loop at three different locations. One mass flow rate sensor was placed at the top port of tank number 1 (blue line), one at the inlet of the extended loop (red line), one at tank number 5 port (green line). All mass flow rate sensors are labeled in figure 55. As seen in figure 66, the mass flow rate value can be negative, this only depends on the orientation of the sensor in the loop. So, when the mass flow rate is negative the flow is going in the opposite direction.

It can also be analyzed that there cannot be a flow over the extended loop and tank 5 mass flow rate sensors simultaneously. This will suggest if the system is in charging or discharging or fully charged operation mode. Analyzing each line individually, if the mass flow rate sensor value of tank 1 is positive then it is discharging. And, if the value of the extended loop mass flow rate sensor is positive then the directional control valve (DCV) switch is active and the loop is in operation. This means, that the system is fully charged. Finally if tank 5's mass flow rate sensor (mfr) is positive then the system is discharging and cold city water is entering tank 5, if it is negative then it means it is charging however, did not reach to fully charged operation conditions yet.

From the figures it can be summarised, that in case 1 the system run mostly in fully charged operation. Where it was rejecting heat to the ambient via the extended loop, except at the time of peak demand. In the other two peak demands, the tanks were still fully charged and the water temperature at the bottom port of tank 5 is over 40^OC.

The extended loop is still in operation, even when hot water is leaving tank 1 because hot water production (HWP) is bigger than the demand (HWD). This is not favorable, as it means alot of the heat would be wasted to the ambient, and the system is oversized. To overcome this without changing the system, a larger or additional water tanks can be used. Or an interesting way to use the waste heat is using the heat to warm a pool water rather than rejecting it to the ambient. This could be something to do for future work (section 7).

With the increase of hot water demand compared to case 1, case 2 had a more balanced operation, sharing similar amounts of time in each type of operation. In all three peak demand times, the system worked in discharging mode and used the available hot water stored in the tank. So, in off peak hours the system recharges with hot water rather than just rejecting heat to the ambient. This says that the heat pump system is oversized for case 1 and is better optimized for case 2. This means if the hotel wanted a small expansion then the heat pump system installed will still be able to provide for the extra demand.

Finally, in case 3 the system was mostly run in in discharge operation, where the system was not able to produce enough hot water to be charged into the tanks, and was only in full charge operation between 02:00hr till 06:30hr. In this case, more hot water production was needed, and

since the compressor is oversized for this case. The extended loop on the cold water circuit will activate which warms the return water to the evaporator to higher temperature, to increase the cooling load, which increases the mass flow rate of CO_2 over the gas cooler since the frequency of the compressor increases. Hence, the mass flow rate of water in the hot water loop is increased to keep the outlet temperature of water at 70^OC, leading to more hot water production. This can be investigated further in the future as suggested in section 7.

Figure 67, further dissect the hot water operation, where it shows when the system is fully charged by showing the temperature of water at the bottom port of tank 5, as well as, the direction of the switch which either directs the water into the extended loop or towards the gas cooler pump directly. More accurately, it can be know how many times was the extended loop utilized and for how long. It can be analyzed that when the temperature sensor is 40^OC or more then the switch direction flips and now the flow is directed towards the extended loop (switch value 0) only if HWP is bigger than the HWD. The sudden drop of the temperature occurs when the flow is switched, and the system is discharging. Due to the hot water demand being much higher than the hot water production. So at that instance the water drops to 25^OC which is the cold city water temperature. As is it can be seen, whenever the switch value switches to 1 it is when the hot water tanks are being discharged and the temperature suddenly drops. In case 3, the temperature of water also reaches 40^OC at one point, but the switch value does not switch to 1. This is due to the fact, that the instant it reached 40^OC, the hot water demand was higher than hot water production and the flow was reversed. Hence, there are two boundary conditions for the switch to activate and direct the flow to the extended loop. One, is the hot water production is higher than hot water demand. Second, the water temperature at the bottom port of tank number 5 must be over 40^OC.

Figure 68, explores the effect of hot water demand on the water temperature supplied to the building. Where the red line represents the temperature of water supplied, the blue line is the temperature of water in top of tank 1. The dotted black line is the hot water demand flow rate and the green dotted lined is the mass flow rate in and out of tank 1. Hence, when the mass flow rate of green dashed line is positive that means that the system is discharging, because hot water demand is higher than the hot water production. As it can be seen in case 1 the supplied water temperature is almost always at 70^OC and the temperature from tank 1 drops to 68^OC. In case 2, the supplied water temperature to the building reaches 64^OC at its lowest which occurred during peak hours. In case 3, the supplied water temperature was less than 70^OC for much longer periods. At two points, tank 1's temperature sensor suddenly lifts to 70^OC, at that instant the tanks are charging and since the hot water produced is 70^OC the sudden lift happens. It can also be seen that the tanks fully discharged in case three where the water temperature leaving tank 1 has reached 30^OC.

Figure 69, presents the average temperature inside each of the tanks over the simulation period of 24 hours. It is said when the outlet temperature of tank number 5 is 40^OC and above then the tanks are fully charged. Hence, case 1 finishes the day with fully charged conditions. Same as with case 2. In case 1 and 2 water stratification between tank 1 and 2 was maintained and never crossed. However, stratification between the remainder of the tanks was not maintained this is mainly caused by the return temperature and which switches are activated as seen in figure 70. It can be seen that the stratification was mainly broken between tank 3 and 4.

Figure 70, can further explain why the stratification was not maintained. As been suggested earlier, the switches on the valves for the building return water are only bounded by the return water temperature. But it should have been bounded with the return water temperature and the temperature inside the tanks at that instant and open the valve accordingly. When the temperature of return water is between 50^OC and 60^OC then tank switch 3 is going to be activated as seen in all three cases. When the temperature of return water is between 40^OC and 50^OC then tank 4 switch is going to be activated. This explains why at peak hours the stratification between tank 2 and 3 is broken. Since, both tanks are fully discharged and then 50^OC water enters tank 3 while tank 2 water temperature is below that. The same reason is applied to why the other tanks did not maintain stratification. In both cases 1 and 2, the return water temperature is mainly 50^OC and above which is why tank 3 switch is mostly activated, while in case 3 the return water is lower than 50^OC mostly which is why tank 4 switch is mainly activated.

Figure 71, shows the temperature of water before and after the gas cooler in correlation with the temperature of supplied water. It can be seen that no matter the temperature of the water before the gas cooler, the outlet temperature is always 70^OC confirming pump's 1 PI controller accuracy. With the increase of hot water demand, the supplied water temperature is not always maintained at 70^OC. Due to the hot water demand being much larger than production.

After analyzing the data it can be said that the heat pump system is over sized for case 1. Which is, a representation of the hotel demands. However, it will still give consistent 70^OC hot water throughout the entire day no matter the time, which was only achieved in case 1. Case 2, seemed to have the best results as it supplies 70^OC water most of the time, at the lowest it was 65^OC and the system did not waste as much heat as case 1. Finally with case 3, the supplied water temperature fell just under 55^OC, and the system was not capable of producing enough hot water to supply the demand, which was the cause of the supplied water temperature dropping. A solution to all these case problems is given in further work section 7.

7   Further Work

Last but not least, by over-viewing the findings in section 6, a great system can be accomplished. Capable of achieving great performance results in all conditions. Making a one heat pump for all, working from cold to hot climates.

However, with the limited time available for the master thesis; not everything was possible to explore and creating one system that works in harmony described would be too complex.

Hence, in future work; First task would be to control cooling demand. As it is the solution for the case problems issued in end of subsection 6.3. It is important to note that they all rose from one limitation faced during the simulation. Which is the fact that the cooling demand was constant. So, if the cooling demand would have been controlled; then when the system is producing too much hot water like in case 1 the cooling demand would decrease. Since, in the simulation it was at highest value the entire period, which lead to such high production and would not be the real life case. In case 2 and 3, if the cooling demand would have been controlled, then when there is a need of extra hot water production, the system will add fake load via the use of the hot and cold water extended loops, where the circulating warm water in the closed extended loop will lift the temperature of the water returning to the evaporator which will increase the cooling demand and in return the hot water production will increase. This is possible since the compressor was also oversized to suit all these possibilities as mentioned earlier.

This is achievable with more experience and knowledge in modelica and should be explored further to really show the novelty of the system, and build the road for future simulations and greater achievements.

Two other controls that must be explored further, is controlling the high side pressure of the heat pump so that the pinch point is at the outlet and the approach temperature is the lowest possible. This is done by defining an expression to control the ejector effective flow area based on the approach temperature of the gas cooler. For a higher efficiency and cooling effect, allowing for a higher capacity and COP and decrease the expansion losses.

The other control to be explored further, is the return water from building to tanks switches so that they switch based on both the return water temperature and temperature inside each of the tanks at that instant and then the switch is activated accordingly.

To make the simulation as realistic as possible. The addition of an ambient temperature profile, and a hot and cooling demand profile for the entire year and specific to the season. That way exploring the system while operating in all season winter, summer, autumn and spring will give the system developer and costumer a better understanding of the system operation and performance. Also validate the results of the simulation with the system installed, since in the time of making this thesis the system was not yet installed.

Other future ideas to keep in mind that can enhance the overall efficiency of the system are presented below;

One way is to increase the cooling capacity of the medium pressure evaporator in the simulation, as discussed earlier is the use of gravity fed evaporation. Since, the refrigerant inlet to the evaporator will be 100% liquid (vapor fraction is 0), this means there will be a higher heat exchange coefficient. Since, the vapor fraction at the outlet of the medium pressure evaporator is limited to a max vapor fraction of 0.5-0.7 so that there would be liquid in the separator then the entire area of the evaporator could be used. In return, increasing the cooling capacity, cooling COP and total COP.

Another important addition to the system, is the addition of a low pressure receiver/separator since the LT evaporator is running in flooded operation, hence separating the liquid refrigerant from the vapor refrigerant is important for the efficiency of the vapor ejector as well as the addition of an additional liquid ejector would be required to lift the low pressure liquid in the separator to the medium pressure.

To avoid doing the aforementioned; is the addition of another internal heat exchanger between the

ejector suction line and the ejector outlet liquid line, since the heat exchange is enough to possibly run the low pressure evaporator in flooded condition utilizing all its advantageous without worrying about adding a low pressure accumulator or a liquid ejector. Since, the return liquid will evaporate through the added internal heat exchanger. While simultaneously, increasing the cooling capacity of the medium pressure evaporator. Because, the vapor fraction of the refrigerant entering the evaporator will decrease. The later reason is only true for the simulated model since the medium pressure evaporator is not run in gravity fed operation. But in actual system the addition of the internal heat exchanger, will lower cost of building it in real life. (Remove the need of both LP accumulator and liquid ejector for an additional internal heat exchanger).

After applying all of the above the system can achieve very high COP and efficiencies. It is also capable of supplying the costumer, in this case the hotel in India, with its hot and cold water demands. Even if the water inlet temperature on the gas cooler side is 30^OC which is significantly high and close the CO_2 critical temperature the system was able to achieve good COP.

8   Conclusion

In conclusion, the constant growing need to protect the environment, cost effective solutions that are easy and safe to maintain lift the potential of CO_2 as a refrigerant on a pedestal, with its great thermo-physical properties for space and water heating, chilling of rooms (AC), cold and freezing storages, makes R744 the king of refrigerants for such uses. With the increase of research and dedicated development of such systems, the ban of HFC will be very easy to deal with by replacing it with trusted R744 systems. Transcritical R744 systems have recently become the norm for heat pumping and refrigeration in the food industry.

This thesis recognises the developments of R744 refrigeration and heat pump systems. It then explores the use of simulation modelling programs to try and replicate real life systems before installations to find the efficiency of the system and how it operates. As well as come to conclusions that would not have arose without simulating it first. It can be said that the paper achieved most of its goals and failed in others. Where the investigation of R744 systems was achieved via the comprehensive literature review, building a simulation model and analyzing it was able to show how R744 systems are the future for most of installations and how they can be implemented.

As it can be seen in section 7 further work, the system has a very high potential of achieving great results for most needs and can be scaled according to the capacities required. As well as, with the optimizations the system can be considered a state of the art CO_2 heat pump system.

Finally, with the increasing knowledge and experience in the usage of modelling languages and simulation programs such as modelica and dymola respectively. This will result in simulations that are efficiently controlled. Making the use of modelling programs the next future step for developing systems; that are capable of depicting real life scenarios accurately and in many various conditions all over the world. This, will increase the rate of system developments. Moreover, increase the reach of CO_2 to all parts of the world by proving that it is a good choice of refrigerant even at high ambient conditions.

All in all, it can be said that this thesis has accomplished its aim to push the CO_2 equator to the south and help remove the reluctance of retailers for installing such CO_2 systems in their projects rather than HFC units, and saving the environment from high GWP refrigerants will be achieved faster.

Bibliography

Abdin, Mohammad (2022). 'R744 Refrigeration and Heat Pumping Units for Hot Climate Regions'. In.

Banasiak, Krzysztof et al. (2015). 'Development and performance mapping of a multi-ejector expansion work recovery pack for R744 vapour compression units'. In: *International Journal of Refrigeration* 57, pp. 265–276.

Bell, Ian (2004). 'Performance increase of carbon dioxide refrigeration cycle with the addition of parallel compression economization'. In: *6th IIR Gustav Lorenzen Natural Working Fluids*.

Cabello, R et al. (2008). 'Experimental evaluation of the energy efficiency of a CO2 refrigerating plant working in transcritical conditions'. In: *Applied thermal engineering* 28.13, pp. 1596–1604.

Cecchinato, L et al. (2007). 'An experimental analysis of a supermarket plant working with carbon dioxide as refrigerant'. In: *Proceedings of the 22nd IIR International Congress of Refrigeration; Beijing, China*.

Cecchinato, Luca et al. (2009). 'Thermodynamic analysis of different two-stage transcritical carbon dioxide cycles'. In: *International Journal of refrigeration* 32.5, pp. 1058–1067.

Cheng, Lixin, Gherhardt Ribatski and John R Thome (2008). 'New prediction methods for CO2 evaporation inside tubes: Part II—An updated general flow boiling heat transfer model based on flow patterns'. In: *International Journal of Heat and Mass Transfer* 51.1-2, pp. 125–135.

Chesi, Andrea et al. (2014). 'Experimental analysis of R744 parallel compression cycle'. In: *Applied Energy* 135, pp. 274–285.

Eckert, M, M Kauffeld and Volker Siegismund (2022). *Natural Refrigerants:Applications and Practical Guidlines*. VDE VERLAG GMBH, ATMOsphere.

Elbel, Stefan and Pega Hrnjak (2008). 'Experimental validation of a prototype ejector designed to reduce throttling losses encountered in transcritical R744 system operation'. In: *International Journal of Refrigeration* 31.3, pp. 411–422.

Elbel, Stefan and Neal Lawrence (2016). 'Review of recent developments in advanced ejector technology'. In: *International journal of refrigeration* 62, pp. 1–18.

Finckh, O, R Schrey and M Wozny (2011). 'Energy and efficiency comparison between standardized HFC and CO2 transcritical systems for supermarket applications'. In: *Proceedings of the 23rd IIR International Congress of Refrigeration, Prague, Czech Republic*, pp. 21–26.

Fricke, Brian et al. (2016). 'Laboratory evaluation of a commercial CO2 booster refrigeration system'. In.

Girotto, S (2017). 'Improved transcritical CO2 refrigeration systems for warm climates'. In: *Proceedings of the 7th IIR Ammonia and CO2 Refrigeration Technologies Conference, Ohrid, Macedonia*, pp. 11–13.

Girotto, Sergio, Silvia Minetto and Petter Neksa (2004). 'Commercial refrigeration system using CO2 as the refrigerant'. In: *International journal of refrigeration* 27.7, pp. 717–723.

Gullo, Paride and Giovanni Cortella (2016b). 'Comparative exergoeconomic analysis of various transcritical R744 commercial refrigeration systems'. In: *29th International Conference on Efficiency, Cost, Optimisation, Simulation and Environmental Impact of Energy Systems, ECOS 2016*. University of Ljubljana.

— (2016a). 'Comparative exergoeconomic analysis of various transcritical R744 commercial refrigeration systems'. In: *29th International Conference on Efficiency, Cost, Optimisation, Simulation and Environmental Impact of Energy Systems, ECOS 2016*. University of Ljubljana.

Gullo, Paride, Giovanni Cortella et al. (2016). 'Overfed evaporators and parallel compression in commercial R744 booster refrigeration systems-An assessment of energy benefits'. In: *12th IIR Gustav Lorentzen Natural Working Fluids Conference, GL 2016*. International Institute of Refrigeration, pp. 261–268.

Gullo, Paride, Brian Elmegaard and Giovanni Cortella (2016). 'Energy and environmental performance assessment of R744 booster supermarket refrigeration systems operating in warm climates'. In: *International Journal of Refrigeration* 64, pp. 61–79.

Gullo, Paride, Armin Hafner and Krzysztof Banasiak (2018). 'Transcritical R744 refrigeration systems for supermarket applications: Current status and future perspectives'. In: *International Journal of Refrigeration* 93, pp. 269–310.

Gullo, Paride, Armin Hafner, Krzysztof Banasiak et al. (2019). 'Multi-ejector concept: A comprehensive review on its latest technological developments'. In: *Energies* 12.3, p. 406.

Gullo, Paride, Konstantinos Tsamos et al. (2017). 'State-of-the-art technologies for transcritical R744 refrigeration systems–a theoretical assessment of energy advantages for European food retail industry'. In: *Energy Procedia* 123, pp. 46–53.

Hafner, A (2015). 'perspectives CO2 refrigeration and heat pump systems'. In: *Proceedings of the 6th IIR Ammonia and CO2 Refrigeration Technologies Conference, Ohrid, Macedonia*, pp. 16–18.

— (2017). 'Integrated CO2 system refrigeration, air conditioning and sanitary hot water'. In: *Proceedings of the 7th IIR Ammonia and CO2 Refrigeration Technologies Conference, Ohrid, Macedonia*, pp. 11–13.

Hafner, A, K Banasiak et al. (2016). 'R744 ejector system case: Italian supermarket, Spiazzo'. In: *12th IIR Gustav Lorentzen Conference on Natural Refrigerants, Edinburgh, Scotland*.

Hafner, A, K Fredslund and K Banasiak (2015). 'Next generation R744 refrigeration technology for supermarkets'. In: *Proceedings of the 24th IIR International Congress of Refrigeration, Yokohama, Japan*, pp. 16–22.

HAFNER, A et al. (2022). 'Experimental investigation on integrated two-stage evaporators for CO2 heat-pump chillers'. In: *Proceedings of the 15th IIR-Gustav Lorentzen Conference on Natural Refrigerants, Trondheim, Norway*, pp. 0–11.

Hafner, Armin (2022). 'Commercial Refrigeration'. In: NTNU, p. 19.

Hafner, Armin, Sven Försterling and Krzysztof Banasiak (2014). 'Multi-ejector concept for R-744 supermarket refrigeration'. In: *International Journal of Refrigeration* 43, pp. 1–13.

Hafner, Armin, Stefano Poppi et al. (2012). 'Development of commercial refrigeration systems with heat recovery for supermarket building'. In: *Proceedings of the 10th IIR Gustav Lorentzen Conference on Natural Refrigerants, Delft, The Netherlands*, pp. 25–27.

Hasnain, S et al. (1996). 'Internal Report'. In: *Energy Research Institute, Riyadh, Saudi Arabia*. KACST.

Hasnain, SM (1998a). 'Review on sustainable thermal energy storage technologies, Part I: heat storage materials and techniques'. In: *Energy conversion and management* 39.11, pp. 1127–1138.

— (1998b). 'Review on sustainable thermal energy storage technologies, Part II: cool thermal storage'. In: *Energy conversion and management* 39.11, pp. 1139–1153.

Hazarika, M M et al. (2022). 'Integration of gravity-fed evaporators in CO2 based heat-pump chillers'. In: *Proceedings of the 15th IIR-Gustav Lorentzen Conference on Natural Refrigerants, Trondheim, Norway*, pp. 0–10.

Javerschek, O, M Reichle and J Karbiner (2016). 'Optimization of parallel compression systems'. In: *12th IIR Gustav Lorentzen Conference on Natural Refrigerants, IIR/IIF, Edinburgh, Scotland*.

Karampour, Mazyar and Samer Sawalha (2018). 'State-of-the-art integrated CO2 refrigeration system for supermarkets: A comparative analysis'. In: *International journal of refrigeration* 86, pp. 239–257.

Llopis, Rodrigo et al. (2015). 'Energy and environmental comparison of two-stage solutions for commercial refrigeration at low temperature: Fluids and systems'. In: *Applied Energy* 138, pp. 133–142.

Matthiesen, O, K Madsen and A Mikhailov (2010). 'Evolution of CO2 systems design based on practical experiences from supermarket installations in Northern Europe'. In: *Proceedings of the 9th IIR Gustav Lorentzen conference on natural working fluids, 12th–14th April*.

Mazzola, D et al. (2016). 'Supermarket application. Effects of sub-cooling on real R744 based trans-critical plants in warm and hot climate. Data analysis'. In: *Proceedings of the 12th IIR Gustav Lorentzen Natural Working Fluids Conference, Edinburgh, UK*, pp. 21–24.

Minetto, S, S Girotto, A Rossetti et al. (2015). 'Experience with ejector work recovery and auxiliary compressors in CO2 refrigeration systems. Technological aspects and application perspectives'. In: *Proceedings of the Ammonia Refrigeration Technology International Conference, Ohrid, Macedonia*. Vol. 1618.

Minetto, S, S Girotto, M Salvatore et al. (2014). 'Recent installations of CO2 supermarket refrigeration system for warm climates: data from field'. In: *Proceedings of the 3rd IIR International Conference on Sustainability and Cold Chain, London, UK*, pp. 23–25.

Pardiñas, Ángel Á, Armin Hafner and Krzysztof Banasiak (2018). 'Novel integrated CO2 vapour compression racks for supermarkets. Thermodynamic analysis of possible system configurations and influence of operational conditions'. In: *Applied Thermal Engineering* 131, pp. 1008–1025.

Purohit, Nilesh, Paride Gullo and Mani Sankar Dasgupta (2017). 'Comparative assessment of low-GWP based refrigerating plants operating in hot climates'. In: *Energy Procedia* 109, pp. 138–145.

Sánchez, D et al. (2016). 'Improvements in a CO2 transcritical plant working with two different subcooling systems'. In: *Proceedings of the 12th IIR Gustav Lorenzen Natural Working Fluids Conference, Edinburgh, UK*, pp. 21–24.

Sánchez, Daniel, Jorge Patiño, Rodrigo Llopis et al. (2014). 'New positions for an internal heat exchanger in a CO2 supercritical refrigeration plant. Experimental analysis and energetic evaluation'. In: *Applied Thermal Engineering* 63.1, pp. 129–139.

Sánchez, Daniel, Jorge Patiño, Carlos Sanz-Kock et al. (2014). 'Energetic evaluation of a CO2 refrigeration plant working in supercritical and subcritical conditions'. In: *Applied thermal engineering* 66.1-2, pp. 227–238.

Sarbu, Ioan and Calin Sebarchievici (2018). 'A comprehensive review of thermal energy storage'. In: *Sustainability* 10.1, p. 191.

Sawalha, Samer (2008). 'Theoretical evaluation of trans-critical CO2 systems in supermarket refrigeration. Part II: System modifications and comparisons of different solutions'. In: *International journal of refrigeration* 31.3, pp. 525–534.

Sawalha, Samer et al. (2017). 'Field measurements of supermarket refrigeration systems. Part II: Analysis of HFC refrigeration systems and comparison to CO2 trans-critical'. In: *Applied Thermal Engineering* 111, pp. 170–182.

Sharma, Vishaldeep, Brian A Fricke and Pradeep Bansal (2015). *Evaluation of a transcritical CO2 supermarket refrigeration system for the USA market.* Tech. rep. Oak Ridge National Lab.(ORNL), Oak Ridge, TN (United States). Building . . .

Sienel, T and O Finckh (2010). 'An overview of development and test capabilities for CO2 commercial refrigeration systems'. In: *Proceedings of the 9th IIR Gustav Lorentzen Conference on Natural Refrigerants, 12th–14th April.*

Singh, Simarpreet, Krzysztof Banasiak et al. (2018). 'Performance evaluation of CO2 ejector system with parallel compressor for supermarket application'. In.

Singh, Simarpreet, Armin Hafner et al. (2018). 'Experimental evaluation of multi-ejector based CO2 cooling system for supermarkets in tropical zones'. In: *17th International Refrigeration and Air Conditioning Conference 2018.*

Singh, Simarpreet, Amshith Reddy et al. (2018). 'Analysis of R744 refrigeration system with liquid ejectors'. In: *Proceedings of the 13th IIR Gustav Lorentzen Conference, Valencia, 2018.* IIR.

Tegethoff, Wilhelm et al. (2011). 'TEMO: Thermische echtzeitfähige Modelle'. In: *Final Project Report.*

Torrella, E et al. (2011). 'Energetic evaluation of an internal heat exchanger in a CO2 transcritical refrigeration plant using experimental data'. In: *International Journal of Refrigeration* 34.1, pp. 40–49.

Tsamos, KM et al. (2017). 'Energy analysis of alternative CO2 refrigeration system configurations for retail food applications in moderate and warm climates'. In: *Energy Conversion and Management* 150, pp. 822–829.

Appendix

A   Appendix A
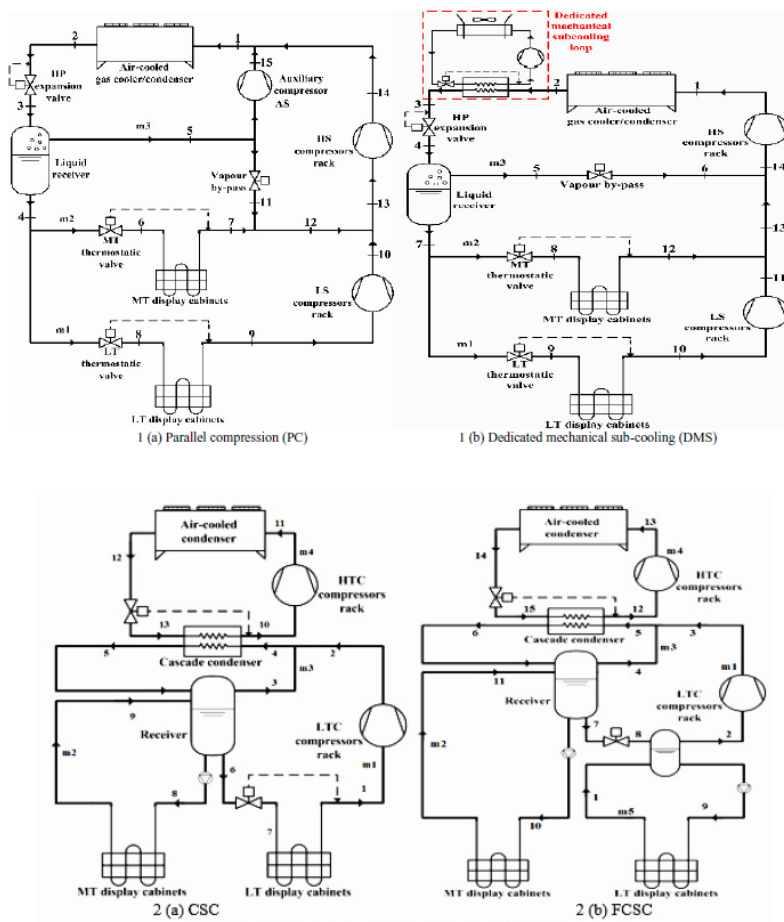
Figure 73: Investigated systems by Purohit et al. 2017

B   Appendix B
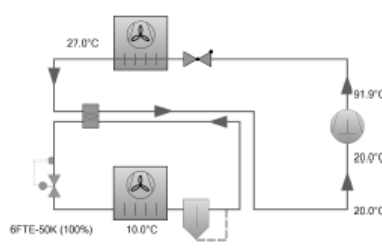
| BITZER Software v6.17.8 rev2725 | Nominal Condition
Carel Ejector
07/07/2022 / All data subject to change. | 1 / 1 |

Selection: Semi-hermetic Reciprocating Compressors

Input Values

Compressor model	6FTE-50K
Mode	Refrigeration and Air conditioning
Refrigerant	R744
Reference temperature	Dew point temp.
Evaporating SST	10.00 °C
High pressure	100.0 bar(a)
Gas cooling outlet	27.0 °C
Suction gas temperature	20.00 °C
Operating mode	Transcritical
Power supply	400V-3-50Hz
Capacity control	100%
Useful superheat	10.00 K

Result

Compressor	6FTE-50K-40P
Capacity steps	100%
Cooling capacity	132.3 kW
Cooling capacity *	132.3 kW
Evaporator capacity	132.3 kW
Power input	34.9 kW
Current (400V)	72.6 A
Voltage range	380-400V
Gas cooler capacity	167.2 kW
COP/EER	3.79
Mass flow	2627 kg/h
Discharge gas temp. w/o cooling	91.9 °C
optimal high pressure	75.0 bar(a)

Tentative Data.
*Compressor-Performance data certified by ASERCOM (see T.Data/ Notes)
Attention, consider operating parameters. See KP-130 or consult BITZER.
*according to EN12900 (10K suction gas superheat)

Application Limits 100% 6FTE-50K

Legend
- mind operating parameters
- M1: motor 1
- Operation above designated line not allowed for following compressor models: 4PTE, 4PTC
- A

Figure 74: System capacities by INDEE++

SWEP

A DOVER COMPANY

SINGLE PHASE - DESIGN
HEAT EXCHANGER: B185Hx151/3P

SWEP SSP G8 2022.620.1.0

Date: 24/06/2022

SSP Alias: B185H/3P

DUTY REQUIREMENTS		Side 1		Side 2
Fluid		R744 (Carbon Dioxide) (100.0 bar)		Water
Flow type			Counter-Current	
Circuit		primary		secondary
Heat load	kW		167.1	
Inlet temperature	°C	91.90		25.00
Outlet temperature	°C	27.00		65.00
Flow rate	kg/h | kg/s	2627		0.9997
Pressure drop (Design PD)	kPa	39.6 (50.00)		35.1 (50.00)
Thermal length		6.774		4.175

PLATE HEAT EXCHANGER		Side 1		Side 2
Total heat transfer area	m²		11.3	
Heat flux	kW/m²		14.8	
Mean temperature difference	K		9.58	
O.H.T.C. (available/required)	W/m²,°C		2710/2740	
Pressure drop - total*	kPa	39.6		35.1
- in ports	kPa	0.698		0.124
Port diameter (up/down)	mm	33.0/33.0		50.0/50.0
Number of channels per pass		25		25
Number of plates			151	
Oversurfacing	%		0	
Fouling factor	m²,°C/kW		-0.004	
Reynolds number		9644		665.8
Port velocity (up/down)	m/s	1.73/1.73		0.515/0.515
Channel velocity	m/s	0.335		0.136
Shear stress	Pa	28.6		25.7
Average wall temperature	°C	44.03		43.57
Largest wall temperature difference	K		1.36	
Min./Max. wall temperature	°C	27.02/69.15		26.80/67.79

Excluding pressure drop in connections.

NOTES

! For a desuperheater installation it is recommended to have the gas enter in the top of the BPHE, etiher in F1 or F2. The reason is to easily remove possible condensate from the BPHE

PHYSICAL PROPERTIES		Side 1	Side 2
Reference temperature	°C	47.88	44.03
Dynamic viscosity	cP	0.0240	0.597
Dynamic viscosity - wall	cP	0.0379	0.612
Density	kg/m³	293.1	990.3
Heat capacity	kJ/kg,°C	3.106	4.180
Thermal conductivity	W/m,°C	0.03970	0.6374
Film coefficient	W/m²,°C	4260	10200

TOTALS		Side 1	Side 2
Total weight empty (no connections)*	kg	77.26	
Total weight filled (no connections)*	kg	89.46	
Hold-up volume (Inner Circuit)	dm³	8.3	
Hold-up volume (Outer Circuit)	dm³	8.77	

SWEP

A DOVER COMPANY

TOTALS		Side 1	Side 2
Port size F1/P1	mm	33	
Port size F2/P2	mm	50	
Port size F3/P3	mm	33	
Port size F4/P4	mm	50	
Carbon footprint	kg	542.93	

Weight depends on the selected product.

DIMENSIONS

A	mm	425.2 ±2
B	mm	203.2 ±1
C	mm	354 ±1
D	mm	126 ±1
E	mm	45 ±1
F	mm	320 ±3%
G	mm	0 ±1
H	mm	342 ±1
J	mm	6
K	mm	35.6
N	mm	41.6
R	mm	41.6

This is a schematic sketch. For correct drawings please use the order drawing function or contact your SWEP representative.

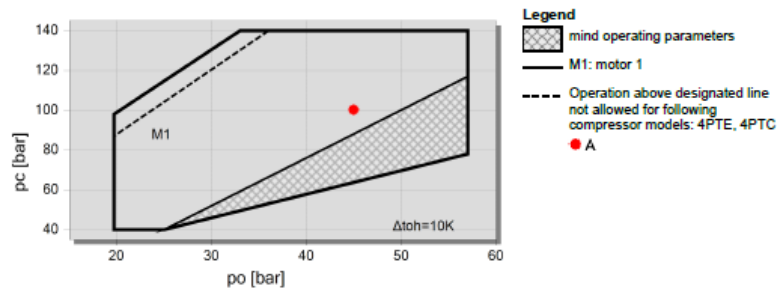Figure 75: Gas Cooler Data by INDEE++

SWEP

SWEP International AB
Box 105, Hjalmar Brantings väg 5
SE-261 22 Landskrona, Sweden

www.swep.net

A DOVER COMPANY

EVAPORATOR - DESIGN
HEAT EXCHANGER: F85Hx62/1P

SWEP SSP G8 2022.620.1.0

Date: 24/06/2022

SSP Alias:	F85			
DUTY REQUIREMENTS			**Side 1**	**Side 2**
Fluid			**R744 (Carbon Dioxide)**	**Water**
Flow type			**Counter-Current**	
Circuit			Inner	Outer
Heat load	kW		60.96	
Subcooled liq. temp.	°C		**21.10**	
Inlet vapor quality			**0.161**	
Outlet vapor quality			**1.000**	
Inlet temperature	°C		**11.08**	**22.00**
Evaporation temperature (dew)	°C		**11.00**	
Superheating	K		**2.00**	
Outlet temperature	°C		**13.00**	**15.00**
Flow rate	kg/h | kg/s		**1314**	2.082
• Inlet vapor	kg/h		212.1	
Fluid vaporized	kg/h		1101	
Pressure drop (Design PD)	kPa		9.32 **(50.00)**	50.1 **(50.00)**

PLATE HEAT EXCHANGER			**Side 1**	**Side 2**
Total heat transfer area	m²		3.60	
Heat flux	kW/m²		16.9	
Mean temperature difference	K		7.80	
O.H.T.C. (available/required)	W/m²,°C		2510/2170	
Pressure drop - total*	kPa		9.32	50.1
– in ports (Inlet/Outlet)	kPa		-1.48/0.836	2.82
Pressure drop in fluid distribution	kPa		195 - 230	
Operating pressure (outlet)	kPa		4620	
Number of channels per pass			30	31
Number of plates			62	
Oversurfacing	%		16	
Fouling factor	m²,°C/kW		0.062	
Port diameter (up/down)	mm		33.0/17.0	33.0/33.0
Recommended inlet connection diameter	mm		6.03 - 9.54	
Recommended outlet connection diameter	mm		11.5 - 25.8	
Reynolds number				1139
Outlet port velocity	m/s		3.05	2.44
Channel velocity	m/s		0.467	0.361
Shear stress	Pa			83.0
Largest wall temperature difference	K		0.53	
Min./Max. wall temperature	°C		13.35/20.41	13.61/20.65

Excluding pressure drop in connections.

NOTES

! Partial film boiling in the two-phase zone.
i Pressure drop in distribution device is 2.0 - 2.3 bar .
! Very high heat flux not experimentally certified (16 kW/m²).
i Superheat less than 5 K.
i Evaporator performance prediction does not use two phase correction factors.

PHYSICAL PROPERTIES			**Side 1**	**Side 2**
Reference temperature	°C		11.06	18.39
Liquid • Dynamic viscosity	cP		0.0809	1.04

SWEP

SWEP International AB
Box 105, Hjalmar Brantings väg 5
SE-261 22 Landskrona, Sweden

www.swep.net

A DOVER COMPANY

PHYSICAL PROPERTIES			**Side 1**	**Side 2**
• Density	kg/m³		853.6	998.5
• Heat capacity	kJ/kg,°C		3.068	4.183
• Thermal conductivity	W/m,°C		0.09687	0.5955
Vapor • Dynamic viscosity	cP		0.0162	
• Density	kg/m³		139.8	
• Heat capacity	kJ/kg,°C		2.667	
• Thermal conductivity	W/m,°C		0.02485	
• Latent heat	kJ/kg		193.3	
Film coefficient	W/m²,°C		2150	15500

TOTALS			**Side 1**	**Side 2**
Total weight (no connections)*	kg		10.51 - 11.34	
Hold-up volume (Inner Circuit)	dm³		2.82	
Hold-up volume (Outer Circuit)	dm³		2.91	
Port size F1/P1	mm		33	
Port size F2/P2	mm		33	
Port size F3/P3	mm		33	
Port size F4/P4	mm		33	
Carbon footprint	kg		79.68	

Weight depends on the selected product.
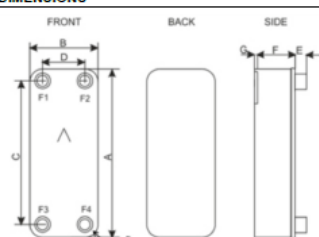
DIMENSIONS

A*	mm	524 - 526 ±2
B*	mm	117 - 119 ±1
C	mm	470 ±1
D	mm	63 ±1
E*	mm	20 - 27 / 45 ±1
F*	mm	118.08 - 124.08 ±3%
G	mm	6 ±1
R	mm	23

Dimensions depend on the selected product.

FRONT   BACK   SIDE

This is a schematic sketch. For correct drawings please use the order drawing function or contact your SWEP representative.

87

Figure 76: Evaporator Medium Pressure Data by INDEE++

SWEP

A DOVER COMPANY

SWEP International AB
Box 105, Hjalmar Brantings väg 5
SE-261 22 Landskrona, Sweden

www.swep.net

EVAPORATOR - DESIGN
HEAT EXCHANGER: F85Hx96/1P

SWEP SSP G8 2022.620.1.0

Date: 24/06/2022

SSP Alias: F85

DUTY REQUIREMENTS		Side 1		Side 2
Fluid		R744 (Carbon Dioxide)		Water
Flow type		Counter-Current		
Circuit		Inner		Outer
Heat load	kW		62.20	
Subcooled liq. temp.	°C	21.10		
Inlet vapor quality		0.202		
Outlet vapor quality		1.000		
Inlet temperature	°C	7.05		15.00
Evaporation temperature (dew)	°C	7.00		
Superheating	K	2.00		
Outlet temperature	°C	9.00		8.00
Flow rate	kg/h | kg/s	1314		2.120
· Inlet vapor	kg/h	265.1		
Fluid vaporized	kg/h	1048		
Pressure drop (Design PD)	kPa	5.66 (50.00)		25.6 (50.00)

PLATE HEAT EXCHANGER		Side 1		Side 2
Total heat transfer area	m²		5.64	
Heat flux	kW/m²		11.0	
Mean temperature difference	K		3.81	
O.H.T.C. (available/required)	W/m²,°C		2930/2890	
Pressure drop - total*	kPa	5.66		25.6
- in ports (Inlet/Outlet)	kPa	-1.64/0.991		2.93
Pressure drop in fluid distribution	kPa	95.1 - 112		
Operating pressure (outlet)	kPa	4180		
Number of channels per pass		47		48
Number of plates			96	
Oversurfacing	%		1	
Fouling factor	m²,°C/kW		0.004	
Port diameter (up/down)	mm	33.0/17.0		33.0/33.0
Recommended inlet connection diameter	mm	6.74 - 10.6		
Recommended outlet connection diameter	mm	12.3 - 27.6		
Reynolds number			622.7	
Outlet port velocity	m/s	3.49		2.48
Channel velocity	m/s	0.340		0.237
Shear stress	Pa		39.8	
Largest wall temperature difference	K		0.43	
Min./Max. wall temperature	°C	7.66/13.92		7.70/14.04

Excluding pressure drop in connections.

NOTES

i Pressure drop in distribution device is 1.0 - 1.1 bar .

i Superheat less than 5 K.

i Evaporator performance prediction does not use two phase correction factors.

| PHYSICAL PROPERTIES		Side 1	Side 2
Reference temperature	°C	7.03	11.41
Liquid · Dynamic viscosity	cP	0.0875	1.26
· Density	kg/m³	882.5	999.5
· Heat capacity	kJ/kg,°C	2.822	4.191

SWEP

A DOVER COMPANY

SWEP International AB
Box 105, Hjalmar Brantings väg 5
SE-261 22 Landskrona, Sweden

www.swep.net

PHYSICAL PROPERTIES		Side 1	Side 2
· Thermal conductivity	W/m,°C	0.1018	0.5826
Vapor · Dynamic viscosity	cP	0.0156	
· Density	kg/m³	122.4	
· Heat capacity	kJ/kg,°C	2.289	
· Thermal conductivity	W/m,°C	0.02254	
· Latent heat	kJ/kg	208.1	
Film coefficient	W/m²,°C	9260	10900

TOTALS		Side 1	Side 2
Total weight (no connections)*	kg	15.59 - 16.41	
Hold-up volume (Inner Circuit)	dm³	4.42	
Hold-up volume (Outer Circuit)	dm³	4.51	
Port size F1/P1	mm	33	
Port size F2/P2	mm	33	
Port size F3/P3	mm	33	
Port size F4/P4	mm	33	
Carbon footprint	kg	115.33	

Weight depends on the selected product.
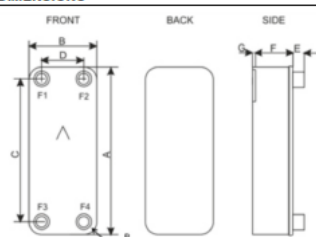
DIMENSIONS

A*	mm	524 - 526 ±2
B*	mm	117 - 119 ±1
C	mm	470 ±1
D	mm	63 ±1
E*	mm	20 - 27 / 45 ±1
F*	mm	180.64 - 186.64 ±3%
G	mm	6 ±1
R	mm	23

Dimensions depend on the selected product.

This is a schematic sketch. For correct drawings please use the order drawing function or contact your SWEP representative.

88

Figure 77: Evaporator Low Pressure Data by INDEE++

SWEP
A DOVER COMPANY

SINGLE PHASE - RATING
HEAT EXCHANGER: B18Hx70/1P

SWEP SSP G8 2022.620.1.0

Date: 24/06/2022

SSP Alias: B18H

DUTY REQUIREMENTS		Side 1		Side 2
Fluid		R744 (Carbon Dioxide) (100.0 bar)		R744 (Carbon Dioxide) (45.0 bar)
Flow type			Co-Current	
Circuit		Inner		Outer
Heat load	kW		12.14	
Inlet temperature	°C	27.00		12.00
Outlet temperature	°C	21.10		20.00
Flow rate	kg/h	2627		2627
Thermal length		1.024		1.389

PLATE HEAT EXCHANGER		Side 1		Side 2
Total heat transfer area	m²		2.79	
Heat flux	kW/m²		4.35	
Mean temperature difference	K		5.76	
O.H.T.C. (available/required)	W/m²,°C		1460/802	
Pressure drop - total*	kPa	7.84		50.8
- in ports	kPa	1.52		10.2
Port diameter (up/down)	mm	24.0/24.0		24.0/24.0
Number of channels per pass		34		35
Number of plates			70	
Oversurfacing	%		83	
Fouling factor	m²,°C/kW		0.564	
Reynolds number		5038		23030
Port velocity (up/down)	m/s	1.96/1.96		13.2/13.2
Channel velocity	m/s	0.154		1.00
Shear stress	Pa	14.4		92.4
Average wall temperature	°C	21.11		20.86
Largest wall temperature difference	K		0.71	
Min./Max. wall temperature	°C	20.86/21.65		20.77/20.96

*Excluding pressure drop in connections.

NOTES

! For a desuperheater installation it is recommended to have the gas enter in the top of the BPHE, etiher in F1 or F2. The reason is to easily remove possible condensate from the BPHE

PHYSICAL PROPERTIES		Side 1	Side 2
Reference temperature	°C	23.99	16.04
Dynamic viscosity	cP	0.0751	0.0161
Dynamic viscosity - wall	cP	0.0798	0.0161
Density	kg/m³	824.1	122.8
Heat capacity	kJ/kg,°C	2.822	1.960
Thermal conductivity	W/m,°C	0.09230	0.02246
Film coefficient	W/m²,°C	4350	2370

TOTALS		Side 1	Side 2
Total weight empty (no connections)*	kg	21.58	
Total weight filled (no connections)*	kg	23.55	
Hold-up volume (Inner Circuit)	dm³	2.07	
Hold-up volume (Outer Circuit)	dm³	2.13	

SWEP
A DOVER COMPANY

TOTALS		Side 1	Side 2
Port size F1/P1	mm	24	
Port size F2/P2	mm	24	
Port size F3/P3	mm	24	
Port size F4/P4	mm	24	
Carbon footprint	kg	151.62	

*Weight depends on the selected product.

DIMENSIONS
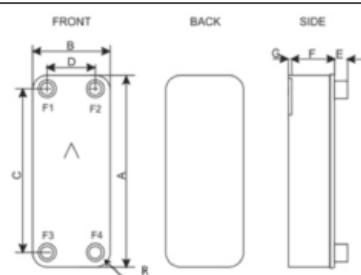
A	mm	377 ±2
B	mm	119.5 ±1
C	mm	329 ±1
D	mm	72 ±1
E	mm	45 (opt. 81) ±1
F	mm	152 +0.5%/-1.5%
G	mm	2 ±1
R	mm	23.5

*This is a schematic sketch. For correct drawings please use the order drawing function or contact your SWEP representative.

Figure 78: Internal Heat Exchanger Data by INDEE++

C   Appendix C Scientific Paper

Development of Transcritical CO_2 Heat Pump Chillers

Mohammad Abdin
Norwegian University of Science and Technology
mohaab@stud,ntnu.no; abdin.mohammad2000@gmail.com

ABSTRACT

This study intends to implement a comprehensive review of the evolution of CO_2 refrigeration and heat pump systems. Covering the most important aspects of the state-of-the-art commercial Transcritical CO_2 systems, which have emerged to overtake its worst counterpart the HFC technologies, and put an end to the use of high GWP refrigerants. It was concluded that, despite the scepticism around CO_2 in warm countries for the adoption of such systems, R744 as an only working refrigerant in transcritical operation with the adoption of the newest technologies proves wrong. This thesis develops an R744 heat pump system for a hotel in India and shows that R744 systems are efficient in warm countries with potential for more upgrades. By the end of the thesis, a transcritical heat pump system capable of achieving great results in all possible conditions was engineered.

1. INTRODUCTION

Heat pump systems and refrigeration systems are increasing with popularity. They account for the highest energy demand in supermarkets and building. With high energy demands, HFC systems impose a great damage to the environment. From their high indirect greenhouse emissions for generating the electricity to keep them running. As well as, they share the responsibility of the largest emitters of high GWP refrigerants, which occurs through leakages during normal operation, extensive pipework, or poor maintenance. Refrigerant leakage is always opted to occur at one point as there is not one system that is 100% leakage free where the estimated average annual leakage is about 15 to 20% of the total charge in the system Armin Hafner, Poppi et al. 2012. Hence, a solution must be developed to cancel out the high global warming potential (GWP) refrigerants with refrigerants with low GWP, and more efficient systems. In other words, a solution to decrease both the direct and indirect emissions. Despite the numerous efforts to phase out high GWP refrigerant R404A which has a GWP factor of 3943 kg_{CO2eq} $kg_{refrigerant}^{-1}$ is still widely used in the food sector around the world especially in warmer countries.

The type of refrigerant and system configuration is the main factor that affects the direct and indirect emissions; hence it is of utmost importance to have a detailed understanding of systems for the preservation of the environment, decrease energy consumption and increase the efficiency of installed systems in commercial refrigeration and heating sector. This project will cover these factors and the developments that come alongside it, to develop the knowledge and skills required to build such systems with high quality. The main objectives and aims of the project are:

- Understanding the newest technologies used for R744 systems, and how far such systems have come from the first-generation system, and analyse their environmental, economical and energy evaluations with comparison to conventional HFC systems.

- Design a heat pump system with cold and hot water loops for a hotel in high ambient temperature city Goa, India.

- Develop a control strategy for optimum working operation for the system.

- Build and develop a working simulation of the designed system.

- Develop a future plan on ways to develop the analyzed system for future work.

The paper aims to move the CO_2 equator south and allow for the use of R744 to be a great viable option for warm countries, as well as, As well as, bring into attention the viability of modelling and simulating heat pump or refrigeration systems using softwares to analyse their performance.

2. System Description

The heat pump system was designed to supply a hotel in Goa, India with domestic hot water for its visitors, as well as cooling for air conditioning use. The entire system can be seen in figure 1. The heat pump system working fluid is CO_2, whereas the secondary fluid is water for both hot and cold loops. CO_2 as working fluid was chosen, for the fact, that its properties allow for large temperature glide on the water side, which enables the heat pump to lift the temperature of cold city water at around 25 to 30 degrees Celsius up to 70 degrees which is the set point for this system on the hot water side. Whereas, on the cold water side decrease the temperature from 12 degrees Celsius down to 7 degrees Celsius. Large temperature glides as were discussed in the chapter 2.5.2 (literature review in main paperwork) will increase the overall energy efficiency of the system. Water was used as a heat source over the evaporators to achieve the cooling demands of the building. Due to its low cost and wide availability in all, countries as the proposed system is highly adaptable to all regions and can be used as a standard system for building applications in the future.
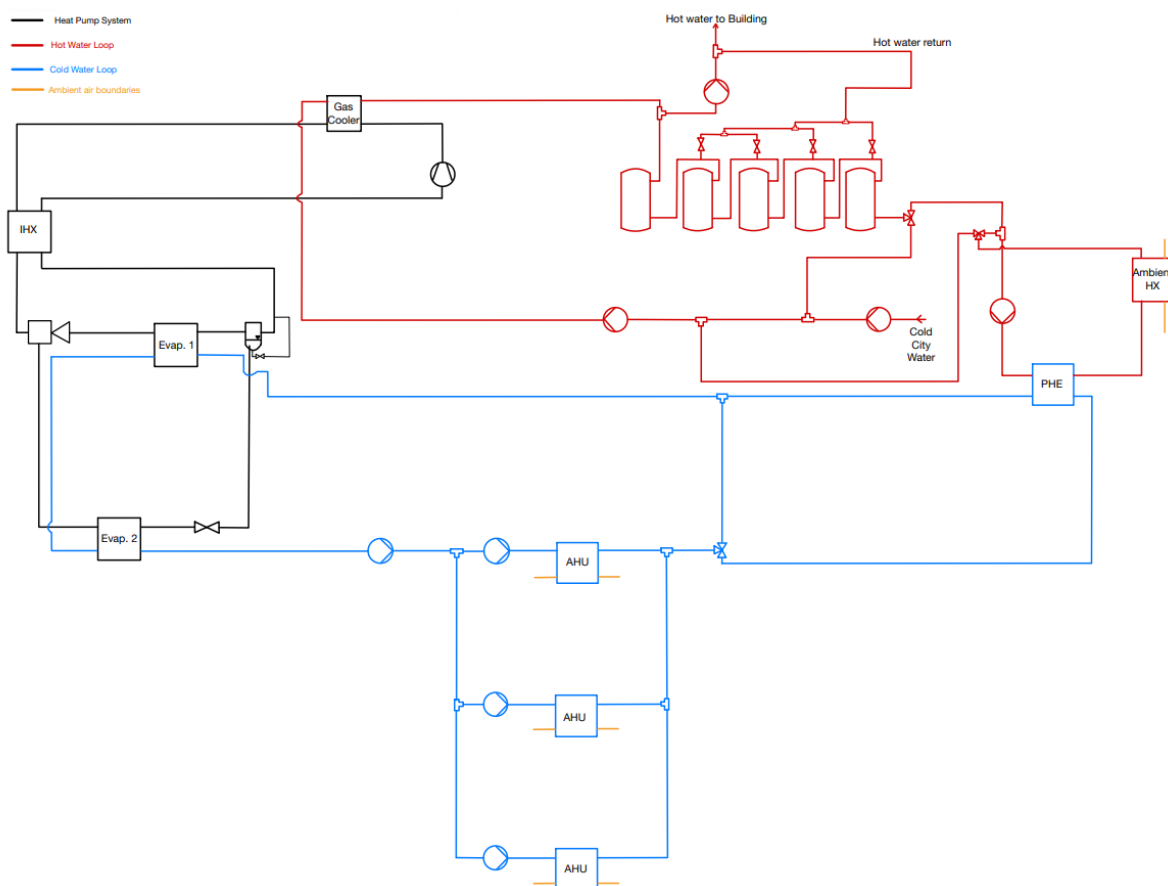

Figure 1: Heat Pump system with hot and cold water loops

For the hot water loop there are three different possible operations as can be seen in figure 2. During the charging process in figure 2a, the hot water demand by the building is less than the hot water production hence, the heat pump system will be able to provide the entire demand, which means the extra hot water production will start to charge the tanks with hot water starting with tank 1 and ending in tank 5, this is true to maintain stratification within the tanks. Simultaneously, while tank 1 is being charged, colder water from tank 5 will be sent to pump number 2 to be pumped to the gas cooler and heated. Based on the temperature of the return water from the building, the corresponding valve will open and fill in its correlated tank. This is true for all operational cases. For better operation, the valve for the return water from the building should open based on

the water return temperature and the water temperature in the tank at that specific moment. This however, was not applied in this modelica model, the reason for this is explained in section methodologies in the main report.
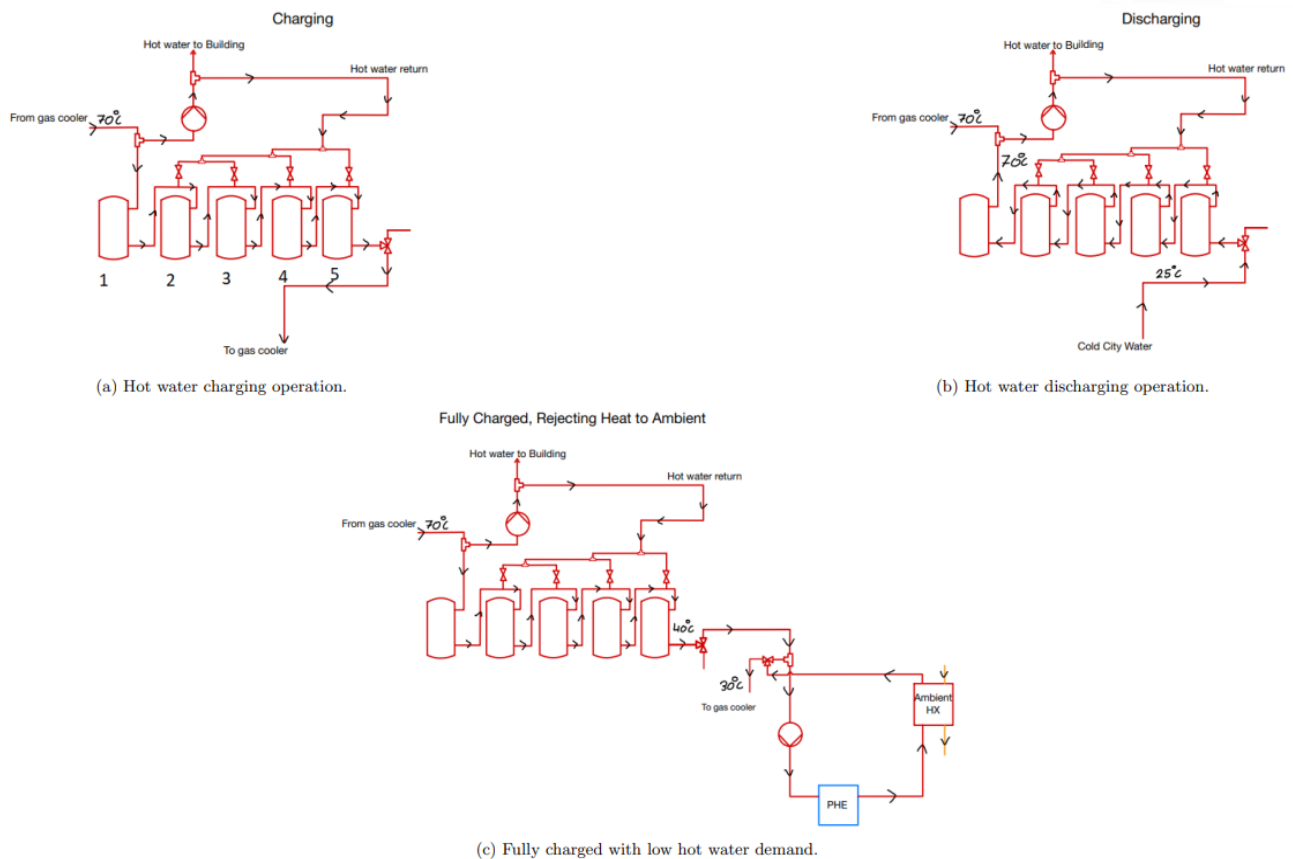

(a) Hot water charging operation.

(b) Hot water discharging operation.

(c) Fully charged with low hot water demand.

Figure 2: Hot water loop operations

During discharging process as seen in figure 2b, the hot water demand is larger than the hot water production, hence, the hot water stored in the tanks combined with the hot water production by the heat pump will add up to provide the total hot water demand by the hotel. The hot water stored in the tanks, will first be sucked from tank number 1 and simultaneously cold city water will enter tank number 5. This maintains stratification within the tanks, and the returned hot water from the building will follow the rule of the charging process. Finally, the third operation occurs when the hot water tanks are fully charged and the hot water demand is lower than the hot water production. The tanks are considered fully charged when the exit water temperature from the fifth tank is 40 degrees Celsius or above. Rather than the hot water exiting the fifth tank is sent directly to the gas cooler as in the charging process, the directional three way valve will switch directions as seen in figure 2c where the hot water will enter the extended loop and will reject heat to the ambient to cool down before being sent back to the gas cooler.

This is done due to the fact, if the hot water at 40 $^{\circ}$C or more is sent back directly to the gas cooler, it will ruin the entire efficiency of the heat pump system. Since, the exit temperature of the CO_2 after the gas cooler is going to be high. The mass flow rate of pump 4 (inside the extended loop) will be determined by the subtraction of the hot water production and hot water demand, to maintain a balanced mass flow rate of the water in the entire loop. Otherwise, cold city water be stuck in the piping between pump 1 and 2 which will increase the system's pressure immensely. More about the control of this pump will be discussed in the upcoming chapter 4. The water temperature after rejecting heat to the ambient will of course depend on the ambient temperature, which will then be mixed with the cold city water before it is pumped to the gas cooler.
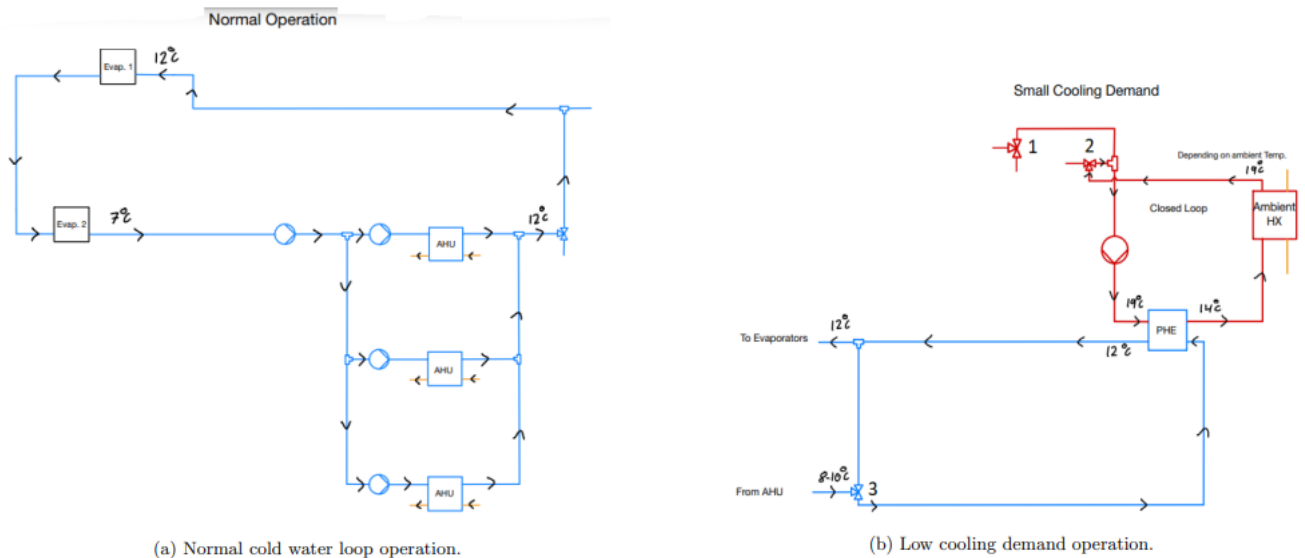
(a) Normal cold water loop operation.

(b) Low cooling demand operation.

Figure 3: Cold water loop operations

For the cold water loop there are two different possible operations as can be seen in figure 3. Where figure 3a represents the normal operation of the cold water loop, cooling water from 12$^{\text{O}}$C to 7$^{\text{O}}$C over both evaporators and sending the chilled water the AHU, however, in the case when there is not enough cold water demand and the exit water temperature from the AHUs is low for example 9$^{\text{O}}$C while there is still hot water demand and hot water production is required meaning that the heat pump system should keep running then the second operation shown in figure 3b takes place. In this operation the directional three way valve (valve number 3) after the AHUs switches direction so that the chilled water is sent towards the PHE rather than directly back to the evaporators. By doing this, it will create a fake load which will increase the cold water temperature back to 12$^{\text{O}}$C, this is done thanks to the extended loop from the hot water loop. As it can be seen in the figure the extended loop is now a closed loop so the water in the pipes is just constantly circulating via the pump which its mass flow rate is controlled to achieve the 12$^{\text{O}}$C water in the cold water loop. So it works as follows, as directional control valve 3 switches direction, directional control valve 1 will operate switch so that no hot water is sent into the loop, and directional control valve 2 switches direction so that the water in the extended loop is not sent back to the gas cooler but kept circulating in the loop.

The pump's mass flow rate in that loop is no longer zero or equal to the subtraction of the hot water production from the hot water demand, but now it is controlled to achieve the temperature setpoint for the chilled water before being sent back to the evaporator, hence creating a fake load. As the warm water in the loop cools down as it heats the cold water to the set point in the PHE it regains its temperature as it warms up again from the ambient heat via the ambient heat exchanger. In figure 3 it can be seen as the warm water goes from 19$^{\text{O}}$C to 14$^{\text{O}}$C then back to 19$^{\text{O}}$C over the ambient HX, and the cold water goes from 9$^{\text{O}}$C to 12$^{\text{O}}$C over the PHE. This operation can also be used in the case where there is high hot water demand, and the tanks are no longer charged, while hot water production is not enough to supply the entirety of the hot water demand, hence this operation takes place in order to heat the water in the cold loop further to increase the cooling demand in return the mass flow rate of CO_2 in the heat pump will increase meaning more hot water production can be achieved to cover the hot water demand.

3.   Methodology

Figure 4, shows the final working iteration of the full heat pump system which includes the heat pump circuit, hot water loop and cold water loop. The development of the system started from scratch for each of the circuits, the heat pump system was built during the project development work and was sized and edited during the master thesis to serve the required capacities. Developing the hot water loop was the most demanding out of all circuits. The final working iteration took around 5 months' worth of work.

In order to build the modelica model, some data to define the model is given by the project group INDEE+ this includes the capacities required to achieve as well as the water temperature setpoints.

Once that was done, the model requires some boundaries in place to further help structure the system and define its operation and function. The heat pump system will deliver water heating and space chilling through a double stage evaporation. The hotel requires a cooling capacity of 130kW, gas cooler capacity of 160kW, with a compression power input of 30kW. Where the high stage circuit has a refrigerant mass flow rate of approximately 2627 kgh^{-1} (0.73 kgs^{-1}) and the medium and low stage circuits have refrigerant mass flow rate of approximately 1314 kgh^{-1} (0.365kgs^{-1}). Where the discharge pressure is at 100 bar, medium pressure is at 45 to 47 bar and low pressure is at 40 to 41 bar, this pressure lift from 40 bar to the medium pressure will be supplied via the ejector. Afterwards a Ph diagram of the system was completed to have a better idea on what could be the best state boundaries, in order to be able to size and configure the system to a higher
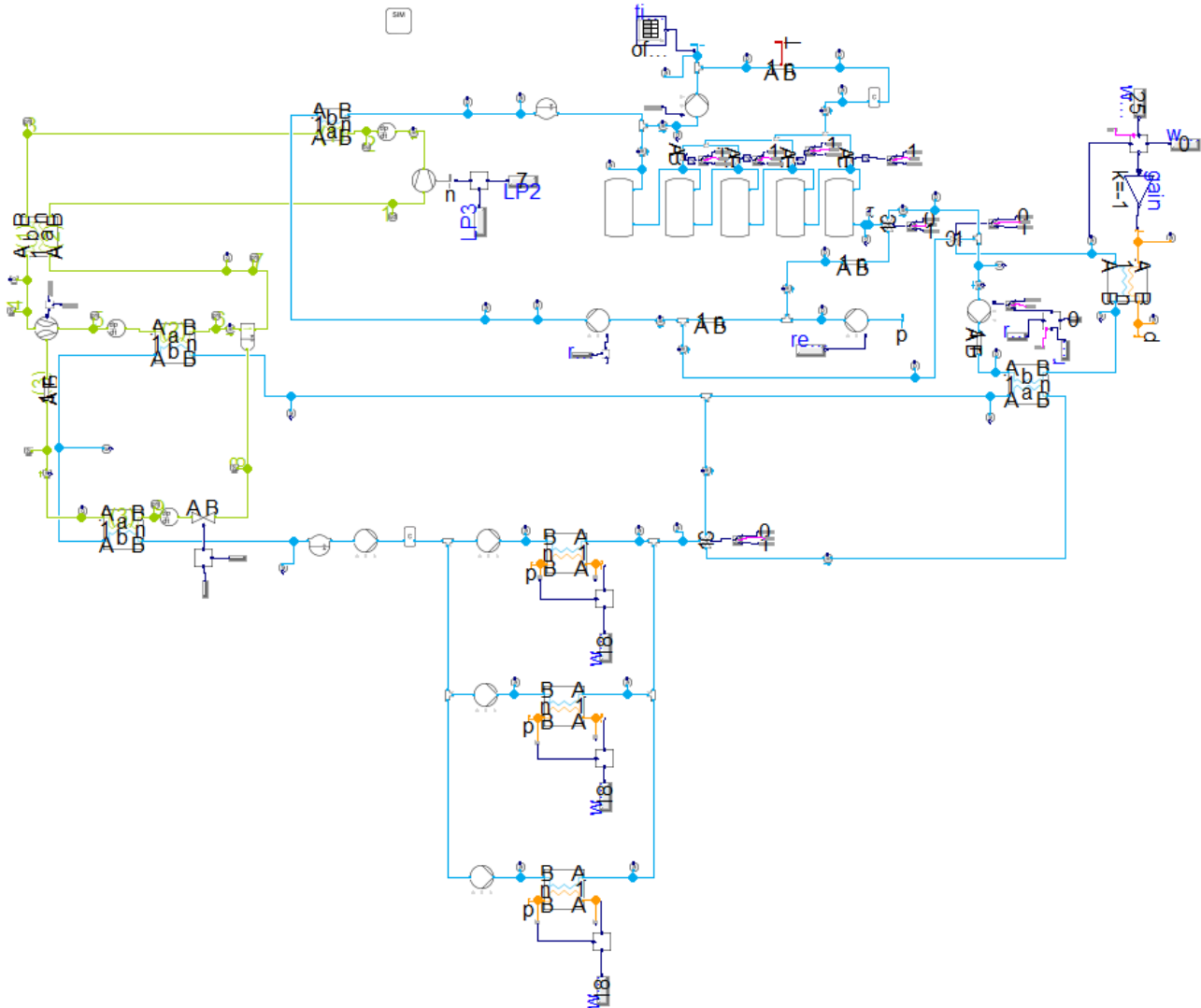

Figure 4: Final iteration of the working Modelica model.

standard.

The liquid separator was also designed and sized to fit the project criteria set by INDEE+. The main criteria was to host the entire charge of CO_2 during standstill conditions. To find the total charge of CO_2 in the system, the volume of all the components in the heat pump circuit must be calculated. This includes the volume over the compressor, gas cooler, internal heat exchanger, both evaporators, ejector and volume of pipes. Since, also sizing the pipes was one of the tasks of this thesis, finding the volume of the pipes was done by choosing a suitable diameter for each section based on the velocity of the refrigerant in said pipe. Detailed version of the calculation is presented in the main thesis paper. After calculating the total volume, the total charge can be found.

After defining the entire system's boundaries and components' sizing, the modelica model can be built. In order to see the system's performance in a dynamic simulation, rather than having static conditions before

building and installing the real system in India, the modelica model was created. The model was created on the programming language Modelica in the programming environment Dymola.

The heat pump circuit was first to be built and modelled. It was produced, through many trials. The final iteration works as follow; via the use of a PI controller which controls the frequency of the compressor the cooling demand is met. Hence, the setpoint is 7°C water at the outlet of the second evaporator. The PI controller of the ejector controls the effective flow area of the ejector so that the high side pressure is maintained at 100 bars. Finally, the PI controller over the expansion valve, controls the effective flow area so that the outlet vapor fraction of CO_2 is 0.8. Via the internal heat exchanger, the CO_2 is subcooled prior to expansion for higher cooling capacity. Then all the state sensors, mass flow rate and temperature sensors were placed accordingly.

To reach the final working iteration of the hot and cold water loops a total of 66 different iterations and trials were created. Three different cases of hot water demands were investigated in this simulation to show the tanks behaviour and storage capacity at different demands. Case 1, which represents the actual hotel's demand, case 2 which is 1.5 times larger than case 1, and case 3 which is 2 times larger than case 1. Where the simulation is done over 1 full day with each hour reflecting real life data on the typical demand of hot water in a 24 hour period. Before starting, it must be noted that a much more detailed explanation is available in the main paper. In simple words, the hot water loop works as follows; based on the hot water demand, cold city water is pumped into the loop, the main pump of the hot water loop is controlled via PI controller that controls the mass flowrate of water pumped so, that the exit water temperature from the gas cooler is 70°C. After this step, based on the conditions in the hot water loop one of the operation types discussed earlier takes place. It is either charging the system so the hot water production will cover the entire hot water demand, as well as, charge the tanks at the same time. While, the hot water returned from the building re-fills in one the tanks based on its temperature. So based on the water return temperature, one of the switches will activate and open the valve prior to the tank accordingly. The water fills up in that tank and maintain stratification. If it was discharging, then the entire hot water production will be needed in addition to hot water stored in the tanks to cover the remainder demand. In last operation, when the system is fully charged and there is a cold demand, a three way valve connected to the last tank on the right, has a switch which is activated only if, the exit water from the tank is over 40°C and the hot water production is bigger than the hot water demand.

In the extended loop there is another pump, that has a switch that either activates a PI controller or a set expression. When the three way valve is activated, the switch position is set to the real expression which states that the mass flow rate is the subtraction between the hot water production and hot water demand. If the three way valve is closed and the extended loop in the cold water operation is activated, then the switch's position will move to the PI controller. Where now, the mass flow rate inside the loop is controlled, so the exit temperature from the plate heat exchange for the cold water is lifted back to 12°C if there is not enough cold water demand. Or, lift it to over 12°C if the hot water production is not enough and the tanks are not charging. Hence, add load to the cooling loop to increase the cooling capacity required. Which increases the displacement of the compressor, hence a higher mass flow rate of CO_2 in the high pressure side. So, a higher mass flow rate of hot water can be maintained. The PI controller on the ambient heat exchanger controls the mass flowrate intake from the ambient so that the outlet water is back to ambient temperature. In the cold water loop, there are PI controllers on the mass flowrate of air intake into the air handling units so the exit air is at 18°C. The switch on the three way valve in the cold loop, activates once the temperature of water leaving the air handling units is lower than 10°C or when extra cooling capacity is required for more hot water production.

4.   Results

After running the simulation, the heat pump results gathered from modelica are presented below. Starting with the Ph diagram of the system seen in figure 5, which was produced via the use of Dave software. Based on the state point values, the calculated pressure lift by the ejector is 7 bars. Via the use of modelica, the average cooling, heating and total COPs are 4.5, 5.4 and 9.9 respectively. With the average total cooling

capacity is 133kW with the capacity of the first evaporator is 88kW and second evaporator 45kW and the heating capacity (gas cooler capacity) 160kW.
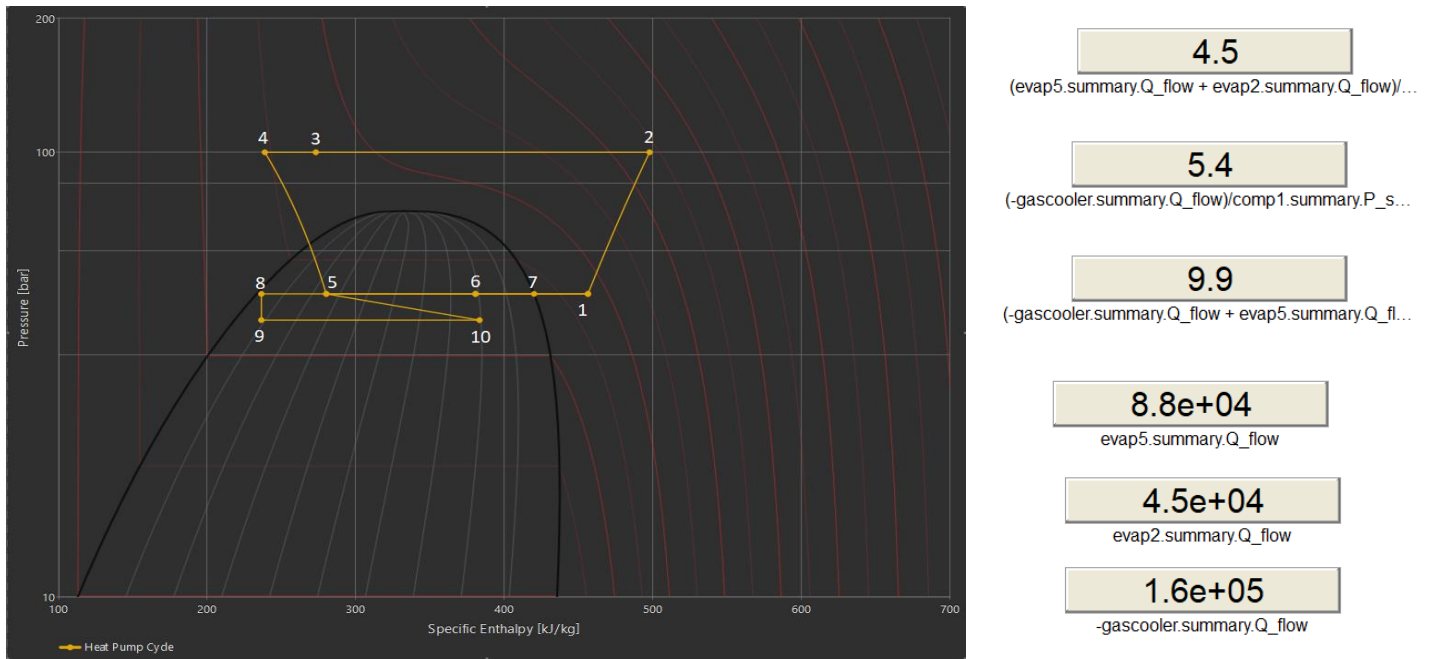

Figure 5: Ph diagram of simulated Heat Pump system

Via the ejector PI controller, the high side pressure is controlled to be at 100 bars. As described in section 2.5.2(literature review of main thesis) earlier this is to achieve a low approach temperature at the exit of the gas cooler. The approach temperature over the entire duration of the simulation, with the average approach temperature between the outlet CO_2 temperature from gas cooler and the inlet water temperature to the gas cooler is $4.43^{O}C$. The average shaft power input is found to be 30.5kW and the average calculated energy demand per day is 731.5kWh. The graphs relative to the approach temperature and energy demand are presented in the main paper.

Other results that have been also analysed for each case are; hot water production vs hot water demand. The total average hot water produced every day is approximately 77400L, which is higher than the total hot water demand over one day in case 1(37500L), 2(56250L) and 3(75000L). However, this production was not adjusted based on the demand peak hours, hence much more data was analyzed to find the operation patterns and system performance in each case. It was found that in case 1 the hot supplied water will always be delivered at $70^{O}C$, however a lot of waste heat is generated for rejecting heat to the ambient via the extended loop. Case 2 had the best operation, where the water supplied was at a minimum of $65^{O}C$ for a very short period and the system did not reject a lot of heat to the ambient. Finally, in case 3 which was the worst out of all since most of the time the supplied water was below much lower than the setpoint of $70^{O}C$. To reach this conclusion, these figures were generated and analysed; 1) To show the effect of the hot water demand on the hot water loop operation, and show that the control strategies for charging, discharging and fully charged operations are successful. 2) A figure that shows the temperature at the bottom of tank 5 and its direct effect on the position of the three directional valve. 3). A figure showing the effect of hot water demand on the temperature of the supplied water as well as exploring how the charging and discharging of tanks occur and what that tells us about the system. 4) A figure to represent the average temperature of water inside each one of the tanks over the period of simulation, which is used to analyse the tank behaviour in three different cases and whether stratification was maintained or not. 5) A figure showing the control operation of the switches connected to the tanks for the return water of the building. 6) A figure that shows the temperature of water at the inlet and outlet of the gas cooler, as well as the supplied water temperature. From these figures the effect of increasing hot water demand on the inlet temperature of the gas cooler and supplied temperature of water can be depicted. As well as, showing that no matter the inlet temperature is the outlet temperature of water from the gas cooler is always $70^{O}C$.

5.   Discussion

After analysing the data, it can be said that the heat pump system is over sized for case 1 which is a representative of the hotel demands, however it will still give consistent 70°C hot water throughout the entire day no matter the time, which was only achieved in case 1. Case 2 seemed to have the best results as it supplies 70 $^{\circ}$C water most of the time at the lowest it was 65°C and the system did not waste as much heat as case 1. Finally with case 3 the supplied water temperature fell just under 55 $^{\circ}$C, and the system was not capable of producing enough hot water to supply the demand, which was the cause of the supplied water temperature dropping. A deeper discussion that covers all the results generated is in the main paper.

For further work, a lot can be done to fix the simulated system and produced even better results. One solution that will solve the problems of each of the cases is the ability to control the cooling demand. Since, all the problems rose from one limitation faced during the simulation. Which is the fact that the cooling demand was constant. So, if the cooling demand would have been controlled, then when the system is producing too much hot water like in case 1, the cooling demand would decrease. Since, in the simulation it was at highest value the entire period, which lead to such high production and would not be the real life case. In case 2 and 3, if the cooling demand would have been controlled, then when there is a need of extra hot water production, the system will add fake load via the use of the hot and cold water extended loops. Where the circulating warm water in the closed extended loop will lift the temperature of the water returning to the evaporator. Which will increase the cooling demand and in return the hot water production will increase. This is possible since, the compressor was also oversized to suit all these possibilities as mentioned earlier.

Two other controls that must be explored further are, controlling the high side pressure of the heat pump so that the pinch point is at the outlet and the approach temperature is the lowest possible. This is done by defining an expression to control the ejector effective flow area based on the approach temperature of the gas cooler. For a higher efficiency and cooling effect, allowing for a higher capacity and COP and decrease the expansion losses. The other control to be explored further, is the return water from building to tanks switches to switch based on both the return water temperature and temperature inside each of the tanks at that instant and then the switch is activated accordingly. More further work suggestions that may not have as a big of an effect on the system as the presented further work, is available in the main thesis paper.
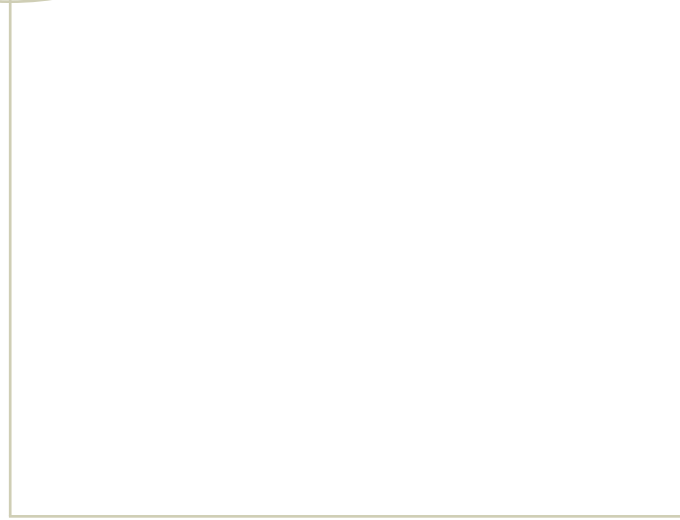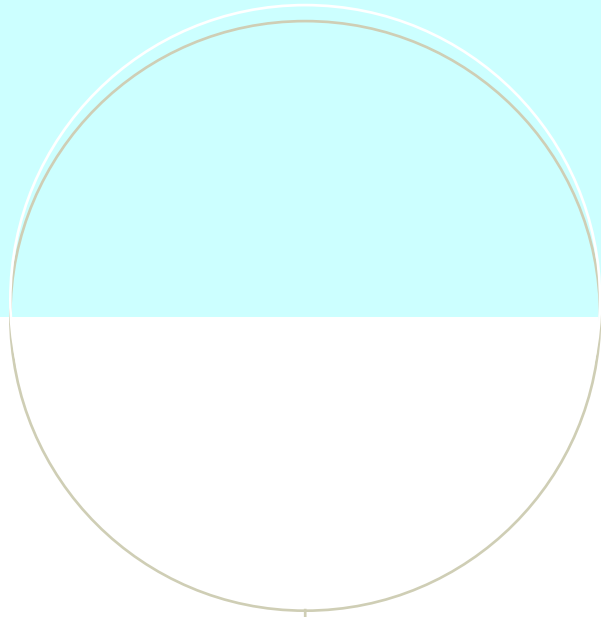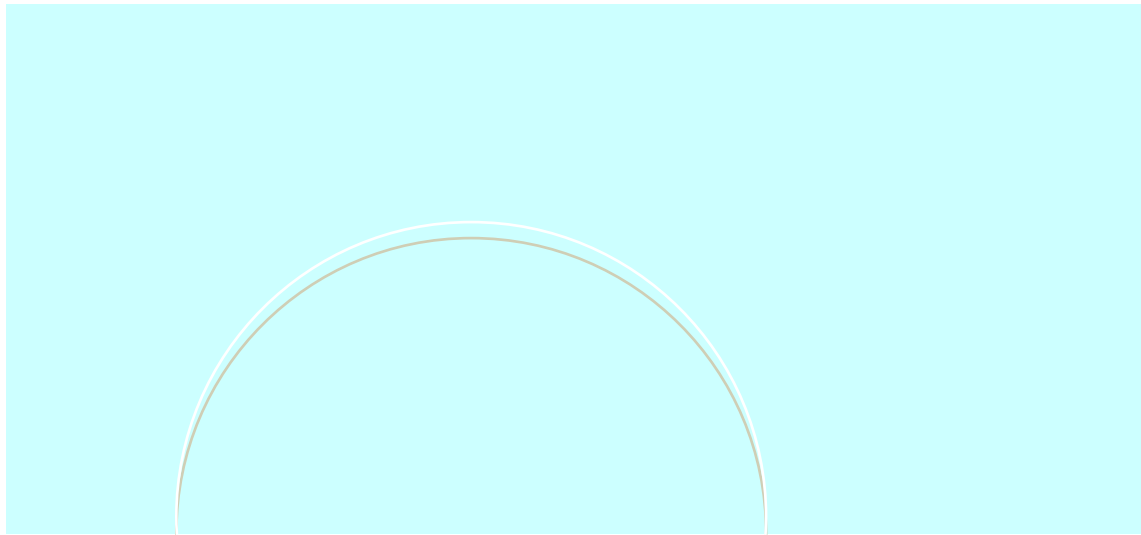
6.   CONCLUSIONS

In conclusion, the constant growing need to protect the environment, cost effective solutions that are easy and safe to maintain lift the potential of CO2 as a refrigerant on a pedestal, with its great thermo-physical properties for space and water heating, chilling of rooms (AC), cold and freezing storages, makes R744 the king of refrigerants for such uses. With the increase of research and dedicated development of such systems the ban of HFC will be very easy to deal with by replacing it with R744 refrigerant. Transcritical R744 systems have recently become the norm for heat pumping and refrigeration in the food industry. This thesis recognises the developments of R744 refrigeration and heat pump systems. It then explores the use of simulation modelling programs to try and replicate real life systems before installations. To find the efficiency of the system and how it operates. In this case scenario, after applying all of that was discussed in the study the heat pump system developed can achieve very high COPs and can supply the costumer "the hotel in India" with its hot and cold water demands, with no problems. The heat pump produced from this extensive research can achieve great performance results in all conditions, making a one heat pump for all. Working from cold to hot climates.

All in all, it can be said that this paper has accomplished its aim to push the CO_2 equator to the south and help remove the reluctance of retailers for installing such CO_2 systems in their projects, rather than HFC units. Saving the environment from high GWP refrigerants will be achieved faster.

7.   REFERENCES

Hafner, Armin, Stefano Poppi et al. (2012). 'Development of commercial refrigeration systems with heat recovery for supermarket building'. In: *Proceedings of the 10th IIR Gustav Lorentzen Conference on Natural Refrigerants, Delft, The Netherlands, pp. 25–27.*

All references used are available in main thesis.